

AD-A086 001

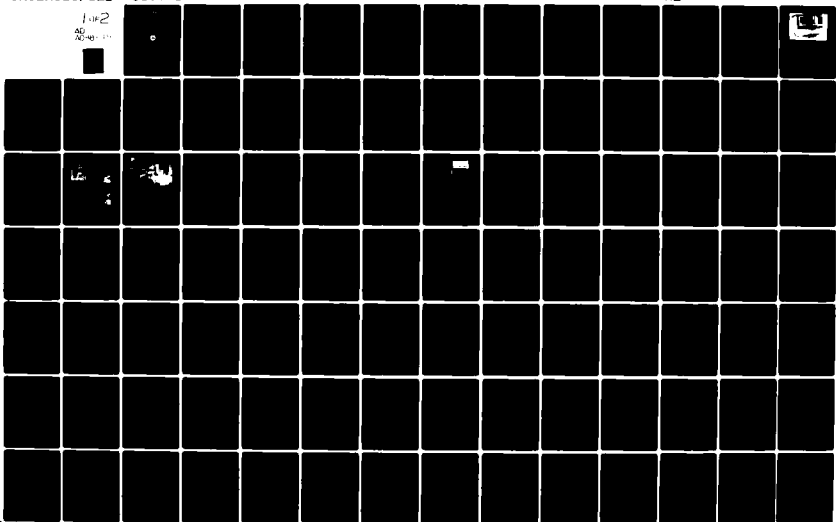
COAST GUARD WASHINGTON D C OFFICE OF RESEARCH AND DE--ETC F/6 17/7  
PRECISION LORAN-C NAVIGATION FOR THE HARBOR AND HARBOR ENTRANCE--ETC(U)  
MAY 80 D L OLSEN, J M LIGON, A J SEDLOCK  
USCG-D-34-80

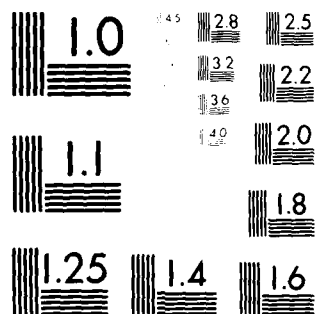
UNCLASSIFIED

NL

1042

2048-171





MICROCOPY RESOLUTION TEST CHART  
 NATIONAL BUREAU OF STANDARDS-1963-A

Report No. CG-D-34-80

**LEVEL**

12

ADA 086001

**PRECISION LORAN-C NAVIGATION FOR THE  
HARBOR AND HARBOR ENTRANCE AREA**



**MAY 1980**

**DTIC**  
**ELECTE**  
**JUN 27 1980**  
**C**

Document is available to the U.S. public through the  
National Technical Information Service,  
Springfield, Virginia 22161

Prepared by

**U.S. DEPARTMENT OF TRANSPORTATION  
United States Coast Guard  
Office of Research and Development  
Washington, D.C. 20593**

DDC FILE COPY

80 6 26 040

### **NOTICE**

**This document is disseminated under the sponsorship of the Department of Transportation in the interest of information exchange. The United States Government assumes no liability for its contents or use thereof.**

**The contents of this report do not necessarily reflect the official view or policy of the Coast Guard; and they do not constitute a standard, specification, or regulation.**

**This report, or portions thereof may not be used for advertising or sales promotion purposes. Citation of trade names and manufacturers does not constitute endorsement or approval of such products.**

## Technical Report Documentation Page

1. Report No. <b>(14) USCG-D-34-80</b>	2. Government Accession No. <b>AD-A086 001</b>	3. Recipient's Catalog No.	
4. Title and Subtitle <b>(6) PRECISION LORAN-C NAVIGATION FOR THE HARBOR AND HARBOR ENTRANCE AREA,</b>		5. Report Date <b>(11) May 1980</b>	6. Performing Organization Code
7. Author(s) <b>(10) D.L. OLSEN, J.M. LIGON, A.J. SEDLOCK, C.E. ISGETT</b>		8. Performing Organization Report No. <b>CG-D-34-80</b>	
9. Performing Organization Name and Address Department of Transportation U.S. Coast Guard Office of Research and Development (G-DST-1) Washington, DC 20593		10. Work Unit No. (TRAIS) <b>2100</b>	11. Contract or Grant No. <b>(12) 154</b>
12. Sponsoring Agency Name and Address Department of Transportation U.S. Coast Guard Office of Research and Development (G-DST-1) Washington, DC 20593		13. Type of Report and Period Covered	
15. Supplementary Notes This report updates and consolidates three papers presented at the Eighth Annual Technical Symposium of the Wild Goose Association in Williamsburg, Virginia, October 17-19, 1979. The papers will be published as part of the proceedings of that symposium.		14. Sponsoring Agency Code <b>G-DST-1</b>	
16. Abstract <p>The U. S. Coast Guard is engaged in a long-term program to evaluate the potential and develop the technology for precision navigation using Loran-C. The Coast Guard has taken a three-pronged approach to harbor and harbor entrance (HHE) navigation—user equipment development, time difference (TD) surveying, and grid stability analysis. These three aspects of HHE Loran-C navigation were addressed in separate papers presented in October, 1979. This report updates and consolidates the three papers, and is intended to serve as a source document on the Coast Guard's approach to HHE Loran-C navigation.</p> <p>User equipment is being developed which combines time differences from a precision Loran-C receiver with survey information from a data tape cassette using simple algorithms to present the plotting situation on a CRT display. The algorithms, hardware, and software are described, and the results of summer and winter 1979 tests on the St. Marys River are given. It is concluded that accuracies of better than 25 meters are achievable.</p> <p>Three methods are described for surveying the Loran-C time difference coordinates of waypoints and prominent physical features of a harbor area for precision Loran-C navigation. Results are presented from field measurements on the St. Marys River Mini Loran-C Chain using existing visual aids to navigation as a position reference. The survey methods described provide for accurate and timely Loran-C grid survey over a wide range of harbor areas. The general features of each method and details of the visual aids to navigation approach are presented. Analysis of field measurements show survey capability on the order of ten nanoseconds.</p> <p>Temporal instabilities on the order of several hundred nanoseconds were measured over the service area of the St. Marys River Mini-Chain between Fall 1977 and Spring 1978. These instabilities, if true, could render the mini-chain unusable for precision navigation on the St. Marys River. A careful recollection effort was deemed necessary to verify the chain's performance and to definitively judge its navigation capabilities. In addition, a methodology is desired for establishing the stability of Loran-C signals in the general harbor and harbor entrance environment. This methodology is being investigated using the mini-chain. Time difference data is being collected at three fixed monitor sites, and is being analyzed by a rather simple model which separates variations into uniform propagation effects, local errors and control errors. The propagation component extracted from the data exhibits a high correlation with temperature, which can be attributed primarily to the vertical lapse rate of the index of refraction.</p>			
17. Key Words  Loran-C, precision navigation, radio-navigation, propagation, inertial surveying, microwave surveying		18. Distribution Statement  Document is available to the U.S. Public through the National Technical Information Service, Springfield, VA 22161.	
19. Security Classif. (of this report)  UNCLASSIFIED	20. Security Classif. (of this page)  UNCLASSIFIED	21. No. of Pages  154	22. Price

## PREFACE

The U. S. Coast Guard is engaged in a long-term program to evaluate the potential and develop the technology for precision navigation using Loran-C. The basic method is to use Loran-C in the repeatable mode for real time 2 or 3 line-of-position precision navigation, or piloting, in the vicinity of surveyed positions. This method can be augmented by offset or proportional differential corrections. The Coast Guard has taken a three-pronged approach to harbor and harbor entrance (HHE) navigation—user equipment development, time difference (TD) surveying, and grid stability analysis. These three aspects of HHE Loran-C navigation were addressed in separate papers presented in October, 1979. This report updates and consolidates the three papers, and is intended to serve as a source document on the Coast Guard's approach to HHE Loran-C navigation.

Section 1 presents the paper by Ligon and Edwards<sup>1</sup> on user equipment development. The PILOT (Precision Intracoastal Loran Translocator) equipment described represents an effort to produce a commercially-realizable precision Loran-C navigator. A basic philosophy in PILOT's design is the minimization of real-time computations. Many of the required parameters are pre-computed and stored on a cassette tape which includes as well the definition of the channel, nav aids and geographic features of a waterway. Included in this section are the results of a brief evaluation of PILOT conducted on the St. Marys River during October, 1979. Several additional sets of this equipment are presently being produced for a 1980-1981 evaluation by various government and commercial interests. Appendices A-I present the development of the algorithms used within PILOT.

Section 2 presents the paper by Sedlock<sup>2</sup> on time difference surveying. A survey is required to determine the repeatable Loran-C TDs which define a waterway, and which are encoded onto cassette tapes for PILOT. A Time Difference Survey Set (TDSS) and accompanying statistical algorithms provide the means for conducting the survey. Several examples show survey data gathered on the St. Marys River.

Section 3 concludes the report with a paper on grid stability analysis by Olsen and Isgett<sup>3</sup>. Grid stability is fundamental to precise navigation using repeatable Loran-C coordinates. The paper concentrates on the St. Marys River Mini-Loran-C Chain, and mentions the extension of the instrumentation and analytical techniques to other HHE areas around the country.

Accession For	<input checked="" type="checkbox"/> <b>NTIS GSAI</b> <input type="checkbox"/> <b>DOC TAB</b> <input type="checkbox"/> <b>Unannounced</b> <input type="checkbox"/> <b>Justification</b>	By	Distribution/	Availability Codes	Avail and/or special Dist <b>A</b>
---------------	---	----	---------------	--------------------	--

# METRIC CONVERSION FACTORS

## Approximate Conversions to Metric Measures

Symbol	When You Know	Multiply by	To Find	Symbol
<b>LENGTH</b>				
in	inches	2.5	centimeters	cm
ft	feet	30	centimeters	cm
y	yards	0.9	meters	m
m	miles	1.6	kilometers	km
<b>AREA</b>				
sq in	square inches	6.5	square centimeters	cm <sup>2</sup>
sq ft	square feet	0.09	square meters	m <sup>2</sup>
sq yd	square yards	0.8	square meters	m <sup>2</sup>
sq mi	square miles	2.6	square kilometers	km <sup>2</sup>
acre	acres	0.4	hectares	ha
<b>MASS (weight)</b>				
ounce	ounces	28	grams	g
pound	pounds	0.45	kilograms	kg
short ton (2000 lb)	short tons	0.9	tonnes	t
<b>VOLUME</b>				
teaspoon	teaspoons	5	milliliters	ml
tablespoon	tablespoons	15	milliliters	ml
fluid ounce	fluid ounces	30	milliliters	ml
cup	cups	0.24	liters	l
pint	pints	0.47	liters	l
quart	quarts	0.95	liters	l
gallon	gallons	3.8	liters	l
cubic foot	cubic feet	0.03	cubic meters	m <sup>3</sup>
cubic yard	cubic yards	0.76	cubic meters	m <sup>3</sup>
<b>TEMPERATURE (celsius)</b>				
Fahrenheit temperature		5/9 (after subtracting 32)	Celsius temperature	°C

\* 1 in = 2.54 (exactly). For other metric conversions and more detailed tables, see NBS Mon. Publ. 286, Units of Length and Masses, Price \$2.25, SD Catalog No. C13.10-286.

## Approximate Conversions from Metric Measures

When You Know	Multiply by	To Find	Symbol
<b>LENGTH</b>			
millimeters	0.04	inches	in
centimeters	0.4	inches	in
meters	3.3	feet	ft
kilometers	1.1	miles	m
kilometers	0.6	miles	mi
<b>AREA</b>			
square centimeters	0.16	square inches	sq in
square meters	1.2	square yards	sq yd
square kilometers	0.4	square miles	sq mi
hectares (10,000 m <sup>2</sup> )	2.5	acres	acre
<b>MASS (weight)</b>			
grams	0.005	ounces	oz
kilograms	2.2	pounds	lb
tonnes (1000 kg)	1.1	short tons	st
<b>VOLUME</b>			
milliliters	0.03	fluid ounces	fl oz
liters	2.1	pints	pt
liters	1.06	quarts	qt
liters	0.26	gallons	gal
cubic meters	35	cubic feet	cu ft
cubic meters	1.3	cubic yards	cu yd
<b>TEMPERATURE (celsius)</b>			
Celsius temperature	9/5 (then add 32)	Fahrenheit temperature	°F

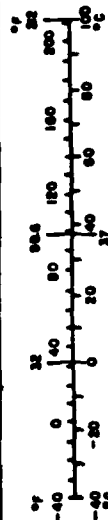


## TABLE OF CONTENTS

<u>Section</u>	<u>Page</u>
<b>1 USER EQUIPMENT DEVELOPMENT</b>	<b>1-1</b>
Loran-C Piloting	1-1
Environmental Requirements	1-2
PILOT	1-3
Hardware Description	1-4
Software Description	1-6
Initial Test Results	1-7
Winter Deployment	1-8
The Future	1-8
Conclusion	1-8
<b>2 TIME DIFFERENCE SURVEYING</b>	<b>2-1</b>
Introduction	2-1
Classic Approach	2-1
A New Approach	2-1
Augmentation Techniques	2-9
Summary	2-10
<b>3 GRID STABILITY ANALYSIS</b>	<b>3-1</b>
Introduction	3-1
Preparations	3-1
Preliminary Stability Analysis	3-4
Harbor Monitor Program	3-8
Conclusions	3-9
Prognosis and Future Efforts	3-9
<b>APPENDIX A — Definition of G Matrix Analysis for USCG HHE Navigation Program</b>	<b>A-1</b>
<b>APPENDIX B — G Matrix Analysis for USCG Loran-C HHE Navigation Program</b>	<b>B-1</b>
<b>APPENDIX C — Methods for Obtaining Approximate and Exact Solutions to a LORAN Navigation Equation</b>	<b>C-1</b>
<b>APPENDIX D — Design, Simulation and Performance of Digital TD and Heading Filters for the USCG LORAN-C HHE Navigation Program</b>	<b>D-1</b>
<b>APPENDIX E — The Effect of Uncompensated TD Truncation Biases on TD and TD Errors in the USCG LORAN-C HHE Navigation Program</b>	<b>E-1</b>
<b>APPENDIX F — Formulas for Making Short-Range Predictions of Ship's Course in the USCG LORAN-C HHE Navigation Program</b>	<b>F-1</b>
<b>APPENDIX G — Additional Performance Evaluations for the Second-Order a,b Filter</b>	<b>G-1</b>
<b>APPENDIX H — Exact Method for Obtaining Horizontal Components of Ship's Velocity from TD Measurements</b>	<b>H-1</b>
<b>APPENDIX I — Computation of GDOP for St. Marys River Data File</b>	<b>I-1</b>
<b>REFERENCES</b>	<b>R-1</b>



## ABBREVIATIONS

APL/JHU	Applied Physics Laboratory of Johns Hopkins University
CALOC	Calculator Assisted Loran Controller
CCZ	Coastal Confluence Zone
C-LAD	Low Cost Loran-C Assist Device
COGLAD	Coast Guard Loran Assist Device
CRT	Cathode Ray Tube
DR	Dear Reckon
FEHG	Flat Earth Hyperbolic Grid
GDOP	Geometric Dilution of Precision
HHE	Harbor and Harbor Entrance
INS	Inertial Navigation System
ISS	Inertial Survey System
LOP	Line of Position
NOAA	National Oceanic and Atmospheric Administration
OEM	Original Equipment Manufacturer
PILOT	Precision Intracoastal Loran Translocator
SAM	System Area Monitor
TD	Time Difference
TDSS	Time Difference Survey Set
WP	Waypoint

## Section 1

### USER EQUIPMENT DEVELOPMENT

#### LORAN-C PILOTING

##### Introduction

As a navigator proceeds from the Coastal Confluence Zone into harbor entrances, harbors and rivers, his requirements for both positioning accuracy and timeliness increase on the order of 500 times. The number of information sources also increases and the navigator must integrate the data from all of these sources. He has crossed the boundary separating piloting from navigation.

Large areas of the U.S. Coastal Confluence Zone (CCZ) are presently, or will shortly be, covered by Loran-C signals which are charted to an accuracy of 0.4 km. It is known that these signals are repeatable to within a few tens of meters. These signals are also present in harbors and harbor entrances and potentially form the basis for a precision navigation system. This section discusses a method for exploiting these Loran-C signals and describes the PILOTing hardware which is the keystone for this exploitation. The name PILOT—Precision Intracoastal Loran Translocator—is not meant to imply automatic piloting, but rather to highlight the significantly different frame of reference which exists in the piloting domain.

##### Loran-C PILOTing

The first two words forming the acronym "PILOT" refer to the environment; the last two refer to the method.

Intracoastal waters are typically characterized by visible or physical features: channel boundaries, visual aids-to-navigation, coastlines. They are also characterized by significant overland Loran-C propagation paths and warped time difference grids. In these waters, positioning in an absolute, geodetic sense (latitude/longitude) is of little value. Also, the orientation of the vessel is as important as its position. Precision must be relative to these intracoastal realities—"precise" enough for safe, speedy vessel operation.

The method is basically Loran-C translocation. Given a reference site and its corresponding Loran-C time differences, estimate the location of a Loran-C receiver at another site in the vicinity of the reference site, based upon the time difference measurements taken there. This is essentially the same as the method used in conventional satellite position translocation and in many loran waypoint navigation systems.

## ENVIRONMENTAL REQUIREMENTS

### Calibration

If the latitude and longitude of all the essential navigation features in a particular river or harbor were known, and if there were a perfect propagation prediction model, then calibration would be unnecessary. There are over 100,000 visual navigation aids installed in the U.S. intracoastal waters, and the latitude and longitude are known for very few of them; yet, they serve their purpose. In the past, attempts have been made to utilize the most accurate Loran-C prediction methods in the piloting environment, but unfortunately these require a larger geological data base than the corresponding loran data base for river and harbor "calibration" by measurement, and still do not provide sufficient accuracy.<sup>4</sup>

When calibration is by measurement, coding delays or System Area Monitor reference time differences are held constant and the time difference field is measured as it is. No attempt is made to adjust the coding delays to cover the service area in some sort of "least squares" error sense to fit the imperfect propagation model. Calibration by measurement brings up five questions: the questions of density of survey, of coordinate conversion algorithm, of positioning, of survey time difference measurement, and of temporal stability. The questions of density of survey and coordinate conversion algorithm are very tightly coupled. On the St. Marys River, a survey interval of approximately 3 kilometers coupled with navigational aid relative position taken from the river charts and processed using the PILOT coordinate conversion algorithm provided "sufficient" navigational accuracy. That is, the PILOT showed the vessel to be in the center of the channel and passing the proper navigational aids when it appeared to the observer that this was the case. The remaining three questions have been addressed and are discussed in greater detail in Sections 2 and 3, and in the paper by Johler<sup>5</sup>. In summary, there is a very effective method for surveying the Loran-C time differences relative to the visual aids and features used by the pilot himself, and the stability question is vital and is ultimately solved by a form of differential corrections.

### Reliability and Speed

The piloting environment places constraints upon navigational equipment that do not exist in the more open waters. The pilot needs much higher accuracy and reliability. The safety of his vessel cannot tolerate the loss of a fix caused by failure of one of the navigational transmitting stations. In Loran-C this translates to 3-LOP fixes, with drop-back 2-LOP fixes, including those when the Master station has a casualty.

The pilot does not have time to convert numbers to a position on a chart. His navigational display should provide him with an immediate picture of his situation so that he can rapidly respond to it. This translates to a visual plan display with navigational aids, channel boundaries and some shoreline features indicated.

### Other Issues

It is possible, and PILOT is the demonstration case, to meet the requirements of the piloting environment with a compact user equipment for approximately \$20,000, including the cost of a "better grade" Loran-C receiver. The pilot will probably not be

able to obtain satisfactory operations using a low-cost CCZ Loran-C receiver.

## PILOT

### Description

The PILOT, developed for the U.S. Coast Guard by the Applied Physics Laboratory of Johns Hopkins University, is an electronic aid for piloting vessels in harbors and rivers. Prerecorded tape cartridges, containing a sequence of chartlets and other navigation information, provide the PILOT with a degree of "local knowledge." The vessel's present position and heading, continuously determined from a loran receiver and the vessel's gyro, are displayed on the current area chartlets. Chartlets of two different scales (master and detail) are always available for operator selection. Position information relative to waypoints (intermediate destinations) is displayed to the left of the chartlet. A horizontal bar graph, representing the vessel's relative cross track position, can be displayed along the bottom of the CRT. A predictor option displays the ship's future position, based upon present course made good and turning rate, for any operator selectable time period.

There have been many systems constructed for similar purposes in the past. The earliest was probably the Decca track plotter in the early 1960s. Modern track plotters are found on many fishing vessels. Table 1-1 lists some of these coordinate

TABLE 1-1. COMPARISON OF VARIOUS TYPES OF USER EQUIPMENT

TYPE	REPRESENTATIVE EQUIPMENT	TD-XY CONVERSION METHOD	AREA OF USE	DISPLAY	NAVIGATIONAL FEATURES DISPLAYED	COMMENTS
Area TD	DECCA Plotter (Cir 1962)	None, TD of 1 and boundary predicted	CCZ	Strip Chart	As desired.	Distorted chart X-Y
Track-line TD	Several receivers and devices	None	CCZ	Alpha-numeric or analog	None	Distances given in micro-seconds. Could be used in HHE with waypoint survey.
Track-line X-Y	C-LAD, User I, LONA, several receivers	Inverse Prediction	CCZ	Alpha-numeric or analog	None	Use Latitude & Longitude In HHE could be used used with TD waypoint survey, but cannot be used Lat-Long or X-Y.
Area X-Y	COGLAD, several track plotters	Inverse Prediction	CCZ HHE	X-Y plotter	None	Use Latitude and Longitude or X-Y.
	User II	Inverse Prediction	HHE	Video Graphics & Alpha-numerics	As desired.	Shows vessel position and orientation. Ultimately required intensive survey. Primarily an R/D device. Very long chartlet change time.
	Modified User II	Inverse Prediction	HHE	Color Graphics & Alpha-numerics	As desired. Data on disc memory.	Color graphics and RAYDIST and Miniranger sensors added.
	PILOT	G-Matrix with flat earth hyperbolic grid	HHE	Video graphics chartlets analog, & alpha-numerics	As desired. Display and conversion data on tape cassette.	Shows vessel position and orientation. Uses waypoint and limited navaid survey information. Rapid chartlet change and display update. Built to demonstrate technology.

conversion/display devices and comments upon their features as they relate to the harbor and river environment. As can be seen, the PILOT is a logical progression from these devices. It solves the coordinate conversion problem which had in the past been the major obstacle to HHE implementation, and it demonstrates the feasibility of reliable PILOTing using a single, compact video display terminal.

### Navigation Charts

The PILOT is basically a data processor. All coordinate conversion constants and navigational background information are provided on a cassette which is, in effect, a Loran-C navigational chart on a magnetic tape medium. A single cassette can contain as many as 150 to 200 of these chartlets—more than enough to permit a complete transit of the St. Marys River, which is approximately 100 kilometers long. Section 2 contains a deeper discussion of the chartlet calibration. In summary, the method involves the creation of a linked mosaic of ideal flat-earth hyperbolic Loran-C grids fixed at the calibration points, with aids and geographic features charted onto these grids. This implies a slight distortion of the physical world if the real Loran-C grid is distorted. On the St. Marys River, this distortion was small enough to be unnoticeable, even with calibration point separations as great as 10 kilometers. Had the distortion become too great, additional survey points would have been necessary. Since the identical model is used within the PILOT for coordinate conversion, the charting accuracy is as good as the repeatable accuracy.

### HARDWARE DESCRIPTION

#### Graphics Terminal

The nucleus of the PILOT system (Figure 1-1) is a Hewlett Packard 2649A microprogrammable graphics terminal. This OEM device was selected because it has a separate graphics processor with memory, dual tape cartridge units, and an 8080 microprocessor that could be modified and programmed as required. Modifications to the HP-2649A terminal included: converting the 8080 microprocessor from software math to hardware math by adding an Advanced Micro Devices (AMD) 9511 arithmetic processing unit, developing a two-receiver interface board to mount inside the terminal, developing an interface board to connect to the ship's gyro and to a time difference bias (differential correction) box, replacing the large general purpose keyboard with a small predefined keypad, and building a short base for the terminal to serve as a cable junction box. The system block diagram is shown in Figure 1-2.

#### Receiver Interface Board

The dual receiver interface board is designed around an 8085 microprocessor and a second AMD 9511 math unit. This microprocessor performs the following functions: input, convert, identify, edit, filter and dead reckon (DR). The use of two loran receivers permits cross chain position fixes. The data format of most receivers can be accommodated (up to 50 parallel lines per receiver) by changing the input software module. A serial receiver interface board has been designed, and will be used to operate PILOT with the forthcoming Internav model LC-404 Loran-C Navigation and Monitor Receiver, a microprocessor version of the presently-used Internav MK III receiver.



FIGURE 1-1. PILOT

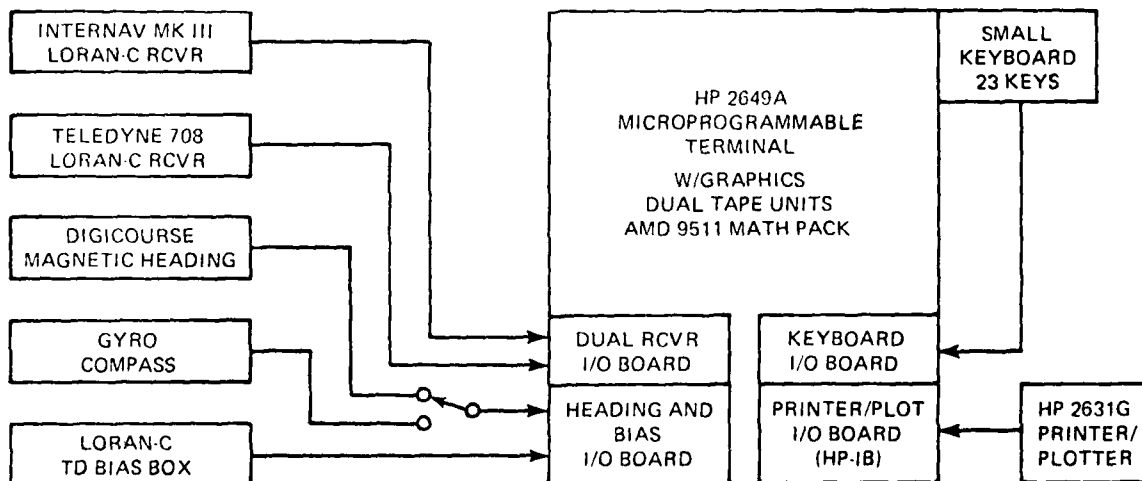


FIGURE 1-2. PILOT SYSTEM BLOCK DIAGRAM



The heading and TD bias board includes a 10-bit synchro-to-digital converter and can accept heading information from either a gyrocompass or a magnetic compass with a shaft encoder. Storage registers on this board can store three sets of TD bias numbers (+ 7999 nanoseconds). These registers can be loaded either by the operator from the keypad or from a remote box or modem via an interface cable.

**Operation of the PILOT terminal was simplified by replacing the HP keyboard (105 keys) with a small keypad (23 keys) having eleven function keys plus twelve numerical and cursor control keys.**

**Figure 1-3 is the PILOT functional data flow diagram.**

**Approximately 17,000 bytes of machine language code were developed at APL for the PILOT terminal, and an additional 40,000 bytes of the original HP code was retained. Structured programming and assembly language was used for maximum efficiency.**

Digital filtering is used on each TD as part of the preprocessing performed on the receiver interface board. An alpha/beta filter was modified to induct turning acceleration feedback. For receivers with relatively slow data rates (i.e., less than

two sets of TDs per second), the TDs are dead-reckoned every 100 milliseconds using the last known velocity and turning acceleration. Three different filter time constants may be selected by the operator from the keypad. The development of PILOT's filter algorithms is given in Appendices D-H.

#### Coordinate Conversion

The 8080 microprocessor performs a full order, iterative transformation approximately twice per second. When three good TDs are available, a 2x3 minimum variance "G" matrix is used. Each term of the matrix is preweighted to produce a best fit with the expected relative signal strength. When only two TDs are available, one of three 2x2 unweighted matrices is used. The development of the "G" matrix and the iterative exact solution to the non-linear loran equations are presented in Appendices A-C.

#### Chartlet Cassettes

Chartlet cassettes contain an index file, master files and detail files. The index file contains a title block and a list of all master chartlets on the cassette. Each master file contains the graphics for 8-16 miles of track, the area matrix coefficients, transmitter coordinates and supplemental data such as display origin, scale, rotation, and geometric dilution of precision (GDOP—developed in Appendix I). Each detail file contains the graphics for 1-2 miles of track, the TDs and x-y coordinates of the current waypoint, bearing angles to and from the WP and supplemental data.

Master chartlets provide "look ahead" by showing the next several waypoints; detail chartlets provide a closer view of the vessel's current situation. Each master file is followed by one or more detail files. North-up or track-up chartlets may be used.

Chartlets can be developed using a digitizer, minicomputer or calculator, plus the PILOT terminal reconfigured as a "stock" HP-2649A terminal. The original chartlet cassettes for the St. Marys River were produced at APL, and the Coast Guard Research and Development Center is currently setting up a system for producing them for other locations.

#### INITIAL TEST RESULTS

The PILOT system was initially tested on the St. Marys River during the first week in October 1979.

##### The Receiver

The Loran-C receiver used was an Internav MK III Survey Receiver. The receiver had been previously tested in the laboratory and could typically be expected to provide an accuracy of 30 nanoseconds under a variety of signal conditions. The St. Marys River signal environment was so benign that performance in the 10 nanosecond range (relative to a reference Austron-5000 monitor receiver) was observed.

##### The PILOT

Overall performance was excellent. The PILOT successfully combined the receiver TDs with survey data taken during August and September and chartlets prepared from the



NOAA navigational charts to provide accurate position and situation information. The references in most areas were visual ranges and buoys, and were quite good. The navigational solutions were based upon waypoint surveys, and the chartlets were calibrated by using the surveyed location of a single aid on each one. Quantifiable accuracy tests will be completed next year, but visual accuracy was excellent. There was no noticeable grid warp—possibly the result of the low conductivity of both the fresh water and the Laurentian Shield upon which the area is located. A repeatable mode error budget is given in Section 3.

#### WINTER DEPLOYMENT

Following the preliminary field tests, the PILOT system was installed aboard the U.S. Coast Guard Cutter Katmai Bay for operational deployment during the winter of 1979-1980. Receiver and PILOT operation was easily mastered by all members of the ship's bridge crew. The display of alphanumerics, graphics and the cross-track distance bar offered something for each of the various levels of interest, from commanding officer to helmsman. PILOT was shown to be useful in thick fog and for starting turns based upon the distance to go. Though the expiration of the winter navigation program limited icebreaking activities, the consensus is that PILOT should be a useful aid in breaking channel edges not marked with buoys.

#### THE FUTURE

A data logging capability is planned for PILOT, whereby a record of a voyage will be recorded on the second tape drive of the HP-2649A terminal. The remaining development tasks include interfacing to the LC-404 Loran-C receiver and installing the algorithms to allow a fall-back Master independent 2-LOP capability.

PILOT will be reinstalled aboard the Katmai Bay in June 1980 for further evaluation and for demonstration to commercial shipping interests. Several PILOT systems have been offered to the carriers for evaluation aboard their vessels in the St. Marys River and on the Great Lakes between August and December 1980. These deployments will be followed by quantitative and human factor tests.

A "stripped-down" version of PILOT, designated PLAD for Portable Loran Assist Device, is presently under development at the Applied Physics Laboratory. PLAD will use a simple digital display in a hand-held data terminal in lieu of the graphical display of the HP-2649A, and will store waypoint information in semiconductor memory. The device is planned for initial testing on the Delaware Bay during the winter of 1980-1981.

#### CONCLUSION

The PILOT opens an entirely new area for precision Loran-C navigation.

## Section 2

### TIME DIFFERENCE SURVEYING

#### INTRODUCTION

The Coast Guard is currently engaged in a development program for precision Loran-C navigation in harbor areas. The key element in this program is the PILOT user equipment described in Section 1. PILOT provides position estimates based upon Loran-C time difference (TD) measurements, a flat-earth hyperbolic grid (FEHG) coordinate conversion algorithm, and chartlets stored on a magnetic tape cartridge. The chartlets contain position and TD coordinates for waypoints, a description of channel boundaries and aids to navigation, and computational constants for the FEHG algorithm. If harbor areas were accurately surveyed (in the geodetic sense) and Loran-C propagation models were highly accurate, the data necessary to produce chartlets could be directly calculated. Since neither is true, a technique has been developed to survey the TD coordinates for waypoints and to test for TD grid warp which could affect the accuracy of the navigation solution. This survey technique applies to a wide range of navigation scenarios including relatively wide open areas such as San Francisco Bay and severely restricted channels such as the St. Marys River. In addition, the survey technique is cost effective, and data reduction and analysis can be accomplished in the field as the survey progresses.

#### CLASSIC APPROACH

The classic approach to the survey problem is to use a high accuracy reference system to position a survey vessel at a point and simultaneously record position and TD coordinates. This is the basic approach that was used in initial attempts to survey waypoints on the St. Marys River. Several difficulties arise with this approach. An accurate geodetic description of channel boundaries and aids to navigation does not exist, and where accurate coordinates do exist, they are not always consistent with geodetic control points ashore. Often existing geodetic control points ashore are not recoverable or are in locations unsuitable for locating the reference system transponders, and additional control points must be surveyed. The cost of establishing the necessary geodetic control ashore, operating the position reference system, and performing the TD survey are substantial. As the navigation channel becomes more restrictive the inconsistency between survey coordinates and coordinates for channel boundaries and aids to navigation becomes intolerable. The costs both in time and dollars for a geodetic survey of channel boundaries and aids to navigation for an entire harbor are totally prohibitive.

#### A NEW APPROACH

The basic problem producing chartlets for precision Loran-C navigation is relating the Loran-C TD grid to the navigation situation of channel boundaries, shoals, aids-to-navigation, etc. This section describes an approach which has been developed

for determining TD coordinates of the physical features of a harbor by surveying. In addition, analysis tools are used to obtain position coordinates which describe the spatial orientation of the physical features consistent with the TD grid. Although these position coordinates are accurate enough in a local sense that deviations from geodetic coordinates are imperceptible, no attempt is made to tie the position coordinates to a geodetic reference.

Since visual aids-to-navigation form the basic position reference, the approach has been termed the Visual Grid Survey. A TD measurement set has been developed by the Coast Guard Research and Development Center to accurately and efficiently measure, record and process TD information. Analysis tools include the techniques for determining waypoint TDs and x-y coordinates using the FEHG algorithm developed for the PILOT user equipment. The FEHG algorithm calculates position relative to a reference waypoint based upon the difference between observed TDs and the TDs for the reference point.

#### General Procedure

The general procedures for a Visual Grid Survey are:

- a. Choose waypoints from harbor charts and estimate the waypoint coordinates (e.g. latitude, longitude).
- b. Compute the FEHG parameters for these positions.
- c. Estimate the positions of surrounding features needed for PILOT chartlets relative to the waypoint, i.e. construct first cut chartlets.
- d. Survey the TDs of ranges, shoals, channel edges, aids-to-navigation, etc. in the area of each waypoint.
- e. Define the TDs of each waypoint.
- f. Refine the actual position offsets of charted features with respect to each waypoint using the FEHG algorithm and channel edge TD data.
- g. Link the chartlets from a central or major waypoint by calculating the position of adjacent waypoints from the surveyed waypoint TDs and the FEHG algorithm.

This procedure results in chartlets that are locally exact models of reality. Charting and chart-pickoff errors are removed but local grid warp and TD survey errors remain.

#### Waypoints

As outlined above, the first step in the survey chartlet preparation process is the selection of waypoints. The waypoints are defined based upon navigation charts and the knowledge of traffic patterns. The intersection of two ranges, intersection of two channel centerlines, intersection of right half channel centerlines, or the intersection of two commonly used tracklines all define possible waypoints. There are two general approaches to determining waypoint TDs. The first approach is used where the waypoint is defined by the intersection of two visual ranges. The visual ranges provide

very precise crosstrack information. In a small region near the waypoint the Loran-C TD grid can be approximated by the linear model below:

$$\text{TDX} - \text{TDX}_0 = a_{11}(x - x_0) + a_{12}(y - y_0) + n_x \quad (2-1)$$

$$\text{TDY} - \text{TDY}_0 = a_{21}(x - x_0) + a_{22}(y - y_0) + n_y \quad (2-2)$$

$$\text{TDZ} - \text{TDZ}_0 = a_{31}(x - x_0) + a_{32}(y - y_0) + n_z \quad (2-3)$$

where

TDX, TDY, TDZ are observed TDs

TDX<sub>0</sub>, TDY<sub>0</sub>, TDZ<sub>0</sub> are waypoint TDs

x, y are position coordinates of the observation

x<sub>0</sub>, y<sub>0</sub> are waypoint position coordinates of the waypoint

a<sub>i,j</sub> are coefficients of the gradient matrix (directional derivatives of the TD grid)

n<sub>x</sub>, n<sub>y</sub>, n<sub>z</sub> are error terms due to noise and nonlinearity

Along the centerline of a visual range,

$$(y - y_0) = m(x - x_0) \quad (2-4)$$

where

$$m = \arctan(\text{course line})$$

Substituting equation (2-4) into equations (2-1), (2-2), and (2-3) results in a set of equations for the trackline in TD space.

$$(\text{TDY} - \text{TDY}_0) = C_1(\text{TDX} - \text{TDX}_0) + n_1 \quad (2-5)$$

$$(\text{TDZ} - \text{TDZ}_0) = C_2(\text{TDY} - \text{TDY}_0) + n_2 \quad (2-6)$$

$$(\text{TDX} - \text{TDX}_0) = C_3(\text{TDZ} - \text{TDZ}_0) + n_3 \quad (2-7)$$

where

$$C_1 = (a_{21} + a_{22}m) / (a_{11} + a_{12}m)$$

$$C_2 = (a_{31} + a_{32}m) / (a_{21} + a_{22}m)$$

$$C_3 = (a_{11} + a_{12}m) / (a_{31} + a_{32}m)$$

$$n_1 = n_y - n_x C_1$$

$$n_2 = n_z - n_y C_2$$

$$n_3 = n_x - n_z C_3$$

Linear regression can be used to fit a straight line to TD data collected along each of the tracklines using a visual range as a position reference. The resultant regression lines of TDs are in the form:

$$(\text{TDY} - \text{TDY}_i) = a_i(\text{TDX} - \text{TDX}_i) \quad (2-8)$$

$$(\text{TDZ} - \text{TDZ}_i) = b_i(\text{TDY} - \text{TDY}_i) \quad (2-9)$$

$$(\text{TDX} - \text{TDX}_i) = c_i(\text{TDZ} - \text{TDZ}_i) \quad (2-10)$$

where

$TDX_i$ ,  $TDY_i$ ,  $TDZ_i$  are averages

$i = 1, 2$  (i.e. trackline 1 and trackline 2)

Each of the above pairs of simultaneous equations can be solved to estimate the waypoint time differences. Two estimates for each of the waypoint TDs are obtained. The agreement of these estimates is one measure of quality of the survey.

The quality of the resultant waypoint survey is a function of several factors. The location of the ranges is an important consideration. In the ideal case, both sets of range markers are near the waypoint. The ability of the operator to determine when the survey vessel is on the range decreases as a function of distance from the range markers. The confidence bounds on the regressive lines are minimum at the mean values; therefore the ideal survey pattern is an "X" centered (approximately) at the waypoint. This pattern is not always realizable since there may be insufficient water beyond the waypoint, or range markers may become obscured shortly after the waypoint is passed. The survey tracklines should be kept short to insure linearity of the TD grid over the survey area. Several runs are made on each trackline to randomize errors in positioning the survey vessel on the trackline.

The crossing angles of the survey lines also affect the accuracy of the solution. In general, when the tracklines cross at a shallow angle on the navigation chart, the TD tracklines will also cross at shallow angles.

Figures 2-1, 2-2, and 2-3 illustrate the determination of waypoint TDs based on TDs measured on two intersecting ranges on the St. Marys River. This is almost an ideal

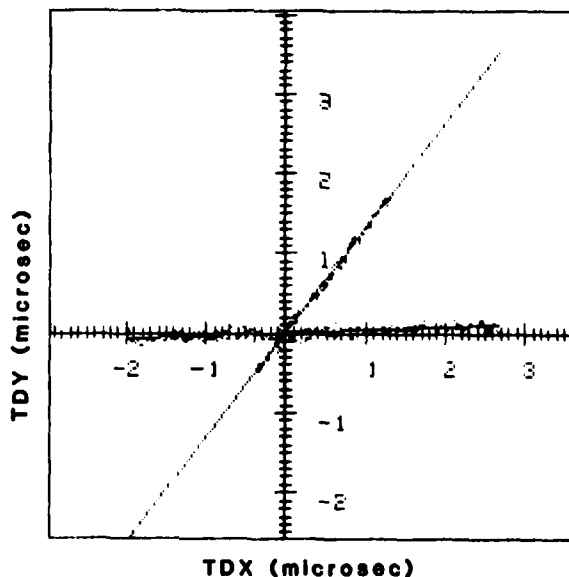
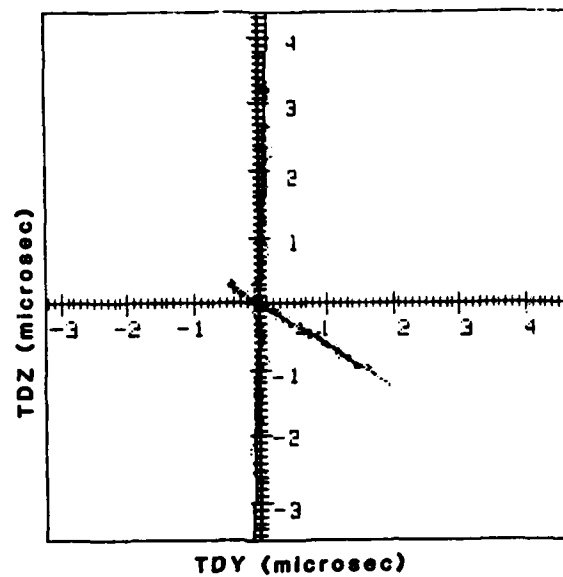
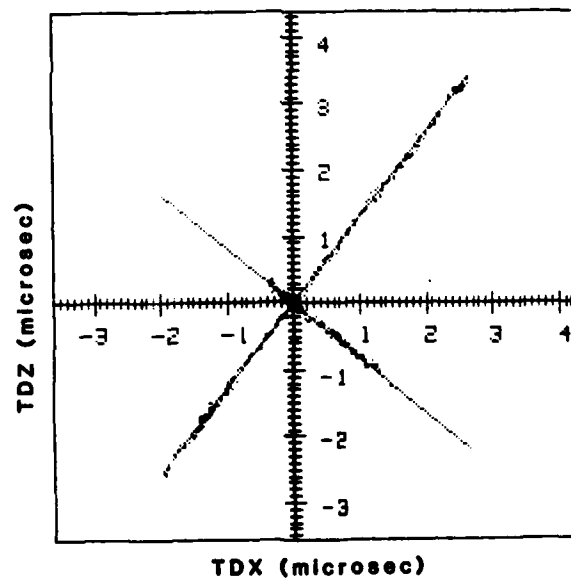


FIGURE 2-1. TDY VS TDX MEASURED ON TWO INTERSECTING VISUAL RANGES WITH RESULTING REGRESSION LINES



**FIGURE 2-2. TDZ VS TDY MEASURED ON TWO INTERSECTING VISUAL RANGES WITH RESULTING REGRESSION LINES**



**FIGURE 2-3. TDZ VS TDX MEASURED ON TWO INTERSECTING VISUAL RANGES WITH RESULTING REGRESSION LINES**

case. Both sets of range markers were near the waypoint and it was possible to bracket the waypoint in an "X" survey pattern. The crossing angles are near ideal (50-88 degrees). The resultant solutions display excellent agreement as shown in Table 2-1.

TABLE 2-1. COMPARISON OF WAYPOINT CALCULATIONS FOR EACH PAIR OF REGRESSION LINES SHOWN IN FIGURES 2-1, 2-2 & 2-3

<u>DATA SET</u>	<u>TDX</u>	<u>TDY</u>	<u>TDZ</u>
TDX/TDY	11260.256	22332.410	-
TDY/TDZ	-	22332.410	33299.094
TDX/TDZ	11260.257	-	33299.092

Unfortunately not all channels are marked by ranges. The approach in this case is an interactive one which utilizes the FEHG algorithm and the survey officer's judgement. The first step is to survey the TDs of the channel features (channel edges, aids-to-navigation, shoals, etc.) in the area around the waypoint. A fathometer can be used to detect channel edges and shoals. Buoys and fixed aids are marked by circling or stationing near them. An initial estimate is made of the waypoint TD from a simple prediction program and the FEHG algorithm can be used to plot the channel features surveyed. If the estimate of the waypoint is incorrect, the location of the waypoint with respect to the channel features will appear offset. The correction which should be applied to correct this offset in x-y coordinates translates into a TD correction for the waypoint. The procedure can be repeated until the survey officer is satisfied that the waypoint is positioned correctly. This procedure works particularly well when one of the channels is marked by a range.

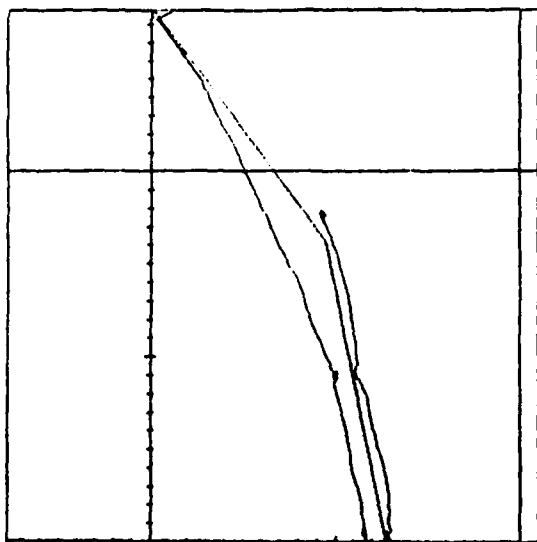


FIGURE 2-4. PLOT OF CHANNEL EDGE FEATURES REFERENCED TO INCORRECT WAYPOINT TDS

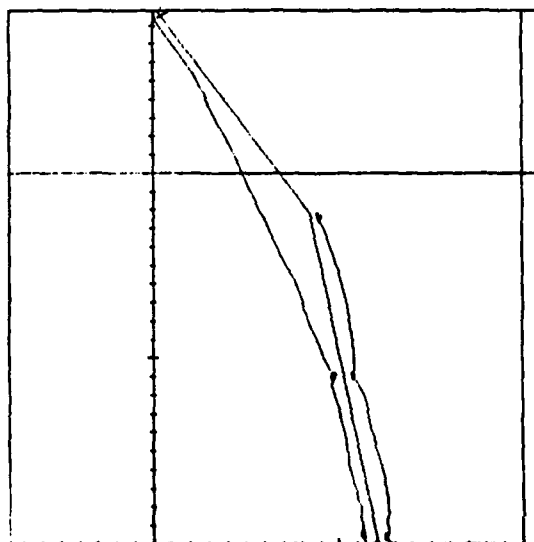


FIGURE 2-5. PLOT OF CHANNEL EDGE FEATURES REFERENCED TO CORRECTED WAYPOINT TDS

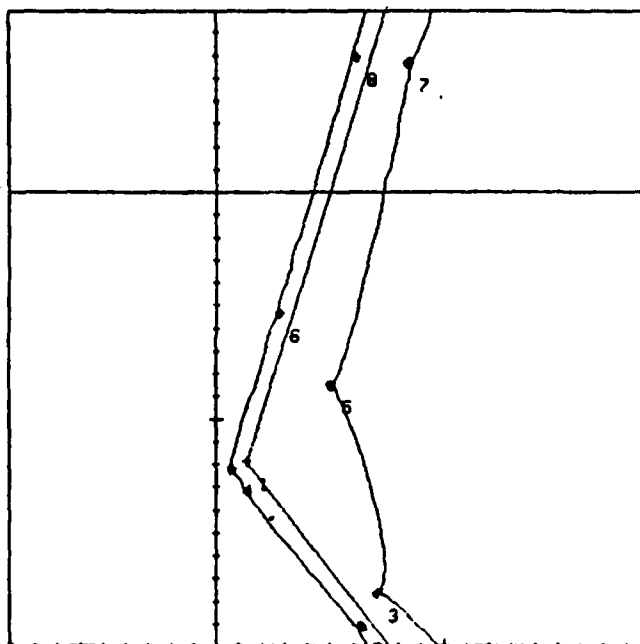


FIGURE 2-6. TYPICAL PLOT OF CHANNEL EDGE FEATURES DERIVED FROM TD MEASUREMENTS

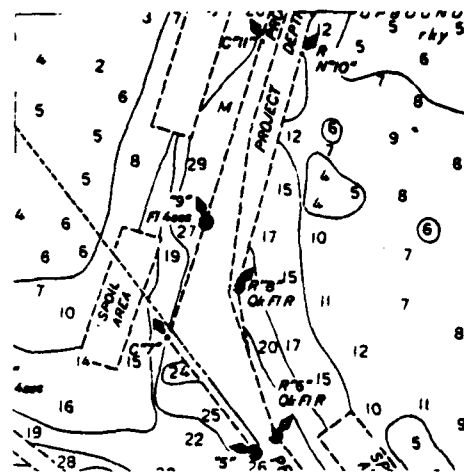


FIGURE 2-7. PORTION OF NAVIGATION CHART FOR AREA SHOWN IN FIGURE 2-6

Figures 2-4 and 2-5 illustrate the above approach applied to a waypoint on the St. Marys River where neither channel was marked by a range. The waypoint in this example was defined as the intersection of the centerlines of two adjacent channels. In Figure 2-4 the buoys on the east side of the channel for the southern trackline plot appear to lie almost on what should be the centerline. On the northern trackline, the channel centerline and western edge coincide. Figure 2-5 shows the result of moving the waypoint such that the tracklines are properly centered in both of the channels.

#### Channel Features

Once the TD coordinates of a waypoint have been determined, the next step in the survey is to determine the position offsets of channel features with respect to the surveyed waypoint. A plot is made using the TD data for the channel features near a waypoint transformed by the FEHG into planar coordinates. The survey officer then digitizes and stores the relative x-y locations of channel edges, shoals, aids-to-navigation, etc.

Figure 2-6 illustrates a typical plot of channel edge features in x-y coordinates in the area around one of the waypoints on the St. Marys River. Figure 2-7 is a portion of the navigation chart covering the same area.



### Daisy-chaining Chartlets

The next step in the survey process is to calculate the position of each of the waypoints based upon the survey data. A central, well-established waypoint is defined as the reference point for the overall survey area. The positions of the waypoints adjacent to the reference waypoint are calculated based on the reference waypoint position and TDs and the surveyed TDs of the adjacent waypoints. Successive waypoint positions are calculated in the same manner from each adjacent waypoint. The differences between projected waypoint positions and the original positions estimated from nautical charts are due to original charting errors, chart pickoff errors, cumulative Loran-C grid warp waypoint-to-waypoint, and TD survey errors.

### Short-distance Grid Warps

While the procedure of daisy-chaining waypoints absorbs the effects of long-distance grid warps, there may exist short-distance grid warps along tracklines. This error can be minimized by introducing trackpoints, which are reference points located between two waypoints. Both the position and TDs for a trackpoint can be estimated from the channel feature data.

### Survey Equipment

A Time-Difference Survey Set (TDSS) was fabricated at the U.S. Coast Guard Research and Development Center to permit collection and analysis of Loran-C TD data. The TDSS consists of an Austron-5000 monitor receiver interfaced to a Hewlett Packard 9845 calculator. The TDSS provides real time data display, processing, and storage during the data collection phase, and provides data reduction and analysis during post mission analysis. During data collection, three sets of TDs are processed and stored. The TDSS provides a real time display of the data in the form of a TD-TD plot on the calculator's CRT display. Cumulative statistics are calculated as the data is collected and are displayed in two forms. A bar graph on the CRT display indicates the confidence bound on the regression lines calculated. The survey officer may also obtain a printout of the cumulative statistics on command. At the end of a data run the calculator outputs a hard copy of the plot and a printout of the statistical data. If a waypoint is being surveyed using two ranges, the survey officer may calculate the mean waypoint TDs on location. Depending on the results of the calculation, he may choose to resurvey one or more of the tracklines or to move on to the next task. TD data collected along channel edges may be translated to x-y coordinates and plotted on the CRT on location for an on-scene check of the data collected.

A fathometer and highly maneuverable shallow draft vessel complete the equipment necessary for a "visual survey." With the fathometer and suitable vessel, it is a relatively simple task to find the dredged channel boundaries and maneuver along them. The shallow draft and maneuverability features of the vessel simplify the task of marking aids to navigation and collecting data on ranges outside channel boundaries. A typical survey crew is comprised of a survey officer, equipment operator/technician, and vessel operator.

## AUGMENTATION TECHNIQUES

The line where a harbor area begins and the Coastal Confluence Zone ends is a fuzzy one. Areas such as the approach to New York Harbor, areas of Puget Sound, Chesapeake Bay, Delaware Bay, etc., may not be suitable for using Visual Grid Survey. In general, such areas are relatively wide open and there are a minimum of aids marking channels. The problem is more to survey channel separation zones rather than well marked restricted navigation channels. Inconsistencies as large as several hundred feet between positions estimated from navigation charts and a position reference are undetectable by the mariner in such situations. In these areas it may be more efficient to use a survey system which incorporates a position reference. Two such systems have been conceptualized.

### Inertial Survey System

As its name implies, the Inertial Survey System (ISS) uses a survey grade inertial navigation system (INS) incorporating special operating procedures and post mission data analysis as a position reference, and a helicopter as the survey vessel. Loran-C TD data is collected as the helicopter hovers over the waypoint. The helicopter pilot receives guidance information from a navigation display driven by the INS. Waypoint positions input to the INS are estimated from the navigation charts for the area being surveyed. Position corrections to account for inertial drift between updates are calculated at the end of the data collection period. The Loran-C TDSS used for visual survey is too heavy and bulky for helicopter deployment, and a helicopter TD measurement package will have to be developed to fill this need.

The ISS using a helicopter as the survey platform has the advantage of being able to cover a large area in a short time. The biggest disadvantage is cost to lease and the availability of inertial survey services. Geodetic control points must also be established as update points for the ISS. This adds to the total survey costs and time to implement.

### Microwave Survey Reference

The microwave survey system conceptually consists of the Loran-C TD measurement system used for the visual survey system with an added position reference system input. As in the ISS approach, waypoint positions are estimated from navigation charts. Instead of hovering over the waypoint, the survey vessel records TD and position data while maneuvering in a cloverleaf pattern about the waypoint. The position of the waypoint and the location of the vessel are displayed on the calculator CRT. Waypoint TDs are calculated by reflecting the measured TDs to the waypoint using a linear transformation.

$$\underline{TDp} = \underline{TD} + A (\underline{Zp} - \underline{Z}) \quad (2-11)$$

where

TDp is the estimated waypoint TD vector

TD is the measured TD vector

Zp is the waypoint position vector

Z is the position vector at the measurement point

A is a gradient matrix which is a function of the positions of the Loran-C transmitting stations and the waypoint.

Individual samples are averaged until the confidence bound of the mean is within some preset tolerance level.

Data is also collected along tracklines between waypoints and perpendicular to the tracklines using the positioning system as a reference. This data is used to determine the presence of grid warp and to bound the navigation errors.

#### SUMMARY

The Visual Survey Method is the ultimate approach for Loran-C TD grid survey in restricted waterways. This approach ties together the Loran-C TD grid and the world of the mariner. The result is a set of waypoint position and TD coordinates and relative position coordinates for harbor features such as channel edges and aids-to-navigation which are incorporated into chartlets for Loran-C user equipment. The position coordinates for these channel features are calculated from TD measurements based on waypoint TD and position coordinates. The waypoint positions are calculated in a daisy-chain fashion from a central waypoint based on the difference in TDs between adjacent waypoints. This procedure eliminates charting and chart pick-off error and absorbs long range grid warp. The remaining error sources are due to errors in the TDs for the waypoints and channel features and local grid warp. The effects of local grid warp are minimized by establishing trackpoint(s) as necessary between waypoints.

In some areas it may not be feasible to apply the visual technique. Two approaches have been conceptualized to survey these areas. At this time it is not clear whether these approaches will be required. The accuracy of relatively simple propagation models may be more than adequate to calculate waypoint TD coordinates in these cases.

## Section 3

### GRID STABILITY ANALYSIS

#### INTRODUCTION

Precise position determination with Loran-C depends on the existence of a stable, repeatable time difference (TD) grid. Grid stability analysis, together with the development of user equipment and TD surveying techniques, constitute the Coast Guard's three-pronged approach to harbor and harbor entrance (HHE) navigation. The Coast Guard's signal stability measurement program has concentrated on the St. Marys River mini-chain.

Data was first collected over the mini-chain's service area between fall 1977 and spring 1978 as input to the design and calibration of a grid prediction algorithm.<sup>6</sup> TD variations at several sites were unusually large, with an average of 300 nanoseconds and a maximum of 850 nanoseconds.<sup>7</sup> These instabilities, if true, could render the mini-chain unusable for precision navigation on the St. Marys River. Although reasonable care was taken in performing the measurements, the data remained suspect due to the equipment and methodology used. A careful recollection effort was deemed necessary to verify the chain's performance and to definitively judge its navigation capabilities.

#### PREPARATIONS

Preparations for a one year in-depth study of the mini-chain's stability were completed in early May 1979. The major tasks involved the creation of three fixed monitor sites plus the improvement of equipment and staffing at the System Area Monitor (SAM) station. Figure 3-1 shows the layout of the chain.

##### Fixed Monitor Sites

The new monitor sites are on the south end of the river at DeTour Village, mid-river at Dunbar Forest, and at Point Iroquois near the river's northern end. Each site has a 35-foot whip antenna with a groundplane and multicoupler. DeTour (Figure 3-2) and Dunbar are equipped with a Magnavox AN/BRN-5 receiver plus an Internav LC-204 receiver. Point Iroquois (Figure 3-3) has two LC-204 receivers. This setup enables each site to monitor all three baselines.

##### System Area Monitor

Figure 3-4 shows the SAM site, which has been converted to a Coast Guard standard suite. Control had previously been achieved using an Internav Model 303 monitor receiver, a short whip antenna, and an early prototype CALOC (Calculator Assisted Loran Controller) system. Since 4 May 1979, control has been performed using the 35-foot whip antenna and Austron 5000-CALOC system that is becoming standard

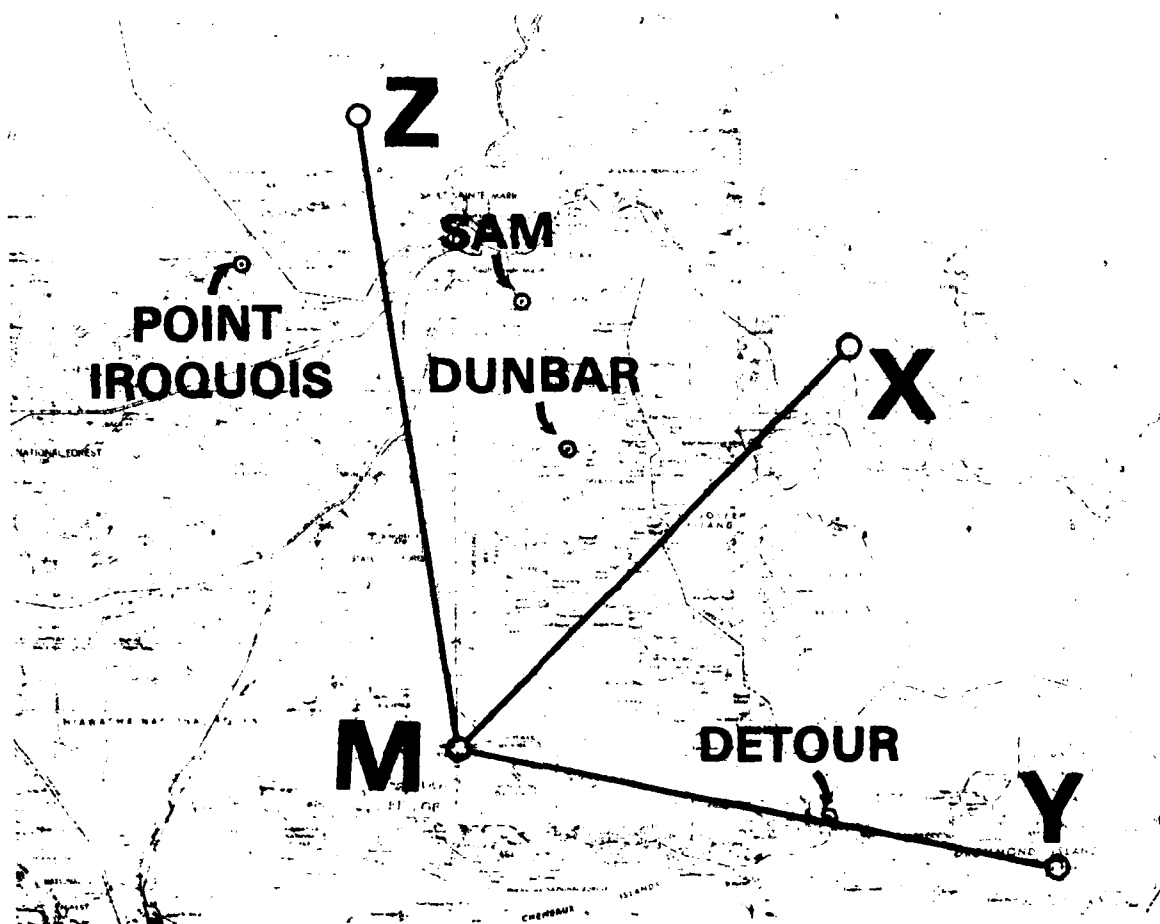


FIGURE 3-1. LAYOUT OF MINI-CHAIN WITH RECONFIGURED M-X

equipment for long-baseline Loran-C chains. The mini-chain's group repetition interval was slowed from 4930 to 5930 to satisfy the Austron 5000's processing time requirements, and has since been changed to 6980 to preclude interference from the Canadian East Coast Chain.

#### Chain Reconfiguration

The final step in preparation for the stability study was accomplished on 9 May 1979 when the Master and Xray station designations were interchanged. The switch was made to improve Master station availability. Prime power failures have been more frequent at the Gordon Lake, Canada site than at the Pickford, Michigan site. Power failures are significant since the transmitters have no emergency generators for backup. Also, repairs can be effected more quickly at the Pickford site due to the shorter travel times involved.



FIGURE 3-2. DETOUR VILLAGE MONITOR

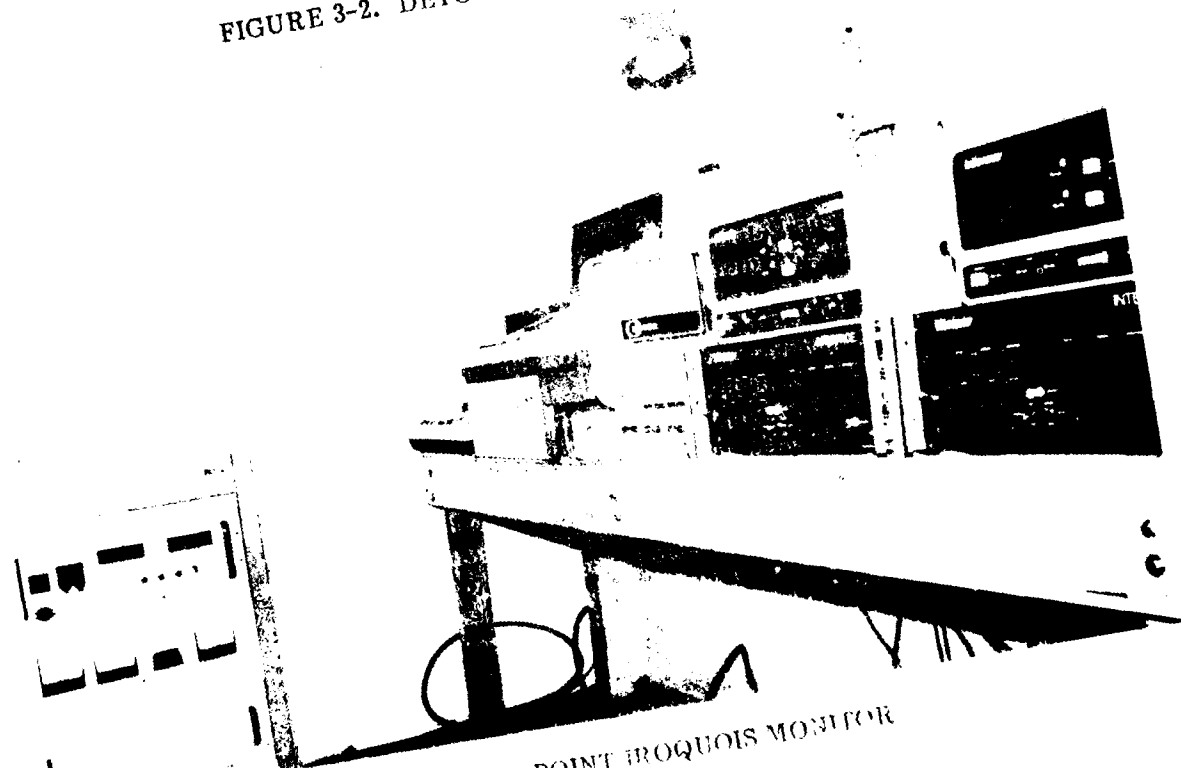


FIGURE 3-3. POINT IROQUOIS MONITOR

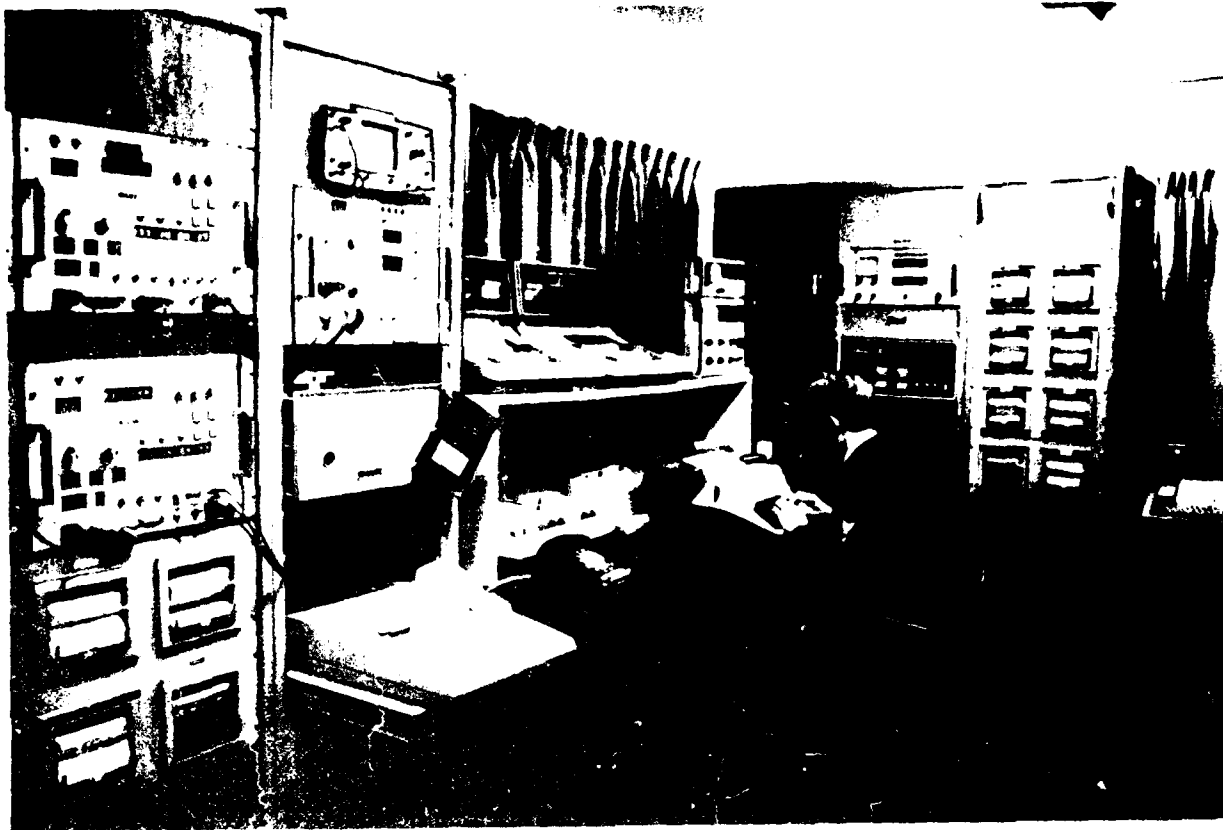


FIGURE 3-4. SYSTEM AREA MONITOR

#### PRELIMINARY STABILITY ANALYSIS

The basic analysis relies upon one hour averages, termed the System Samples, collected at midday and midnight. The initial analysis period includes not only environmental changes, but also the above-mentioned refinements in the monitor and control equipment. The data cannot be considered the final measure of the mini-chain's performance, but are nonetheless informative. Figure 3-5 shows the midday TD fluctuations for one baseline at the three monitor sites. The worst case variation is approximately 180 nanoseconds.

#### Variations Model

The TD data has been analyzed by a rather simple yet elegant model:

$$\hat{Z} = \hat{A} \times \begin{bmatrix} \Delta TD \\ \hat{C} \end{bmatrix} + \hat{\epsilon} \quad (3-1)$$

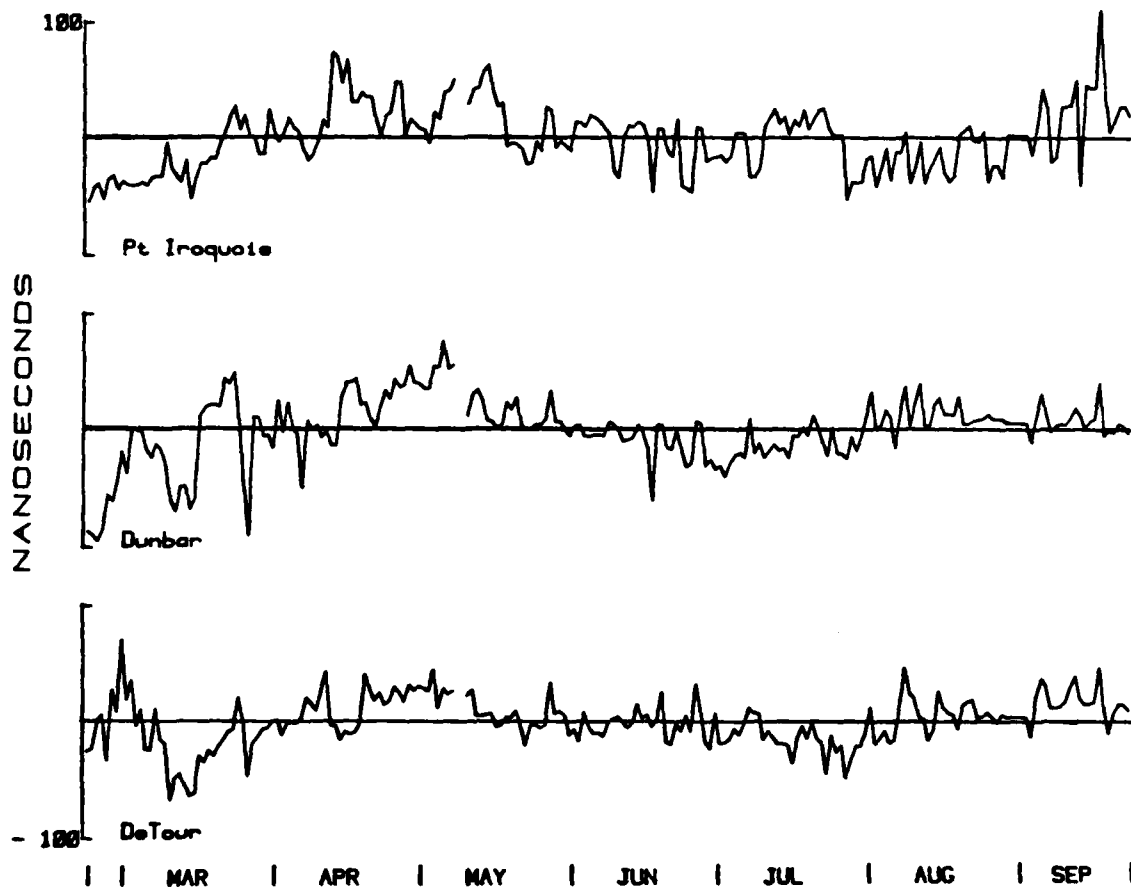


FIGURE 3-5. MASTER-ZULU MIDDAY TIME DIFFERENCE VARIATIONS

where  $Z$  is the observation matrix containing the three TD records at each of the three monitor sites,  $A$  is the transformation or geometry matrix describing the position of each site with respect to the baselines and the control station,  $\Delta TD$  is a uniform change in propagation velocity,  $C$  is the common error matrix containing variations seen only by and corrected by the control station; and  $\epsilon$  is the matrix containing local errors, unique to each site. The common variations are erroneous in the sense that no other site detected the changes that were compensated by the resulting transmitter timing adjustments. Any non-uniform propagation effects will be included in the local error terms. The least squares solution to the model is:

$$\begin{bmatrix} \Delta TD \\ \hat{C} \end{bmatrix} = \begin{bmatrix} \hat{A}^T \hat{A} \end{bmatrix}^{-1} \hat{A}^T \hat{Z} \quad (3-2)$$



TABLE 3-1. COMMON CONTROL ERRORS

	Nanoseconds (RMS)		
	C <sub>x</sub>	C <sub>y</sub>	C <sub>z</sub>
22 Feb-8 May 1979	46	18	28
11 May-24 Sep 1979	7	7	6

TABLE 3-2. TYPICAL UNIFORM  
VELOCITY TIME DIFFERENCE  
CHANGES (NANOSECONDS)

	M-X	M-Y	M-Z
Gros Cap (North End)	40	-88	125
Six Mile Point (Near SAM)	-1	-2	9
DeTour Light (South End)	48	-95	132

Table 3-1 lists the common control errors extracted from the data for the periods before and after the chain reconfiguration and monitor station upgrade. Considerable improvement can be seen in the second set of numbers.

Figure 3-6 shows the uniform velocity of propagation effects extracted from the data, in units of nanoseconds per kilometer of difference distance (differential Master-Secondary distance of point of interest vs SAM). The propagation component is extracted as an estimate, based upon how each site would react to the postulated uniform propagation change. Such a change is expected to be primarily caused by temperature affecting the vertical lapse rate of the index of refraction<sup>8,9</sup>.

The peak-to-peak propagation velocity change extracted from the data to date is approximately two nanoseconds per kilometer. The corresponding time difference variations are obtained by multiplying the plotted values by the difference distances for each site. (The difference distance is zero for a site on the same hyperbolic TD line as the SAM and increases with distance from this line.) Typical values are listed in Table 3-2.

The uniform propagation changes are interesting in that they represent a fundamental performance limit in the system. The significant point is that the information provides a bound on a physical effect which cannot be improved upon through equipment or procedural changes at the SAM, but which might be improved with an "altimeter correction" applied within the user equipment.

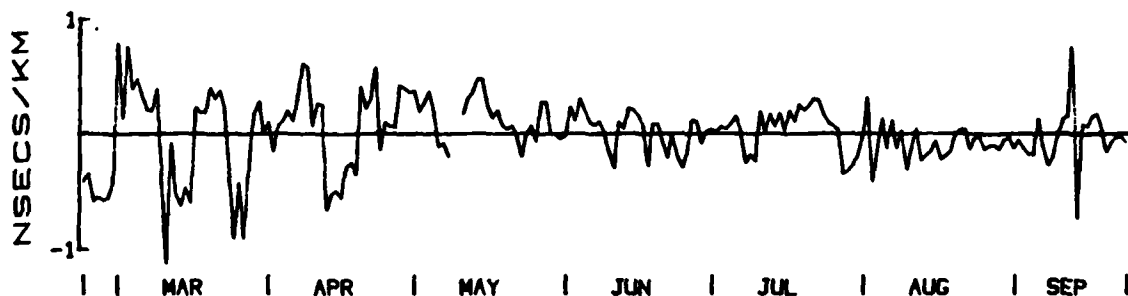


FIGURE 3-6. UNIFORM PROPAGATION VELOCITY CHANGES

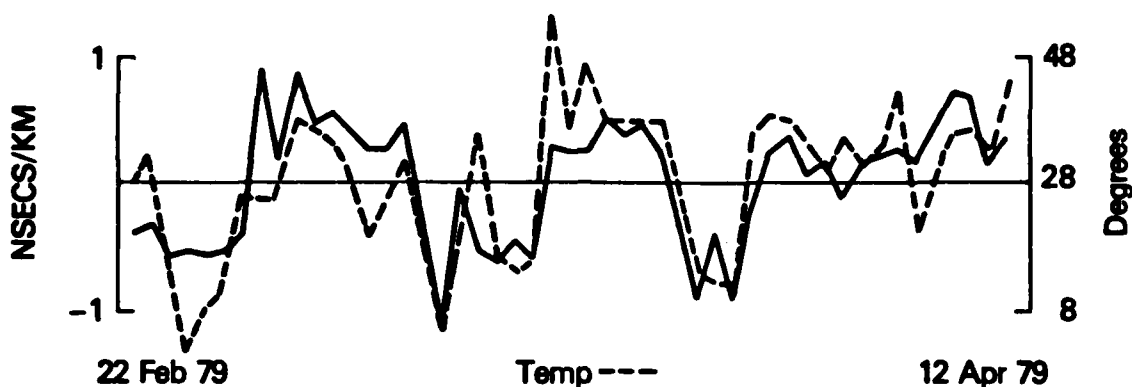


FIGURE 3-7. WINTER PROPAGATION VELOCITY CHANGES

Figure 3-7 shows the mid-February to mid-April propagation velocity changes, superimposed with a plot of temperature recorded at the SAM. The correlation coefficient for these plots is approximately 0.7. This relatively high correlation confirms the expected temperature dependency. The correlation diminishes rapidly during late April and early May, after which there is negligible correlation with temperature. This diminishing correlation is expected, since the temperature dependency of the vertical lapse rate is predominantly a winter effect.<sup>8,9</sup>

#### Error Budget Analysis

Knowing the nature and source of the grid variations is interesting, but of no immediate value to the user. However, having determined the expected TD fluctuations, it is now possible to calculate the positioning errors that would result. Figure 3-8 is the plot of an error budget analysis for a series of points along the St. Marys River. A user's time difference error has been allocated to three sources:

1. Uniform Propagation Velocity Changes. The maximum variation experienced to date (two nanoseconds per kilometer of baseline length) is used, recognizing that the river might be surveyed during one extreme and navigated during the opposite extreme. The narrower portions of the navigation channel are nearer the SAM and will experience the smallest variations, as can be seen from Table 3-2.

2. Control Errors. The "erroneous" control station adjustments are applied as normally distributed random numbers with a zero mean and a standard deviation equal to the smaller RMS values from Table 3-1.

3. Receiver Offsets. Assuming the use of a survey-quality receiver, 15 nanoseconds is allowed for the offset between a user's receiver and the calibration receiver which surveyed the river. The sign of the offset is allowed to vary randomly for each of the three TDs.

Radial error values are determined by computing a minimum variance three-TD "fix" according to the "G-Matrix" algorithm developed in Appendix B. The 99 percent curve was determined by running a Monte Carlo simulation and plotting the resulting probability histogram. Also plotted is the halfwidth of the navigation channel. It can

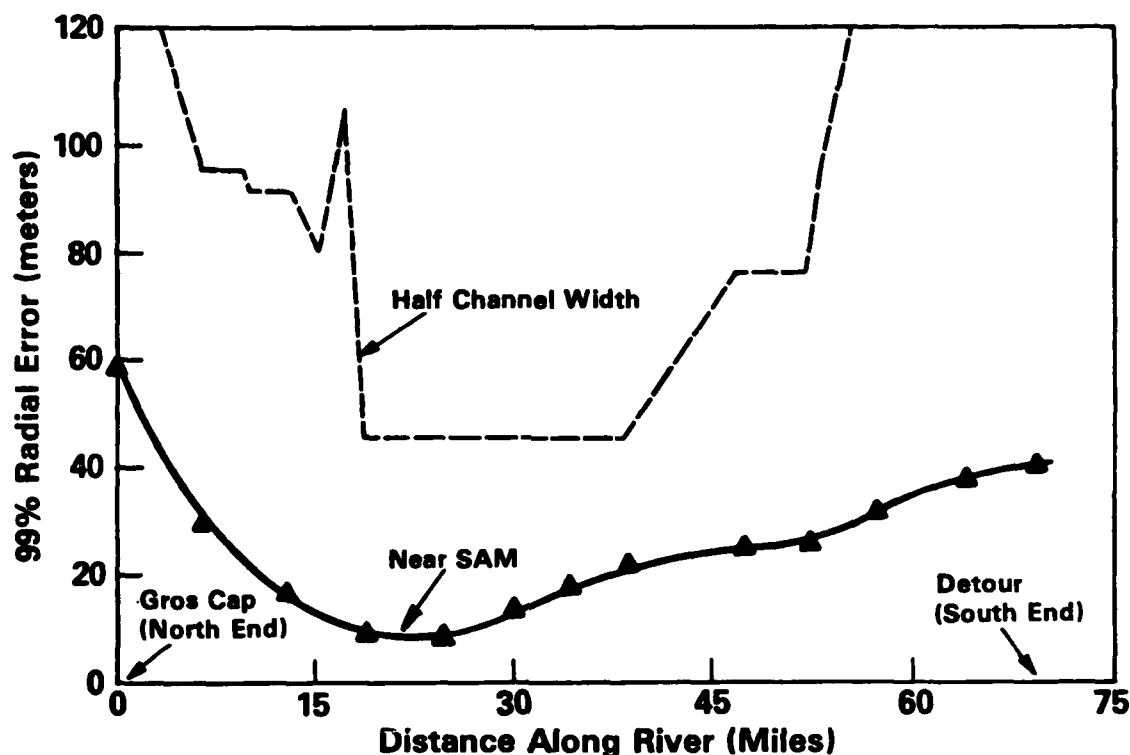


FIGURE 3-8. ERROR BUDGET ANALYSIS

be seen that the 99 percent error is well within this half-channel distance for the entire river. This makes an interesting comparison, but the intent is not to imply that the half-channel width is an acceptable error in a radionavigation system. Allowances must also be made for navigation error and the half-width of the user's vessel (up to 16 meters).

#### HARBOR MONITOR PROGRAM

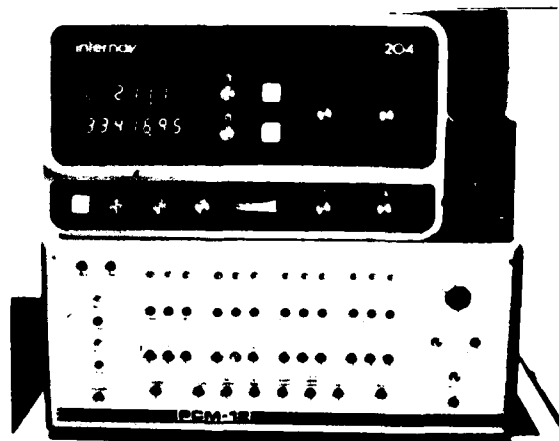
The Office of Research and Development is responsible for evaluating the effectiveness of the Loran-C system in providing the accuracy necessary to serve as a reliable, all-weather radio aid within the HHE environment. The desired technical approach is to extract the inherent accuracy of the system through improved understanding of the bounding physical elements. This understanding will be developed through analysis, model development, testing and verification.

The objective of the Harbor Monitor Program is to characterize the stability of the existing grid in the HHE areas of the United States. Quantification of the year-round temporal variations is required as input to an error budget analysis for each HHE area of interest.

Several sets of equipment have been developed previously for monitoring the operation of both the West Coast chain and the St. Marys River mini-chain. The Coast Guard Research and Development Center has constructed a prototype monitor system (Figure

3-9) consisting of hardware and software to allow remote dial-up access to the daily System Samples. These prototypes are presently deployed at the St. Marys River monitor sites.

Improved versions of the remote monitoring hardware will be installed in each harbor area studied. Up to ten sets will be installed during 1980. Two monitoring sites should be sufficient to characterize the grid stability in most regions. Boston Harbor, the Delaware Bay and the Chesapeake Bay have been chosen for the first installations.



## CONCLUSIONS

FIGURE 3-9. HARBOR MONITOR SYSTEM

The preliminary results have established that the grid is reasonably stable, and that earlier reports showing much larger variations were apparently incorrect.

An analysis of the data has revealed a limiting physical effect in the form of changes in the velocity of propagation, uniform throughout the chain. These propagation changes have been as large as 130 nanoseconds at the ends of the river, but are much smaller near the control station.

An error budget analysis has projected three-TD fixes that are well within the half-width of the river's navigation channels. However, the addition of navigation error and the half-width of a typical vessel preclude making the implication that the mini-chain is capable of providing safe electronic-only navigation in every section of the St. Marys River at all times.

## PROGNOSIS AND FUTURE EFFORTS

The mini-chain stability study has recently been completed (May 1980), and analysis of the additional data collected since September 1979 should enable a definitive judgement to be made on the navigation capabilities of the St. Marys River mini-chain.

The geometry of the Great Lakes Loran-C chain is excellent in the St. Marys River area. Consideration is being given to providing precision coverage of the river by supplementing the long-baseline chain with a single mini-Loran-C station — a much more cost effective approach — in lieu of providing an entire mini-chain. Present plans call for terminating the mini-chain concept after the St. Marys River is closed to navigation for the 1980-1981 winter season. The Gordon Lake station will then be brought on-air as a low-powered secondary on the Great Lakes rate (8970). A new experiment will be developed to verify the validity of this augmented coverage concept. Data collection for this new experiment was started on the Great Lakes chain at several of the St. Marys River monitor sites during the 1979-1980 winter season, and was recently expanded to include all sites.

S2R-78-307  
ZT70S2R0  
December 6, 1978

TO: J. G. Wall

FROM: L. J. Levy

SUBJECT: Definition of G Matrix Analysis for USCG LORAN-C  
HHE Navigation Program

REFERENCES: 1) APL/JHU Technical Program Plan for the USCG  
LORAN-C Harbor-Estuary Navigation Program,  
Enclosure (1) of AD-7599

2) LORAN-C HHE Navigator, Handwritten Notes by  
Cmdr. Don Feldman, USCG

The program plan for the USCG LORAN-C Harbor-Harbor-Entrance (HHE) Navigator program in Ref. 1 states that APL is to "Perform the 'G' matrix analysis...". Based on discussions with Lt.Cdr. Dan Garrison, USCG, discussions with the USCG at the December 4 meeting, and the notes in Ref. 2, the G matrix analysis to be performed by APL can now be defined.

The objective of the G matrix study is to recommend to the USCG an algorithm to calculate the G matrix under the following three conditions:

a) 2TD Case

Given the location of the master, two slave stations, and a surveyed point, calculate the unique G matrix for that surveyed point.

b) 3TD, Weighting Vector Case

Given the location of the master, 3 slave stations, and a surveyed point and a set of TD weighting parameters, reflecting the confidence in each TD, calculate a G matrix for that surveyed point using a weighted-least-squares criterion on the TD residual.

c) 3TD Statistical Minimization Case


Given the location of the master, 3 slave stations, and a surveyed point, calculate the G matrix for that surveyed point such that the statistical mean square error in estimating X and Y is minimized. It is to be assumed that the noise level into the LORAN receivers is equal and Gaussian. APL will provide an algorithm for computing the required TD error covariance matrix to be primarily based upon calculated signal strength and assumed background noise considerations.

Additionally, it is assumed that:

- 1) All G matrices will transform TDs in units of nano-seconds to position in the X-Y coordinate system in units of yards.
- 2) Since it was agreed that the generation, tape storage, and use of new G matrix coefficients could be easily accomplished for each waypoint, no linearity analysis or sensitivity analysis need be performed over tracklines not including the waypoint used in the calculation of a particular G matrix. Only a linearity analysis over the adjacent tracklines will be performed to determine if an additional waypoint, with associated new G coefficient, is needed.
- 3) APL will also provide to the USCG an algorithm to evaluate linearity and an algorithm to evaluate the covariance performance.
- 4) A limited amount of covariance performance analysis will be done for each case to show the utility of the covariance analysis algorithm.
- 5) A Geometrical Dilution of Precision (GDOP) number will be calculated for each waypoint.
- 6) The algorithms presented to the USCG will be in standard mathematical equation form. Non optimized coding of these algorithms may be supplied if requested by the USCG.
- 7) Grid warpage will be controlled by insertion of additional trackpoints to be determined by the USCG. Decisions as to the choice of G matrix algorithm is the responsibility of the USCG.

The APL report, recommending the algorithms for the three above cases, plus providing the associated linearity and covariance

analysis algorithms will be submitted to the USCG by January 15, 1979. A follow-on report providing the linearity analysis of item (2), the limited covariance performance analysis of item (4), and the GDOP analysis of item (5) will be provided to the USCG by February 30, 1979.

  
\_\_\_\_\_  
L. J. Levy

LJL:nt  
Distribution  
GEBaer  
CREdwards  
LJLevy  
TThompson  
JGWall  
Archives  
S2R File

S2R-79-008  
ZT70S2R0  
January 19, 1979

TO: J. G. Wall

FROM: L. J. Levy/V. Schwab

SUBJECT: G Matrix Analysis for USCG Loran-C HHE Navigation Program

REFERENCES: 1) Loran-C HHE Navigator, Handwritten Notes by Cmdr Don Feldman, USCG

2) Definition of G Matrix Analysis for USCG Loran-C HHE Navigation Program, S2R-78-307, by L. J. Levy, December 6, 1978

3) C-LAD - A Low Cost Loran-C Assist Device; Vol II - Software, L. M. Marshall, C. R. Edwards, APL/JHU CP034B, June 1974

#### INTRODUCTION

The G Matrix technique, as defined in Reference 1, is essentially a method for converting 2 or more measured TDs into horizontal navigator position. It yields a linear estimate referenced to the surveyed values of a "near" waypoint or track point as

$$\hat{\underline{Z}}_Q = \underline{Z}_P + G \left[ \underline{TD}_Q - \underline{TD}_P \right] \quad (1)$$

where

- $\underline{Z}_P$  ~ surveyed position vector of point P, a nearby TP (track point) or WP (waypoint)
- $\hat{\underline{Z}}_Q$  ~ estimate of receiver position vector at point Q
- $\underline{TD}_P$  ~ vector of surveyed time differences at point P
- $\underline{TD}_Q$  ~ vector of measured time differences from receiver at point Q



G ~ G matrix which transforms the vector TD residual into vector position residual in some optimal fashion

In general, the G matrix is a function of the surveyed position of the WP or TP, surveyed position of the master and slave stations, an assumed estimation error minimization criterion, and possibly of the expected relative error characteristics or quality factors of  $\underline{TD}_Q$ . Its validity is based upon the assumption that the residual TD vector (measured TD vector minus the surveyed TD vector) is linearly related to the position residual (position of navigator minus surveyed position of the WP or TP).

The significance of the G matrix technique is that the G matrix can be precomputed for each WP or TP, thereby significantly reducing the amount of real time computation of the navigator in transforming measured TDs into navigator position.

The objective of the G matrix analysis is to recommend to the USCG the algorithms to calculate the G matrix under the three conditions specified in Reference 2. This report will present these recommended algorithms along with the associated covariance and linearity analysis algorithms.

### 1. General G Matrix Solution

This section will define the navigation problem and present the general G matrix solution. Given an m-vector of measured TDs,  $\underline{TD}_Q$ , at navigator position Q; the corresponding vector of surveyed TDs,  $\underline{TD}_P$ , for a nearby point P; and the surveyed position 2-vector,  $\underline{Z}_P$ , of the nearby point P; determine the position of the navigator. From Appendices B and C, it is shown that when point Q is sufficiently near point P,

$$u = A\bar{x} + e \quad (2)$$

where  $A$  is a function of the positions of the master, slaves, and the surveyed point  $P$ ,

$$u = \frac{TD}{Q} - \frac{TD}{P} \quad (3)$$

$$\bar{x} = \frac{z}{Q} - \frac{z}{P} \quad (4)$$

and  $e$  is the  $m$ -vector of TD measurement errors at point  $Q$ . Since  $\frac{z}{P}$  is known, then an estimate of  $x$ ,  $\hat{x}$ , will yield an estimate of  $\frac{z}{Q}$ ,  $\hat{z}_Q$ , by

$$\hat{x} = \hat{z}_Q - \frac{z}{P} \quad (5)$$

As shown in Appendix A, the general form of the estimate of  $\bar{x}$  is given by

$$\hat{x} = G u \quad (6)$$

where

$$G = (A^T W A)^{-1} A^T W \quad (7)$$

For the 2 TD case,  $m=2$ , the  $G$  matrix reduces to

$$G = A^{-1} \quad (8)$$

Otherwise, the specific value of the  $G$  matrix is dependent upon the weighting matrix,  $W$ . If  $W=I$ , the measurements are equally weighted and Eqs. (6) and (7) yield the standard least squares estimate of  $\bar{x}$ . For a general  $W$ , we have a weighted least squares estimate. For  $W=R^{-1}$ , where  $R$  is the covariance of  $e$ , we have the minimum variance estimate.

Combining Eqs. (3), (5), and (6) we obtain the desired result of estimating the navigator position at point Q via Eq. (1).

## 2. Specific Algorithm for the 2 TD Case

Given the location of the master station,  $(x_m, y_m)$ ; the slave stations,  $(x_{sj}, y_{sj})$ ,  $j=1,2,3$ ; and the surveyed position of the WP or TP,  $(x_p, y_p)$ ; calculate the unique G matrix for each 2 TD case. Here  $(x, y)$  are the components in the planar coordinate frame.\* (For the St. Marys River system the coordinate center (i.e., point of tangency) is at the Loran monitor station ( $46^\circ 28.1244'$  N,  $84^\circ 17.9343'$  W)). At the coordinate center  $x$  is east and  $y$  is north. For the 2 TD case, G is given by

$$G(i, j) = \begin{bmatrix} g_{xi} & g_{xj} \\ g_{yi} & g_{yj} \end{bmatrix} \quad (9)$$

where  $g_{\alpha k}$  transforms the  $k^{\text{th}}$  station TD ( $k=i, j$ ) into the  $\alpha$  position coordinate ( $\alpha=x, y$ ). The  $G(i, j)$  matrix transforms the  $i$  and  $j$  station TDs into the  $x$  and  $y$  position estimates. Now from Appendix B,

$$r_1 = \sqrt{(x_p - x_m)^2 + (y_p - y_m)^2} \quad (10)$$

$$r_{2j} = \sqrt{(x_p - x_{sj})^2 + (y_p - y_{sj})^2} ; j = 1, 2, 3 \quad (11)$$

where  $r_1$  is the slant range from the surveyed point P to the master station,  $r_{2j}$  is the slant range from the surveyed point P to the  $j^{\text{th}}$  slave station. The gradient matrix values are

---

\* Planar coordinate frame defined in Reference 3, pp. 30-35, 141-144;  $x = \rho \sin \Psi$ ,  $y = \rho \cos \Psi$ , where  $\rho$ =geodetic arc length from origin to desired point,  $\Psi$ =heading angle of geodetic arc.

$$a_{jx} = \frac{1}{v} \left\{ \frac{x_p - x_{sj}}{r_{2j}} - \frac{x_p - x_m}{r_1} \right\}; j = 1, 2, 3 \quad (12)$$

$$a_{jy} = \frac{1}{v} \left\{ \frac{y_p - y_{sj}}{r_{2j}} - \frac{y_p - y_m}{r_1} \right\}; j = 1, 2, 3 \quad (13)$$

where

$a_{jx}$  is the derivative of the  $j^{\text{th}}$  TD with respect to  $x_p$ ,

$a_{jy}$  is the derivative of the  $j^{\text{th}}$  TD with respect to  $y_p$ ,

and

$v$  is the propagation velocity.

Then

$$\left. \begin{aligned} \Delta(i,j) &= a_{ix} a_{jy} - a_{iy} a_{jx} \\ &\text{for } i=1 \ j=2, \ i=1 \ j=3, \ i=2 \ j=3 \end{aligned} \right\} \quad (14)$$

and for  $G(i,j)$

$$\left. \begin{aligned} g_{xi} &= a_{jy} / \Delta(i,j) \\ g_{xj} &= -a_{iy} / \Delta(i,j) \\ g_{yi} &= -a_{jx} / \Delta(i,j) \\ g_{yj} &= a_{ix} / \Delta(i,j) \end{aligned} \right\} \quad \begin{aligned} &\text{for } i=1 \ j=2 \\ &\quad \quad i=1 \ j=3 \\ &\quad \quad i=2 \ j=3 \end{aligned} \quad (15)$$

Thus, 3 separate and distinct G matrices are possible for the 2 TD case. Note, for instance, that  $g_{x1}$  in  $G(1,2)$  does not equal  $g_{x1}$  in  $G(1,3)$ . Finally, note that if  $x$  and  $y$  are in units of yards,  $v$  in units of yards/nanoseconds, then the elements of the G matrix are in units of yards/nanoseconds. Equations (9) through (15)

comprise the recommended algorithm for calculating the three G matrices for the 2 TD case.

### 3. Specific Algorithm for the 3 TD, Weighting Vector Case

Given the location of the master, 3 slave stations, a surveyed position at point P, and a set of TD weighting parameters,

$$\bar{W} = \begin{bmatrix} w_1 \\ w_2 \\ w_3 \end{bmatrix} \quad (16)$$

reflecting the confidence (i.e., large  $w_i$  implies high confidence in the  $i^{\text{th}}$  TD) in each TD, calculate the G matrix for the surveyed point P using a weighted-least-squares criterion.

First of all, it must be noted that the weighting parameters do not need to be normalized (i.e.,  $w_1 + w_2 + w_3 = 1$ ) although it may be meaningful from an interpretation standpoint. This can be seen by substituting  $\alpha W$  for  $W$  in Eq. (7) where  $\alpha$  is a scalar. The value of G remains the same.

For this case we set the weighting matrix by

$$W = \begin{bmatrix} w_1 & 0 & 0 \\ 0 & w_2 & 0 \\ 0 & 0 & w_3 \end{bmatrix} \quad (17)$$

We see by Appendix A that this will result in weighting the square of each TD residual according to our respective confidence in each TD in the weighted-squared-residuals function that is minimized.

The resulting least squares estimate is given by the G matrix in Eq. (7) using Eq. (17). The specific result using Eq. (17) in Appendix C and taking into account the zeroes in W,

$$b_{xj} = a_{jx} w_j \quad j=1,2,3 \quad (18)$$

$$b_{yi} = a_{jy} w_j \quad j=1,2,3 \quad (19)$$

$$\left. \begin{aligned} c_{xx} &= \sum_{j=1}^3 b_{xj} a_{jx} \\ c_{xy} &= \sum_{j=1}^3 b_{xj} a_{jy} \\ c_{yx} &= \sum_{j=1}^3 b_{yj} a_{jx} = c_{xy} \\ c_{yy} &= \sum_{j=1}^3 b_{yj} a_{jy} \\ \Delta &= c_{yy} c_{xx} - c_{xy}^2 \end{aligned} \right\} \quad (20)$$

$$\left. \begin{aligned} c_{xx}^{-1} &= c_{yy} / \Delta \\ c_{xy}^{-1} &= -c_{xy} / \Delta \\ c_{yx}^{-1} &= c_{xy}^{-1} \\ c_{yy}^{-1} &= c_{xx} / \Delta \end{aligned} \right\} \quad (21)$$

then

$$\left. \begin{aligned} g_{xj} &= c_{xx}^{-1} b_{xj} + c_{xy}^{-1} b_{yj} \\ g_{yj} &= c_{yx}^{-1} b_{xj} + c_{yy}^{-1} b_{yj} \end{aligned} \right\} \quad j=1,2,3 \quad (22)$$

Note that the  $a_{jx}$ ,  $a_{jy}$ ,  $g_{xj}$ , and  $g_{yj}$  are defined in Section 2. The resulting G matrix for this case is

$$G(1,2,3) = \begin{bmatrix} g_{x1} & g_{x2} & g_{x3} \\ g_{y1} & g_{y2} & g_{y3} \end{bmatrix} \quad (23)$$

Equations (10)-(13), (18)-(23) comprise the recommended algorithm for calculating the G matrix for the 3 TD weighting vector case.

#### 4. Specific Algorithm for the 3 TD Statistical Minimization Case

Given the location of the master, 3 slave stations, and a surveyed point P, calculate the G matrix for that point such that the variance of the error in estimating the navigator position is minimized. It is to be assumed that the noise into the 4 tracking loops, measuring receipt times of the 3 slave and master pulses, are equal and Gaussian.

From Appendix A, the minimum variance criterion results in setting  $W=R^{-1}$  in Eq. (7). An accurate determination of R requires specific knowledge of the signal-to-noise ratios at the receiver antennae (which are receiver configuration independent), and many additional parameters that are specific to the receiver configuration. Thus, each different receiver configuration would require a detailed error analysis to ultimately yield a specific G matrix. We believe this to be impractical and will strive to obtain a G matrix for this case that is configuration independent.

The constraint that the noise into the 4 tracking loops are equal can be justified under the following assumptions:

- a) The dominant noise into the tracking loop is external noise (receiver noise is negligible).
- b) RF receiver input bandwidths are equal (if the RF gain from antenna input to the tracking loop differs between receivers, the signal-to-noise ratios for the external noise remain the same, yielding the same relative noise performance between receivers).

Also, it is assumed that the relative noise performance between tracking filters from the tracker filter input to the input to the G matrix transformation remains invariant. This can be satisfied if:

- 1) all tracking filters are equal,
- 2) quantization noise in the counting process is negligible,
- 3) any further smoothing beyond the counting process is equivalent between receivers.

Under assumptions (a)-(c), (1)-(3), the G matrix is receiver configuration invariant and dependent only on the effective transmitted power of each slave station,  $P_i$ ,  $i=1,2,3$ , the effective transmitted power of the master station, and the slant ranges,  $r_{2j}$ ;  $j=1,2,3$  and  $r_1$ . From Appendix D, the calculation is

$$\left. \begin{aligned} R_{ii} &= k_1 \left( \frac{r_{2i}^2}{P_i} + \frac{r_1^2}{P_m} \right) ; \quad i=1,2,3 \\ R_{ij} &= k_1 \left( \frac{r_1^2}{P_m} \right) \quad i \neq j \end{aligned} \right\} \quad (24)$$

where  $k_1$  is arbitrarily set so that the above elements of R are roughly around unity. (It is shown in Appendix D that only the relative values of  $R_{ij}$  will affect the G matrix.)



Then

$$R^{-1} = \begin{bmatrix} R_{11}^{-1} & R_{12}^{-1} & R_{13}^{-1} \\ R_{12}^{-1} & R_{22}^{-1} & R_{23}^{-1} \\ R_{13}^{-1} & R_{23}^{-1} & R_{33}^{-1} \end{bmatrix} \quad (25)$$

with

$$\left. \begin{aligned} \Delta &= R_{11}R_{22}R_{33} + 2 R_{12}R_{23}R_{13} \\ &\quad - R_{13}^2 R_{22} - R_{12}^2 R_{33} - R_{11}R_{23}^2 \\ R_{11}^{-1} &= (R_{22}R_{33} - R_{23}^2)/\Delta \\ R_{12}^{-1} &= (R_{13}R_{23} - R_{33}R_{12})/\Delta = R_{21}^{-1} \\ R_{13}^{-1} &= (R_{12}R_{23} - R_{22}R_{13})/\Delta = R_{31}^{-1} \\ R_{22}^{-1} &= (R_{11}R_{33} - R_{13}^2)/\Delta \\ R_{23}^{-1} &= (R_{12}R_{13} - R_{11}R_{23})/\Delta = R_{32}^{-1} \\ R_{33}^{-1} &= (R_{11}R_{22} - R_{12}^2)/\Delta \end{aligned} \right\} \quad (26)$$

From Appendix C, substituting  $M=R^{-1}$ ,

$$\left. \begin{aligned} b_{xj} &= \sum_{i=1}^3 a_{ix} R_{ij}^{-1} ; j = 1, 2, 3 \\ b_{yj} &= \sum_{i=1}^3 a_{iy} R_{ij}^{-1} ; j = 1, 2, 3 \end{aligned} \right\} \quad (27)$$

The rest of the required equations are given by Eqs. (20)-(23).

Equations (10)-(13), (24), (26), (27), (20)-(23) comprise the recommended algorithm for calculating the G matrix for the case considered in this section.

##### 5. Linearity and Covariance Analysis Algorithms

From Appendix A, the general form of the error covariance is  $C = GRG^T$ , where G is any G matrix of the form in Eq. (7) with any W, and R is the actual covariance of TD measurement error vector (not necessarily the R matrix computed in Section 4). Define

$$\tilde{\Delta x} = \hat{x}_Q - x_Q$$

$$\tilde{\Delta y} = \hat{y}_Q - y_Q$$

then

$$C \equiv \begin{bmatrix} \langle \tilde{\Delta x}^2 \rangle & \langle \tilde{\Delta x} \tilde{\Delta y} \rangle \\ \langle \tilde{\Delta x} \tilde{\Delta y} \rangle & \langle \tilde{\Delta y}^2 \rangle \end{bmatrix}$$

For

$$R(i,j) = \begin{bmatrix} R_{ii} & R_{ij} \\ R_{ij} & R_{jj} \end{bmatrix}$$

with  $G(i,j)$  given by Eq. (9), then

$$C(i,j) = G(i,j)R(i,j)G(i,j)^T \quad (28)$$

for any pair of TDs,  $i,j$ .

For any 3 TD case, set

$$R = \begin{bmatrix} R_{11} & R_{12} & R_{13} \\ R_{12} & R_{22} & R_{23} \\ R_{13} & R_{23} & R_{33} \end{bmatrix}$$

with  $G$  given by Eq. (23), then  $C = GRG^T$ .

The linearity of  $G$ , generated for surveyed point  $P$ , is evaluated at point  $Q$  as follows:

- 1) Use  $G_p$  computed for particular 2 TD case, along with surveyed TDs at point  $Q$  and point  $P$ , and surveyed position,  $\underline{z}_p$ , in Eq. (1) to get  $\hat{\underline{z}}_Q$ .
- 2) Linearity error at point  $Q$  relative to point  $P$  is given by differencing the surveyed position  $\underline{z}_Q$  with  $\hat{\underline{z}}_Q$ .
- 3) Repeat steps (1) and (2) for each 2 TD case and single 3 TD case.

L. V. Levy  
L. V. Levy

V. Schwab  
V. Schwab

LJL/VS:nt

## Appendix A

### LINEAR ESTIMATION

(Derivations of Formulae Due to S. T. Haywood)

A set of  $m$  linear equations in  $n \leq m$  unknowns will be represented by

$$(A.1) \quad u = A\bar{x} + e$$

in which we define:

- A     $m \times n$  matrix of rank  $n$
- e     $n \times 1$  noise vector
- $\bar{x}$     $m \times 1$  vector of true values of the state variables
- u     $n \times 1$  vector of observations or measurements

In (A.1)  $u$  and  $A$  are presumed known;  $e$  and  $\bar{x}$  are unknowns.

The problem to be considered next is that of obtaining an estimate of  $\bar{x}$ . Let

$$(A.2) \quad d = Ax - u$$

where

- d     $n \times 1$  vector of residuals
- x     $m \times 1$  vector representing an estimate of  $\bar{x}$

In classical least squares estimation an estimate of  $x$  is obtained which minimizes the scalar

$$d^T d = |d|^2 = \delta_1^2 + \delta_2^2 + \dots + \delta_n^2.$$

We shall now derive the weighted least squares estimate of  $\bar{x}$  which minimizes  $d^T W d$ , where  $W = W^T > 0$  is the weighting matrix. Ordinary least squares estimate will be obtained as the special case,  $W = I$ .

From (A.2) we obtain

$$\begin{aligned} d^T W d &= (Ax - u)^T W (Ax - u) = (x^T A^T - u^T) W (Ax - u) \\ &= x^T A^T W A x - x^T A^T W u - u^T W A x + u^T W u \\ &= x^T (A^T W A) x + u^T W u - x^T A^T W u - u^T W A x \\ &= x^T (A^T W A) x + u^T W u - 2x^T A^T W u \end{aligned}$$

Let  $s = s(x) = d^T W d$ . Then  $s(x+h) = (d + Ah)^T W (d + Ah)$  and

$$\begin{aligned} s(\hat{x} + h) - s(\hat{x}) &= d^T W d + h^T A^T W d + d^T W A h + h^T A^T W A h - d^T W d \\ &= h^T A^T W A h + 2h^T (A^T W A \hat{x} - A^T W u) \end{aligned}$$

The first term on the right above is always non-negative. The second term vanishes if

$$(A.3) \quad \hat{x} = (A^T W A)^{-1} A^T W u$$

Thus if  $\hat{x}$  has the value given by (A.3)  $s(\hat{x} + h) - s(\hat{x}) \geq 0$  for any  $m \times 1$  vector  $h$ . Therefore  $\hat{x}$  is the desired weighted least squares estimate of  $\bar{x}$ . The ordinary (unweighted) least squares solution is given by

$$(A.4) \quad \hat{x} = (A^T A)^{-1} A^T u.$$

We next consider the statistical properties of the noise vector  $e$  which enters into the determination of the covariance matrix associated with the error in the estimate of  $x$ . We shall assume  $\langle e \rangle = 0$  and  $\langle ee^T \rangle = R > 0$ . In other words, we assume the noise in the measurements has zero mean and covariance matrix denoted by  $R$ .

Now, from (A.3),

$$\begin{aligned}\hat{x} &= (A^T W A)^{-1} A^T W u = (A^T W A)^{-1} A^T W A \bar{x} - (A^T W A)^{-1} A^T W e \\ &= \bar{x} - (A^T W A)^{-1} A^T W e.\end{aligned}$$

Therefore

$$(A.5) \quad \langle \hat{x} \rangle = \bar{x}.$$

Equation (A.5) asserts that  $\hat{x}$  is an unbiased estimate of  $\bar{x}$ .

The covariance matrix of the error in the estimate  $\hat{x}$  is denoted by  $C$  and given by

$$(A.6) \quad C = \langle (\hat{x} - \bar{x})(\hat{x} - \bar{x})^T \rangle = (A^T W A)^{-1} A^T W R W A (A^T W A)^{-1}.$$

We next consider the problem of finding the estimate  $\hat{x}$  which makes  $C$  a minimum.

$$\text{Let} \quad \hat{x} = Bu = BA\bar{x} + Be$$

$$\text{Then} \quad \langle \hat{x} \rangle = B\langle u \rangle = BA\bar{x} = \bar{x}$$

$$\text{Therefore} \quad BA = I$$

$$\hat{x} - \bar{x} = Bu - \bar{x} = BA\bar{x} + Be - \bar{x} = Be$$

$$C = C(B) = \langle (\hat{x} - \bar{x})(\hat{x} - \bar{x})^T \rangle = BRB^T$$

Next, let H be any matrix having the same dimensions as B. Then

$$I = (B+H)A = I + HA$$

$$\text{Therefore } HA = 0$$

$$\begin{aligned} \text{Then } C(B+H) - C(B) &= (B+H)R(B^T+H^T) - BRB^T \\ &= BRB^T + BRH^T + HRB^T + HRH^T - BRB^T \\ &= HRH^T + BRH^T + HRB^T \end{aligned}$$

$$\text{Let } B = MA^T R^{-1}$$

$$\begin{aligned} \text{Then } BRH^T + HRB^T &= MA^T R^{-1} R H^T + H R R^{-1} A M^T \\ &= MA^T H^T + HAM^T \end{aligned}$$

$$\text{Since } HA = 0, C(B+H) - C(B) = HRH^T \geq 0$$

$$I = BA = MA^T R^{-1} A$$

$$\text{Therefore } M = (A^T R^{-1} A)^{-1}$$

$$\text{Therefore } B = (A^T R^{-1} A)^{-1} A^T R^{-1}$$

and, the estimate,  $\hat{x}$ , which minimizes C is given by

$$(A.7) \quad \hat{x} = (A^T R^{-1} A)^{-1} A^T R^{-1} u.$$

The minimized covariance matrix is given by

$$(A.8) \quad C_{\min} = (A^T R^{-1} A)^{-1}$$

The estimate given by (A.7) is known as the minimum variance estimate. It may be noted that the minimum variance estimate is obtained as the weighted least squares estimate when  $W = R^{-1}$ .

The general expression for the covariance matrix  $C$  is given by

$$(A.9) \quad C = BRB^T$$

in which  $B$  can be any  $n \times m$  matrix of the form

$$B = (A^T W A)^{-1} A^T W$$

In the special case where  $m=n$  (number of equations equal to number of unknowns) and the matrix  $A$  in (A.3) and (A.4) is invertible, then

$$(A^T W A)^{-1} A^T W = A^{-1} (A^T W)^{-1} (A^T W) = A^{-1}$$

Accordingly (A.3) and (A.4) reduce to

$$(A.10) \quad \hat{x} = A^{-1} u$$

and (A.9) reduces to

$$(A.11) \quad C = A^{-1} R (A^{-1})^T$$

when  $m=n$ .



Appendix B

2 TD Case

In Fig. B-1 the master station is at M, a slave station at  $S_j$  and an arbitrary way point at P.

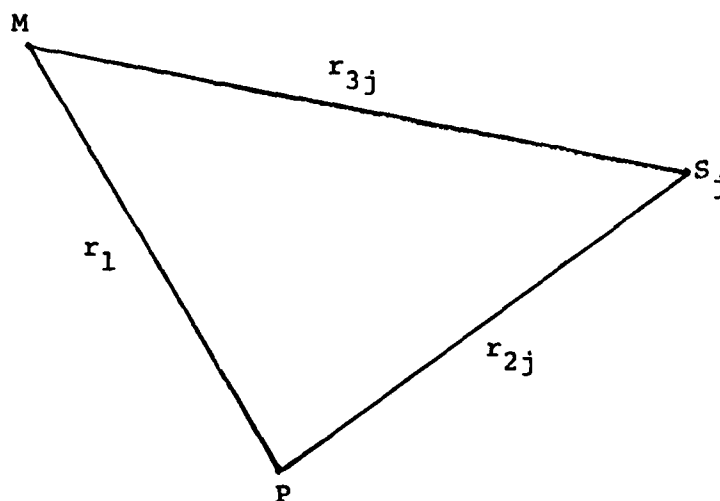


Fig. B-1

Since we are considering 2 slave stations the index  $j$  assumes the values 1 and 2.

The coordinates of M will be denoted by  $(x_m, y_m)$ ; P by  $(x_p, y_p)$ ;  $S_j$  by  $(x_{sj}, y_{sj})$ . The three slant ranges shown in Fig. B-1 are given by

$$(B.1) \quad \left[ \begin{array}{l} r_1 = \sqrt{(x_p - x_m)^2 + (y_p - y_m)^2} \\ r_{2j} = \sqrt{(x_p - x_{sj})^2 + (y_p - y_{sj})^2}, \quad j = 1, 2 \\ r_{3j} = \sqrt{(x_{sj} - x_m)^2 + (y_{sj} - y_m)^2}, \quad j = 1, 2 \end{array} \right]$$

The time differences in the signal receipt times at P are denoted by  $\tau_1$  and  $\tau_2$  and given by

$$(B.2) \quad \left[ \begin{array}{l} \tau_1 = (r_{31} + r_{21} - r_1)/v + \delta\tau_1 \\ \tau_2 = (r_{32} + r_{22} - r_1)/v + \delta\tau_2 \end{array} \right]$$

where the  $\delta\tau$ 's denote the absolute emission delays of the slave stations and  $v$  denotes the speed of signal propagation.

The derivatives of  $\tau_1$  and  $\tau_2$  with respect to  $x_p$  and  $y_p$  appear as elements in a 2x2 A-matrix. These are given in

$$(B.3) \quad \left\{ \begin{array}{l} a_{11} = \frac{d\tau_1}{dx_p} = \frac{1}{v} \left\{ \frac{x_p - x_{s1}}{r_{21}} - \frac{x_p - x_m}{r_1} \right\} \\ a_{12} = \frac{d\tau_1}{dy_p} = \frac{1}{v} \left\{ \frac{y_p - y_{s1}}{r_{21}} - \frac{y_p - y_m}{r_1} \right\} \\ a_{21} = \frac{d\tau_2}{dx_p} = \frac{1}{v} \left\{ \frac{x_p - x_{s2}}{r_{22}} - \frac{x_p - x_m}{r_1} \right\} \\ a_{22} = \frac{d\tau_2}{dy_p} = \frac{1}{v} \left\{ \frac{y_p - y_{s2}}{r_{22}} - \frac{y_p - y_m}{r_1} \right\} \end{array} \right.$$

Let  $\Delta x$  and  $\Delta y$  denote the coordinates of an arbitrary point Q (i.e., navigator) relative to the way point P as shown in Fig. B-2.

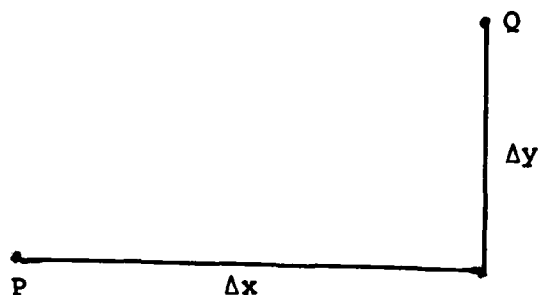


Fig. B-2

Then the time differences observed at Q can be expressed by

$$(B.4) \quad \begin{bmatrix} \tau_1 \\ \tau_2 \end{bmatrix}_Q = \begin{bmatrix} \tau_1 \\ \tau_2 \end{bmatrix}_P + \begin{bmatrix} a_{11} & a_{12} \\ a_{21} & a_{22} \end{bmatrix}_P \begin{bmatrix} \Delta x \\ \Delta y \end{bmatrix}_Q + \begin{bmatrix} \epsilon_1 \\ \epsilon_2 \end{bmatrix}_Q$$

in which  $\epsilon_1$  and  $\epsilon_2$  represent noise terms present in the observations of  $\tau_1$  and  $\tau_2$  made at Q.

In (B.4) let

$$u = \begin{bmatrix} \tau_1 \\ \tau_2 \end{bmatrix}_Q - \begin{bmatrix} \tau_1 \\ \tau_2 \end{bmatrix}_P = \begin{bmatrix} \tau_{1Q} - \tau_{1P} \\ \tau_{2Q} - \tau_{2P} \end{bmatrix}$$

$$A = \begin{bmatrix} a_{11} & a_{12} \\ a_{21} & a_{22} \end{bmatrix}$$

$$\hat{x} = \begin{bmatrix} \Delta x \\ \Delta y \end{bmatrix}$$

$$e = \begin{bmatrix} \epsilon_1 \\ \epsilon_2 \end{bmatrix}$$

Then (B.4) is seen to have the linear form

$$u = A\bar{x} + e$$

of Appendix A in which  $u$  and  $A$  are known and  $\bar{x}$  and  $e$  are unknowns.

In Appendix A it is shown that

$$(B.5) \quad \hat{x} = A^{-1}u$$

is the least squares estimate of  $\bar{x}$  when  $m=n=2$ ,

We shall next proceed to write explicit formulas for  $\Delta x$  and  $\Delta y$ . The  $G$  matrix is defined by

$$(B.6) \quad \hat{x} = Gu$$

Therefore,

$$(B.7) \quad G = A^{-1}$$

where

$$\Delta = a_{11}a_{22} - a_{12}a_{21}$$

$$a_{11}^{-1} = a_{22}/\Delta = g_{11}$$

$$a_{12}^{-1} = -a_{12}/\Delta = g_{12}$$

$$a_{21}^{-1} = -a_{21}/\Delta = g_{21}$$

$$a_{22}^{-1} = a_{11}/\Delta = g_{22}$$

and where

$$G \equiv \begin{bmatrix} g_{11} & g_{12} \\ g_{21} & g_{22} \end{bmatrix}$$

Therefore,

$$(B.8) \quad \begin{cases} \Delta x = g_{11}(\tau_{1Q} - \tau_{1P}) + g_{12}(\tau_{2Q} - \tau_{2P}) \\ \Delta y = g_{21}(\tau_{1Q} - \tau_{1P}) + g_{22}(\tau_{2Q} - \tau_{2P}) \end{cases}$$

## Appendix C

### 3 TD Case

(based on definitions and assumption stated in Appendix B)

In the case where 3 TD signals are employed the slant range equations are given in

$$(C.1) \quad \begin{cases} r_1 = \sqrt{(x_p - x_m)^2 + (y_p - y_m)^2} \\ r_{2j} = \sqrt{(x_p - x_{sj})^2 + (y_p - y_{sj})^2}, \quad j=1,2,3 \\ r_{3j} = \sqrt{(x_{sj} - x_m)^2 + (y_{sj} - y_m)^2}, \quad j=1,2,3 \end{cases}$$

The three time delays are

$$(C.2) \quad \tau_j = (r_{3j} + r_{2j} - r_1)/v + \delta\tau_j, \quad j=1,2,3$$

The six elements of the 3x2 A-matrix are

$$(C.3) \quad \begin{cases} a_{j1} = \frac{1}{v} \left[ \frac{x_p - x_{sj}}{r_{2j}} - \frac{x_p - x_m}{r_1} \right], \quad j=1,2,3 \\ a_{j2} = \frac{1}{v} \left[ \frac{y_p - y_{sj}}{r_{2j}} - \frac{y_p - y_m}{r_1} \right], \quad j=1,2,3 \end{cases}$$

The linear expansion of the three measured time differences made at an arbitrary point Q relative to a way station at P is given by

$$(C.4) \quad \begin{bmatrix} \tau_1 \\ \tau_2 \\ \tau_3 \end{bmatrix}_Q = \begin{bmatrix} \tau_1 \\ \tau_2 \\ \tau_3 \end{bmatrix}_P + \begin{bmatrix} a_{11} & a_{12} \\ a_{21} & a_{22} \\ a_{31} & a_{32} \end{bmatrix}_P \begin{bmatrix} \Delta x \\ \Delta y \end{bmatrix}_Q + \begin{bmatrix} \epsilon_1 \\ \epsilon_2 \\ \epsilon_3 \end{bmatrix}_Q$$

Equation (C.4) will be recognized as the linear form

$$u = A\bar{x} + e$$

of Appendix A in which

$$u = \begin{bmatrix} \tau_1 \\ \tau_2 \\ \tau_3 \end{bmatrix}_Q - \begin{bmatrix} \tau_1 \\ \tau_2 \\ \tau_3 \end{bmatrix}_P = \begin{bmatrix} \tau_{1Q} - \tau_{1P} \\ \tau_{2Q} - \tau_{2P} \\ \tau_{3Q} - \tau_{3P} \end{bmatrix}$$

$$\bar{x} = \begin{bmatrix} \Delta x \\ \Delta y \end{bmatrix} \quad e = \begin{bmatrix} \epsilon_1 \\ \epsilon_2 \\ \epsilon_3 \end{bmatrix} \quad A = \begin{bmatrix} a_{11} & a_{12} \\ a_{21} & a_{22} \\ a_{31} & a_{32} \end{bmatrix}$$

In Appendix A it is shown that the weighted least squares estimate of  $\bar{x}$  and the minimum variance estimate have the same algebraic form which we shall represent here by

$$(C.5) \quad x = (A^T M A)^{-1} A^T M u$$

To obtain the weighted least squares estimate we set  $M=W$ , the least squares weighting matrix. The minimum variance estimate of  $\bar{x}$  is obtained when  $M=R^{-1}$  where  $R = \langle ee^T \rangle$ .

We shall next obtain explicit formulas for the solution of (C.4) in the form (C.5). Either the weighted least squares or minimum variance solutions may then be obtained by making the appropriate substitution for the matrix  $M$ .

$$A^T M A = \begin{bmatrix} a_{11} & a_{21} & a_{31} \\ a_{12} & a_{22} & a_{32} \end{bmatrix} \begin{bmatrix} m_{11} & m_{12} & m_{13} \\ m_{21} & m_{22} & m_{23} \\ m_{31} & m_{32} & m_{33} \end{bmatrix}$$

$$b_{11} = a_{11}m_{11} + a_{21}m_{21} + a_{31}m_{31}$$

$$b_{12} = a_{11}m_{12} + a_{21}m_{22} + a_{31}m_{32}$$

$$b_{13} = a_{11}m_{13} + a_{21}m_{23} + a_{31}m_{33}$$

$$b_{21} = a_{12}m_{11} + a_{22}m_{21} + a_{32}m_{31}$$

$$b_{22} = a_{12}m_{12} + a_{22}m_{22} + a_{32}m_{32}$$

$$b_{23} = a_{12}m_{13} + a_{22}m_{23} + a_{32}m_{33}$$



$$A^T M A = B A = C = \begin{bmatrix} b_{11} & b_{12} & b_{13} \\ b_{21} & b_{22} & b_{23} \end{bmatrix} \begin{bmatrix} a_{11} & a_{12} \\ a_{21} & a_{22} \\ a_{31} & a_{32} \end{bmatrix}$$

$$c_{11} = b_{11}a_{11} + b_{12}a_{21} + b_{13}a_{31}$$

$$c_{12} = b_{11}a_{12} + b_{12}a_{22} + b_{13}a_{32}$$

$$c_{21} = b_{21}a_{11} + b_{22}a_{21} + b_{23}a_{31}$$

$$c_{22} = b_{21}a_{12} + b_{22}a_{22} + b_{23}a_{32}$$

$$\Delta = c_{22}c_{11} - c_{12}c_{21}$$

$$c_{11}^{-1} = c_{22}/\Delta$$

$$c_{12}^{-1} = -c_{12}/\Delta$$

$$c_{21}^{-1} = -c_{21}/\Delta$$

$$c_{22}^{-1} = c_{11}/\Delta$$

$$5) \quad G = C^{-1} B = (A^T M A)^{-1} A^T M$$

$$G = \begin{bmatrix} c_{11}^{-1} & c_{12}^{-1} \\ c_{21}^{-1} & c_{22}^{-1} \end{bmatrix} \begin{bmatrix} b_{11} & b_{12} & b_{13} \\ b_{21} & b_{22} & b_{23} \end{bmatrix} = \begin{bmatrix} g_{11} & g_{12} & g_{13} \\ g_{21} & g_{22} & g_{23} \end{bmatrix}$$

$$g_{11} = c_{11}^{-1} b_{11} + c_{12}^{-1} b_{21}$$

$$g_{12} = c_{11}^{-1} b_{12} + c_{12}^{-1} b_{22}$$

$$g_{13} = c_{11}^{-1} b_{13} + c_{12}^{-1} b_{23}$$

$$g_{21} = c_{21}^{-1} b_{11} + c_{22}^{-1} b_{21}$$

$$g_{22} = c_{21}^{-1} b_{12} + c_{22}^{-1} b_{22}$$

$$g_{23} = c_{21}^{-1} b_{13} + c_{22}^{-1} b_{23}$$

Finally we obtain

$$(C.7) \quad \begin{bmatrix} \Delta x = g_{11}(\tau_{1Q} - \tau_{1P}) + g_{12}(\tau_{2Q} - \tau_{2P}) + g_{13}(\tau_{3Q} - \tau_{3P}) \\ \Delta y = g_{21}(\tau_{1Q} - \tau_{1P}) + g_{22}(\tau_{2Q} - \tau_{2P}) + g_{23}(\tau_{3Q} - \tau_{3P}) \end{bmatrix}$$

#### Appendix D

#### Calculation of $R^{-1}$ for 3 TD Equal Gaussian Noise Case

From Appendices B and C, R was defined as

$$(D.1) \quad R \equiv \langle ee^T \rangle$$

where  $e$  was the vector of time difference measurement noises, assumed to be zero mean. Therefore,

$$(D.2) \quad e = \begin{bmatrix} \epsilon_1 \\ \epsilon_2 \\ \epsilon_3 \end{bmatrix}$$

where  $\epsilon_i$  is the noise on the  $i^{\text{th}}$  time difference measurement. Now, since each time difference measurement,  $T_i$ , is essentially the receipt time of the  $i^{\text{th}}$  slave pulse minus the receipt time of the master pulse, then

$$(D.3) \quad \epsilon_i = n_i - n_m$$

where  $n_i$  is the tracking filter noise jitter on the receipt time of the  $i^{\text{th}}$  slave pulse and  $n_m$  is the tracking filter noise jitter on the receipt time of the master pulse.

Now in actuality, each  $T_i$  has additional noise added to it due to the quantization process of each time difference counter. It is assumed that it is negligible. There may even be additional smoothing (averaging) of each  $T_i$  after the counting process. In any

event, we assume that the relative noise performance between  $T_1$ ,  $T_2$ ,  $T_3$  remains the same through these additional processes. Therefore, it is sufficient, for G matrix purposes, to consider the tracking filter noise jitter since only the relative noise statistics will affect the G matrix.

Assuming  $\langle n_i \rangle = 0$ ,  $\langle n_m \rangle = 0$ , then

$$(D.4) \quad R = \langle ee^T \rangle = \begin{bmatrix} R_{11} & R_{12} & R_{13} \\ R_{12} & R_{22} & R_{23} \\ R_{13} & R_{23} & R_{33} \end{bmatrix}$$

where

$$(D.5) \quad \begin{cases} R_{ii} = \langle \epsilon_i^2 \rangle = \langle n_i^2 \rangle + \langle n_m^2 \rangle & i = 1, 2, 3 \\ R_{ij} = \langle \epsilon_i \epsilon_j \rangle = \langle n_m^2 \rangle & i \neq j \quad \begin{matrix} i = 1, 2 \\ j = 2, 3 \end{matrix} \end{cases}$$

since it is assumed that  $\langle n_i n_j \rangle = 0$ . Now there are many formulae for calculating noise jitter performance out of a tracking filter. They differ according to the order and bandwidth of the tracking loop and the specific mechanization of the phase error detector. We assume that all tracking filters are identical so that

$$(D.6) \quad n_i^2 = k_o / (S/N)_i \quad i = 1, 2, 3, m$$

where  $k_o$  is a function of the specific tracking filter implementation and  $(S/N)_i$  is the power signal-to-noise ratio at the input to each tracking loop. Since atmospheric (external) noise is dominant (receiver noise negligible) and since we assume the RF receiver input bandwidths are all the same, then the noise presented

to each tracker is the same (even if the RF gains from antenna input to tracking loop input is different between receivers, the signal-to-noise ratio remains the same). Therefore,

$$(D.7) \quad \langle n_i^2 \rangle = \frac{k_o^N}{S_i} \quad i = 1, 2, 3, m$$

so that the relative tracking jitter performance is only a function of the signal powers,  $S_i$ , into the receiver antenna input.

$$(D.8) \quad S_i = P_i \left( \frac{\lambda}{4\pi r_{2i}} \right)^2 \quad i = 1, 2, 3$$

and

$$(D.9) \quad S_m = P_m \left( \frac{\lambda}{4\pi r_1} \right)^2$$

where  $P_i$  is the effective transmitter power of the  $i^{\text{th}}$  station;  $\lambda$  = wavelength of carrier frequency;  $r_{2i}$  and  $r_1$  are the slant ranges defined in Appendices B and C. Therefore,

$$(D.10) \quad \begin{cases} \langle n_i^2 \rangle = \frac{k_1 r_{2i}^2}{P_i} & i = 1, 2, 3 \\ \langle n_m^2 \rangle = \frac{k_1 r_1^2}{P_m} \end{cases}$$

so that

$$(D.11) \quad \begin{cases} R_{ii} = k_1 \left( \frac{r_{2i}^2}{P_i} + \frac{r_1^2}{P_m} \right) & i = 1, 2, 3 \\ R_{ii} = k_1 \left( \frac{r_1^2}{P_m} \right) & i \neq j \end{cases}$$

The value of  $k_1$  is unimportant except that it would be good practice to set it so that the elements of  $R$  are near unity. We let

$$(D.12) \quad R^{-1} = \begin{bmatrix} R_{11}^{-1} & R_{12}^{-1} & R_{13}^{-1} \\ R_{12}^{-1} & R_{22}^{-1} & R_{23}^{-1} \\ R_{13}^{-1} & R_{23}^{-1} & R_{33}^{-1} \end{bmatrix}$$

then

$$(D.13) \quad \left\{ \begin{array}{l} \Delta = R_{11} R_{22} R_{33} + 2 R_{12} R_{23} R_{13} \\ \quad - R_{13}^2 R_{22} - R_{12}^2 R_{33} - R_{11} R_{23}^2 \\ R_{11}^{-1} = (R_{22} R_{33} - R_{23}^2) / \Delta \\ R_{12}^{-1} = (R_{13} R_{23} - R_{33} R_{12}) / \Delta \\ R_{13}^{-1} = (R_{12} R_{23} - R_{22} R_{13}) / \Delta \\ R_{22}^{-1} = (R_{11} R_{33} - R_{13}^2) / \Delta \\ R_{23}^{-1} = (R_{12} R_{13} - R_{11} R_{23}) / \Delta \\ R_{33}^{-1} = (R_{11} R_{22} - R_{12}^2) / \Delta \end{array} \right.$$

Note that since the elements of  $R$  are directly proportional to  $k_1$ , then the elements of  $R^{-1}$  are inversely proportional to  $k_1$ . For

this case, from Appendix A,

$$G = (A^T R^{-1} A)^{-1} A^T R^{-1}$$

Therefore,  $A^T R^{-1}$  is inversely proportional to  $k_1$  while  $(A^T R^{-1} A)^{-1}$  is directly proportional to  $k_1$ , resulting in  $G$  being independent of  $k_1$ .

S2R-79-162  
ZT70S2R0  
October 8, 1979

TO: J. G. Wall

FROM: L. J. Levy and V. Schwab

SUBJECT: Methods for Obtaining Approximate and Exact Solutions  
to a LORAN Navigation Equation

REFERENCE: [1] APL/JHU S2R-79-008, G-Matrix Analysis for USCG  
LORAN-C HHE Navigation Program, by L. J. Levy and  
V. Schwab, January 19, 1979

The G-Matrix technique proposed by the U.S.C.G. is a computational method for converting two or more measured LORAN TDs into horizontal coordinates of navigator position. It yields a linear estimate of position referenced to the surveyed values of a 'near' waypoint or track point and employs a precomputed G-matrix to transform the TDs.

In the winter and spring of 1979 the proposed linear G-Matrix scheme as applied to the LORAN mini-chain in the St Marys River was simulated on the IBM 3033 computer at APL. It was then discovered that the navigation errors resulting from the high grid curvatures were much too large to be tolerated; a modification of the linear G-Matrix technique was then sought which would reduce the navigation error to an acceptable level.

Two modifications were studied. The first of these involved the iterated application of a second-order correction to the linear G-matrix solution. The second-order correction greatly reduced the first-order navigation error, but the residual errors were still above an acceptable level. It was then apparent that the exact solution of the LORAN TD equation was needed and also within easy reach if an iterative process for obtaining it were admitted. The method for obtaining the exact solution which was devised retains



the linear G-Matrix solution for its starting estimate of navigation position. It therefore also retains the important feature of the surveyed TDs and locations of the waypoints.

The remaining five sections of this memorandum elaborate on the remarks above. Section 1 contains a derivation of the basic LORAN equation relating the TD vector and navigator's position vector. Section 2 defines the linear G-Matrix solution of the LORAN equation. Section 3 contains a derivation of the second-order correction to the linear G-Matrix solution. The exact solution is presented in Section 4. The three methods of solution are compared quantitatively in Section 5 where they are applied to navigation in the LORAN-C mini-chain of the St. Marys River.

L. J. Levy

V. Schwab  
V. Schwab

LJL/VS:nt  
Distribution  
GEBaer  
CREdwards  
LJLevy  
JBMoffett  
JNagrant  
BSOgorzalek  
VLPisacane  
VSchwab  
JETarr  
TThompson  
JGWall (6)  
GCWeiffenbach  
Archives  
S2R File

# 1. General Form of the LORAN Time Difference Vector

In this section we shall develop the general form for the LORAN time difference vector upon which the three navigation solutions derived in subsequent sections are based.

The cartesian coordinates of the LORAN receiver aboard a ship are denoted by X and Y and these are the components of the vector

$$\underline{z} = \begin{bmatrix} X \\ Y \end{bmatrix}. \quad (1.1)$$

Either two or three time differences (TDs) are measured and for the sake of being definite we shall assume in this memorandum the number is three. The time difference or TD vector is given by

$$\underline{TD} = \begin{bmatrix} TD_1 \\ TD_2 \\ TD_3 \end{bmatrix} \quad (1.2)$$

The slant ranges from the ship to the LORAN slave and master stations are given by

$$r_i = [(X-X_i)^2 + (Y-Y_i)^2]^{1/2}, \quad i=1,2,3,m \quad (1.3)$$

in which  $i=1,2,3$  denotes the three slaves and  $i=m$  the master LORAN station.

The part of the time difference vector due to geometry alone (i.e., the ideal part, ignoring biases and noise) is denoted by  $\underline{h}(\underline{z})$  and given by

$$\underline{h}(\underline{z}) = \begin{bmatrix} (r_1 - r_m)/v \\ (r_2 - r_m)/v \\ (r_3 - r_m)/v \end{bmatrix} = \begin{bmatrix} h_1 \\ h_2 \\ h_3 \end{bmatrix} \quad (1.4)$$

in which  $v$  denotes the propagation speed of the LORAN signal.

The matrix of partial derivatives of the elements of  $\underline{h}$  with respect to  $X$  and  $Y$  is denoted by  $A$  and given by

$$A(\underline{z}) = \begin{bmatrix} \frac{\partial h_1}{\partial X} & \frac{\partial h_1}{\partial Y} \\ \frac{\partial h_2}{\partial X} & \frac{\partial h_2}{\partial Y} \\ \frac{\partial h_3}{\partial X} & \frac{\partial h_3}{\partial Y} \end{bmatrix} \quad (1.5)$$

Let  $\underline{z}_p$  and  $\underline{z}_Q$  represent two different values of  $\underline{z}$ . The vector difference,  $\underline{h}(\underline{z}_Q) - \underline{h}(\underline{z}_p)$ , can be resolved into a linear component equal to the vector  $A_p[\underline{z}_Q - \underline{z}_p]$  and a residual non-linear

component, denoted by the vector  $\underline{f}(\underline{z}_p, \underline{z}_Q)$ . The non-linear component will be defined by

$$\underline{f}(\underline{z}_p, \underline{z}_Q) = \underline{h}(\underline{z}_Q) - \underline{h}(\underline{z}_p) - A_p [\underline{z}_Q - \underline{z}_p] \quad (1.6)$$

At a waypoint P a measured TD vector is represented by

$$\underline{TD}_p = \underline{h}(\underline{z}_p) + \underline{w}_p + \underline{n}_p \quad (1.7)$$

in which  $\underline{w}_p$  represents biases and warpage in the measurement and  $\underline{n}_p$  represents zero-mean noise. Similarly, at an arbitrary nearby point Q the measured TD vector is represented by

$$\underline{TD}_Q = \underline{h}(\underline{z}_Q) + \underline{w}_Q + \underline{n}_Q. \quad (1.8)$$

The surveyed TD vector at  $\underline{z}=\underline{z}_p$  is the mean of many TD measurements of the form (1.7) and is denoted by  $\overline{\underline{TD}}_p$ . Since  $\underline{n}_p$  has zero mean we have

$$\overline{\underline{TD}}_p = \underline{h}(\underline{z}_p) + \underline{w}_p. \quad (1.9)$$

If P and Q are sufficiently close it may be reasonable to assume

$$\underline{w}_Q = \underline{w}_p. \quad (1.10)$$

If we assume (1.10) we find from (1.8) and 1.9)

$$\underline{TD}_Q - \underline{\overline{TD}}_P = \underline{h}(\underline{z}_Q) - \underline{h}(\underline{z}_P) + \underline{n}_Q. \quad (1.11)$$

However by means of (1.6) we are able to eliminate  $\underline{h}(z)$  from (1.11) and obtain

$$\underline{TD}_Q - \underline{\overline{TD}}_P = \underline{A}_P [\underline{z}_Q - \underline{z}_P] + \underline{f}(\underline{z}_P, \underline{z}_Q) + \underline{n}_Q. \quad (1.12)$$

In (1.11) and (1.12)  $\underline{z}_P$  represents the surveyed position of point P. The difference between the mean of many TD measurements made at P,  $\underline{\overline{TD}}_P$ , and  $\underline{h}(\underline{z}_P)$  is, by definition, the warpage or bias at P which is denoted by  $\underline{w}_P$  in (1.7). All three of these vectors are known for each waypoint.

The problem of LORAN navigation is to determine the position vector  $\underline{z}_Q$  given the measurement vector  $\underline{TD}_Q$ . The different ways in which this has been done are explained in the following three sections.

## 2. Linear G-Matrix Navigation Solution

The linear G-Matrix solution to the LORAN navigation problem represented by (1.12) is obtained under the assumption that  $\underline{f}(\underline{z}_P, \underline{z}_Q) = 0$ , or

$$\underline{TD}_Q - \underline{\overline{TD}}_P = \underline{A}_P [\underline{z}_Q - \underline{z}_P] + \underline{n}_Q. \quad (2.1)$$

In the notation of Ref. [1] let

$$u = \underline{TD}_Q - \overline{\underline{TD}}_P$$

$$A = A_P$$

$$\bar{x} = \underline{z}_Q - \underline{z}_P$$

$$e = \underline{n}_Q$$

$$R = \text{Cov}(e)$$

W positive definite, symmetric weighting matrix.

Then (2.1) takes the form

$$u = A\bar{x} + e. \quad (2.2)$$

A solution of (2.2) is represented by

$$\hat{\bar{x}} = G u \quad (2.3)$$

in which

$$G = (A^T W A)^{-1} A^T W. \quad (2.4)$$

Note from (2.4) that  $GA=I$ . The solution given by (2.3) is called the ordinary least squares solution when  $W=I$ ; the weighted least squares solution when

$$W = \begin{bmatrix} \dot{w}_1 & 0 & 0 \\ 0 & w_2 & 0 \\ 0 & 0 & w_3 \end{bmatrix};$$

the minimum variance solution when  $W=R^{-1}$ . In any case the solution of (2.1) is denoted by  $\hat{z}_Q = \hat{x} + z_p$  and is given by

$$\hat{z}_Q = z_p + G_p [\underline{TD}_Q - \overline{\underline{TD}}_p]. \quad (2.5)$$

### 3. G-Matrix Solution with 2nd Order Correction

In Appendix A we obtain the second-order expansion of a vector function (TD) of two variables (X,Y). The result is expressed by (A.6). When we apply this result to (1.12) we find

$$\begin{aligned} \underline{TD}_Q - \overline{\underline{TD}}_p &= A_p [z_Q - z_p] + n_Q \\ &+ (1/2) \sum_{i=1}^3 \underline{\psi}_i [z_Q - z_p]^T B_{pi} [z_Q - z_p] \end{aligned} \quad (3.1)$$

in which

$$\underline{\psi}_1 = \begin{bmatrix} 1 \\ 0 \\ 0 \end{bmatrix}, \quad \underline{\psi}_2 = \begin{bmatrix} 0 \\ 1 \\ 0 \end{bmatrix}, \quad \underline{\psi}_3 = \begin{bmatrix} 0 \\ 0 \\ 1 \end{bmatrix} \quad (3.2)$$

and

$$B_{pi} = \begin{bmatrix} \frac{\partial^2 h_i}{\partial x^2} & \frac{\partial^2 h_i}{\partial x \partial y} \\ \frac{\partial^2 h_i}{\partial x \partial y} & \frac{\partial^2 h_i}{\partial y^2} \end{bmatrix}, \quad i=1,2,3 \quad (3.3)$$

and  $A_p$  is defined by (1.5).

The solution of (3.1) is obtained through an iterative process. In the first iteration we compute the linear approximation defined by (2.5), i.e.,

$$\hat{z}_Q^1 = z_p + G_p [\underline{TD}_Q - \overline{TD}_p]. \quad (3.4)$$

The corresponding second-order correction term is denoted by  $\hat{a}$  and given by

$$\hat{a}^1 = (1/2) \sum_{i=1}^3 \psi_i [\hat{z}_Q^1 - z_p]^T B_{pi} [\hat{z}_Q^1 - z_p]. \quad (3.5)$$

In the second iteration we have

$$\hat{z}_Q^2 = z_p + G_p [\underline{TD}_Q - \overline{TD}_p - \hat{a}^1] = \hat{z}_Q^1 - G_p \hat{a}^1 \quad (3.6)$$

and

$$\hat{a}^2 = (1/2) \sum_{i=1}^3 \psi_i [\hat{z}_Q^2 - z_p]^T B_{pi} [\hat{z}_Q^2 - z_p] \quad (3.7)$$



In general,

$$\hat{\underline{a}}^{n-1} = (1/2) \sum_{i=1}^3 \underline{\psi}_i [\hat{\underline{z}}_Q^{n-1} - \underline{z}_P]^T \underline{B}_{Pi} [\hat{\underline{z}}_Q^{n-1} - \underline{z}_P] \quad (3.8)$$

and

$$\hat{\underline{z}}_Q^n = \hat{\underline{z}}_Q^1 - \underline{G}_P \hat{\underline{a}}^{n-1}. \quad (3.9)$$

The iterative process may be terminated when the change in  $\hat{\underline{a}}$  from the previous iteration becomes negligible.

#### 4. Exact Solution of the Non-Linear LORAN Equation

We shall present in this section an iterative scheme for obtaining an exact solution to the non-linear LORAN equation given by (1.12) or

$$\underline{TD}_Q - \underline{TD}_P = \underline{A}_P [\underline{z}_Q - \underline{z}_P] + f(\underline{z}_Q, \underline{z}_P) + \underline{n}_Q. \quad (4.1)$$

Again we use the linear G-matrix solution as the starting estimate in the first iteration. Thus we have

$$\hat{\underline{z}}_Q^1 = \underline{z}_P + \underline{G}_P [\underline{TD}_Q - \underline{TD}_P]. \quad (4.2)$$

Then from (1.6) we obtain

$$\hat{\underline{f}}^1 = \underline{h}(\hat{\underline{z}}_Q^1) - \underline{h}(\underline{z}_P) - \underline{A}_P [\hat{\underline{z}}_Q^1 - \underline{z}_P]. \quad (4.3)$$

For the second iteration we find

$$\hat{z}_Q^2 = z_p + G_p [\underline{TD}_Q - \underline{TD}_p - \hat{f}^1] = \underline{z}_Q^1 - G_p \hat{f}^1 \quad (4.4)$$

and

$$\hat{f}^2 = \underline{h}(\hat{z}_Q^2) - \underline{h}(z_p) - A_p [\hat{z}_Q^2 - z_p]. \quad (4.5)$$

In general,

$$\hat{f}^{n-1} = \underline{h}(\hat{z}_Q^{n-1}) - \underline{h}(z_p) - A_p [\hat{z}_Q^{n-1} - z_p] \quad (4.6)$$

and

$$\hat{z}_Q^n = \hat{z}_Q^1 - G_p \hat{f}^{n-1}. \quad (4.7)$$

A simpler scheme than that represented by (4.6) and (4.7) can be obtained by avoiding  $\underline{f}$  and dealing with  $\underline{h}$  alone.

In (4.4) if we substitute from (4.3) for  $\hat{f}^1$  we obtain

$$\hat{z}_Q^2 = \hat{z}_Q^1 - G_p [\underline{h}(\hat{z}_Q^1) - \underline{h}(z_p)] + G_p A_p [\hat{z}_Q^1 - z_p]$$

or, since  $G_p A_p = I$ ,

$$\hat{z}_Q^2 = 2\hat{z}_Q^1 - z_p - G_p [\underline{h}(\hat{z}_Q^1) - \underline{h}(z_p)]. \quad (4.8)$$

For the third iteration we find from (4.7)

$$\hat{\underline{z}}_Q^3 = \hat{\underline{z}}_Q^1 - G_P \hat{\underline{f}}^2. \quad (4.9)$$

From (4.9) and (4.5) we obtain

$$\begin{aligned} \hat{\underline{z}}_Q^3 &= \hat{\underline{z}}_Q^1 - G_P [\underline{h}(\hat{\underline{z}}_Q^2) - \underline{h}(\underline{z}_P)] - A_P [\hat{\underline{z}}_Q^2 - \underline{z}_P] \\ &= \hat{\underline{z}}_Q^1 + \hat{\underline{z}}_Q^2 - \underline{z}_P - G_P [\underline{h}(\hat{\underline{z}}_Q^2) - \underline{h}(\underline{z}_P)]. \end{aligned} \quad (4.10)$$

If we add the term

$$\hat{\underline{z}}_Q^1 - \hat{\underline{z}}_Q^1 + G_P [\underline{h}(\hat{\underline{z}}_Q^1) - \underline{h}(\underline{z}_P)] = 0$$

to the right-hand side of (4.10) and apply (4.8) to the result we find

$$\begin{aligned} \hat{\underline{z}}_Q^3 &= 2\hat{\underline{z}}_Q^1 - \underline{z}_P - G_P [\underline{h}(\hat{\underline{z}}_Q^1) - \underline{h}(\underline{z}_P)] + \hat{\underline{z}}_Q^2 - \hat{\underline{z}}_Q^1 \\ &\quad - G_P [\underline{h}(\hat{\underline{z}}_Q^2) - \underline{h}(\hat{\underline{z}}_Q^1)] \end{aligned}$$

or

$$\hat{\underline{z}}_Q^3 = 2\hat{\underline{z}}_Q^2 - \hat{\underline{z}}_Q^1 - G_P [\underline{h}(\hat{\underline{z}}_Q^2) - \underline{h}(\hat{\underline{z}}_Q^1)]. \quad (4.11)$$

In general,

$$\hat{\underline{z}}_Q^n = 2\hat{\underline{z}}_Q^{n-1} - \hat{\underline{z}}_Q^{n-2} - G_P [h(\hat{\underline{z}}_Q^{n-1}) - h(\hat{\underline{z}}_Q^{n-2})] \quad (4.12)$$

The iterative scheme represented by (4.12) may be terminated when the change in  $\hat{\underline{z}}$  from the previous iteration is sufficiently small to be negligible.

5. Comparison of the Navigation Solutions Obtained by Means of the Linear, Linear with 2nd Order Correction and Exact Methods of Solving the LORAN TD Equation

A comparison of the results obtained by the three methods of solving the LORAN TD equation (1.12) has been made for navigation between selected waypoints in the LORAN-C mini-chain in the St. Marys River connecting Lakes Superior and Huron.

In Table 5-1 the integers NWAY denote waypoint numbers; S represents the distance from a waypoint P to a point Q on the straight line joining waypoint P with the next waypoint. When S=0, Q is at P; when S attains its maximum value at a waypoint (e.g., S=11.19 at waypoint 1) Q is at the next waypoint. ATE and CTE denote the along-track error and cross-track error in navigated position at point Q.

Each row in Table 5-1 represents a navigation run. The distance S, of point Q from Point P is increased until the next waypoint is reached.

The three double columns of ATE and CTE contain the navigation errors which result using the linear G-Matrix solution defined

in Section 2; the iterative G-Matrix solution with second-order correction defined in Section 3; the iterative exact solution defined in Section 4.

It may be seen from Table 5-1 that the navigation errors increase with increasing S except in the case of the exact method of solution. Also, while the second-order correction achieves a considerable reduction in navigation error over the straight linear method, the errors remain unacceptably large especially when the distance between waypoints is great.

TABLE 5-1. COMPARISON OF METHODS OF SOLUTION

NWAY	S (KYDS)	Linear		2nd Order Correction		Exact	
		ATE (FT)	CTE (FT)	ATE (FT)	CTE (FT)	ATE (FT)	CTE (FT)
1	0.0	0.0	0.0	0.0	0.0	0.0	0.0
1	1.10000	-118.0	10.0	0.6	-0.1	0.05	-0.01
1	2.20000	-468.6	39.2	5.1	-1.3	0.03	-0.00
1	3.30000	-1044.3	86.1	19.0	-4.5	-0.11	0.01
1	4.40000	-1834.7	148.9	48.5	-11.3	0.28	-0.03
1	5.50000	-2827.4	225.4	100.2	-22.9	0.21	-0.02
1	6.60000	-4008.1	313.1	180.2	-40.8	0.20	-0.02
1	7.70000	-5361.6	405.6	294.6	-66.3	0.23	-0.02
1	8.80000	-6871.9	512.1	448.5	-100.7	0.28	-0.03
1	9.90000	-8522.9	617.9	646.5	-145.0	0.37	-0.03
1	11.00000	-10298.7	724.5	892.0	-200.4	0.49	-0.04
1	11.15034	-10617.6	742.8	939.6	-211.2	-0.37	0.03
2	0.0	0.0	0.0	0.0	0.0	0.0	0.0
2	1.00000	-48.2	-25.5	-0.5	-0.8	0.00	0.00
2	2.00000	-155.0	-105.2	-3.7	-6.3	-0.01	-0.01
2	3.00000	-443.4	-244.2	-11.7	-20.7	0.02	0.01
2	4.00000	-756.1	-447.4	-26.0	-48.1	-0.03	-0.02
2	5.00000	-1255.9	-719.4	-47.6	-91.8	0.04	0.03
2	5.41751	-1480.3	-854.6	-58.9	-115.6	0.08	0.05
3	0.0	0.0	0.0	0.0	0.0	-0.00	-0.00
3	0.86379	-20.9	-23.2	-0.0	-0.6	-0.02	-0.02
4	0.0	0.0	0.0	0.0	0.0	-0.00	-0.00
4	1.00000	11.5	7.8	0.4	-0.4	0.00	0.00
4	1.56471	28.6	18.6	1.7	-1.5	0.01	0.02
5	0.0	0.0	0.0	0.0	0.0	-0.00	-0.00
5	1.00000	-11.5	-31.6	0.2	-1.1	0.00	0.00
5	2.00000	-45.1	-131.0	2.0	-8.9	0.03	0.04
5	3.00000	-99.5	-305.2	7.1	-29.7	-0.02	-0.03
5	4.00000	-173.5	-560.9	18.0	-69.3	0.02	0.02
5	4.28515	-198.0	-649.6	22.5	-84.8	0.03	0.04
6	0.0	0.0	0.0	0.0	0.0	-0.00	-0.00
6	1.00000	-39.2	-35.1	0.4	0.4	0.00	0.00
6	2.00000	-155.1	-138.7	3.1	3.3	0.04	0.02
6	3.00000	-344.6	-307.0	10.8	12.0	-0.02	-0.01
6	3.59555	-460.9	-436.4	18.8	21.6	-0.06	-0.04
7	0.0	0.0	0.0	0.0	0.0	0.0	0.0
7	1.00000	-34.5	-12.4	0.8	1.0	-0.02	-0.00
7	2.00000	-125.2	-46.0	5.9	7.7	0.01	0.00
7	3.00000	-297.4	-95.4	19.3	25.6	-0.00	-0.00
7	2.25662	-356.7	-112.4	25.4	33.9	-0.01	-0.00
8	0.0	0.0	0.0	0.0	0.0	0.0	0.0
8	0.50921	-4.3	13.3	0.2	0.2	-0.00	0.00
9	0.0	0.0	0.0	0.0	0.0	0.0	0.0
9	1.00000	-12.3	16.6	0.3	0.4	-0.00	0.00
9	2.00000	-48.1	67.6	2.5	2.6	0.00	-0.00
9	2.02567	-49.4	69.4	2.6	2.9	0.00	-0.00

## APPENDIX A

### Expansion to the 2nd Order of a Vector Function of Two Variables

To the second order in  $h$  and  $k$  the Taylor expansion of the scalar function  $f(x,y)$ , where  $x$  and  $y$  are independent variables, is given by

$$\begin{aligned} f(z+h,y+k) = f(x,y) + \{hf_x(x,y) + k f_y(x,y)\} \\ + (1/2!) \left\{ h^2 f_{xx}(x,y) + 2hkf_{xy}(x,y) + k^2 f_{yy}(x,y) \right\}. \end{aligned} \quad (A.1)$$

We define the  $1 \times 2$  matrix  $A$ , the  $2 \times 2$  matrix  $B$  and the  $2 \times 1$  vector  $\underline{y}$  by the expressions in

$$\begin{aligned} A &= \begin{bmatrix} f_x & f_y \end{bmatrix} \\ B &= \begin{bmatrix} f_{xx} & f_{xy} \\ f_{xy} & f_{yy} \end{bmatrix} \quad \underline{y} = \begin{bmatrix} h \\ k \end{bmatrix} \end{aligned} \quad (A.2)$$

The matrices and vector defined in (A.2) permit us to write (A.1) in the form

$$f(x+h,y+k) = f(x,y) = A\underline{y} + (1/2!) \underline{y}^T B \underline{y} \quad (A.3)$$

To verify (A.3) observe from (A.2) that

$$A_y = [hf_x + kf_y]$$

$$B_y = \begin{bmatrix} hf_{xx} + kf_{xy} \\ hf_{xy} + kf_{yy} \end{bmatrix}$$

$$\underline{v}^T B_y = [h \ k] \begin{bmatrix} hf_{xx} + kf_{xy} \\ hf_{xy} + kf_{yy} \end{bmatrix} = h^2 f_{xx} + 2hkf_{xy} + k^2 f_{yy}$$

and note that these results agree with (A.1).

Consider next the 3x1 vector function  $\underline{F}(x,y)$  defined by

$$\underline{F}(x,y) = \begin{bmatrix} f_1(x,y) \\ f_2(x,y) \\ f_3(x,y) \end{bmatrix} \quad (A.4)$$

Again we wish to form the second-order Taylor expansion of  $\underline{F}(x,y)$ . For this purpose we define the 3x2 matrix A, the 2x2 matrices  $B_i$ ,  $i=1,2,3$  and the 3x1 vector  $\psi_i$ ,  $i=1,2,3$  in



$$A = \begin{bmatrix} f_{1x} & f_{1y} \\ f_{2x} & f_{2y} \\ f_{3x} & f_{3y} \end{bmatrix} \quad B_i = \begin{bmatrix} f_{ixx} & f_{ixy} \\ f_{ixy} & f_{iyy} \end{bmatrix}, \quad i=1,2,3$$

$$\underline{\psi}_1 = \begin{bmatrix} 1 \\ 0 \\ 0 \end{bmatrix} \quad \underline{\psi}_2 = \begin{bmatrix} 0 \\ 1 \\ 0 \end{bmatrix} \quad \underline{\psi}_3 = \begin{bmatrix} 0 \\ 0 \\ 1 \end{bmatrix} \quad (A.5)$$

Then, to the second order in  $h$  and  $k$ ,

$$\underline{F}(x+h, y+k) = \underline{F}(x, y) = A\underline{v} + (1/2!) \sum_{i=1}^3 \underline{\psi}_i \underline{v}^T B_i \underline{v} \quad (A.6)$$

where  $\underline{v}$  has been defined in (A.2).

S2R-79-166  
ZT70S2R0  
October 22, 1979

TO: J. G. Wall

FROM: L. J. Levy/V. Schwab

SUBJECT: Design, Simulation and Performance of Digital TD and Heading Filters for the USCG LORAN-C HHE Navigation Program

REFERENCES: [1] APL/JHU TYA-0-002, Compilation of Characteristics of the Second-Order Digital Filter, by R. J. McConahy, August 29, 1963

[2] IRE Transactions PGAC, Vol. AC-7, July 1962, Synthesis of an Optimal Set of Radar Track-while-scan Smoothing Equations, by T. R. Benedict and G. W. Bordner

[3] APL/JHU S2R-79-162, Methods for Obtaining Approximate and Exact Solutions to a LORAN Navigation Equation, by L. J. Levy and V. Schwab, October 8, 1979

The time difference (TD) measurements made in the USCG LORAN-C HHE Navigation Program may be expected to contain zero-mean noise errors ranging in size up to tens of nanoseconds. Since the TD measurements are converted directly to display ship's position on a scope, it is desirable to filter out large fluctuations in the TDs before computing position.

In the absence of ship's maneuver (turning) the TDs can be effectively filtered by a conventional second-order digital filter which has zero velocity lag. However large velocity lags and position errors are introduced by this filter during the frequent turns required on the St. Mary's River. It has been demonstrated that this deficiency of the conventional filter can be essentially eliminated by the addition of a first-order filter which provides a filtered value of acceleration normal to the ship's course. The raw acceleration measurement is obtained from differential measurements of ship's

heading angle which, in turn, measure the turning rate of the ship.

The main body of this memorandum is divided into three parts:

- I Filter Design
- II Filter Simulation
- III Filter Performance

The section on filter design is divided into two parts. The first part reviews the theory of the conventional second-order digital a,b-filter; the modification to the filter required when aged measurements and display delay are present; the reduction of velocity lag by means of acceleration-aided prediction in the filter. The general filter equations developed in the first part are applied in the second part to the particular problem of filtering LORAN TD measurements.

The section on filter simulation contains a fairly detailed description of a digital simulation prepared for the IBM 3033 Computer at APL in the spring of 1979. The purpose of the simulation was the provision of the possibility of the computation of filter performance in order to confirm the choices of filter gains and other optional system parameters.

The section on filter performance presents a small representative sample of the simulation runs which were made on the 3033 Computer. The particular series of four runs were chosen to show the effect on filter performance of variations in the gain of the heading (acceleration) filter. These runs show clearly: (1) the need to greatly reduce velocity lag; (2) the ability of the heading filter to essentially eliminate velocity lag.

LJL/VS:nt

L. J. Levy  
V. Schwab

### I-1.1 The Conventional a,b-Filter

The following description of a second-order digital filter used for filtering and estimating the rate of change of a digital data sequence follows closely the excellent account given in Ref [1]. The sequel is often nearly but not precisely verbatim and the notation of the present text also differs slightly from that of Ref [1].

Suppose one has a sequence

$$x^*(n), n=0,1,2,\dots$$

of input or raw data. We suppose this sequence is measured (or delivered) at a sample period of  $\Delta t$  seconds. Then  $x^*(n)$  would be the measurement of the quantity 'x' at time  $t=n\Delta t$ .

Obviously the individual measurements will contain noise. It is often desirable to smooth them so that the system functions which use the data will not operate wildly and erratically, as they might if nothing were done. But, more than this, there is usually a desire to estimate the rate of change,  $\dot{x}$ , of the quantity x. This is very useful in case there is a sudden fade in the data sequence  $x^*(n)$  and we are forced to 'coast' awhile.

One of the simplest filtering or estimation schemes that will allow us simultaneously to smooth the data and estimate rate of change is the second-order filter defined by

$$\begin{aligned} r(n) &= x^*(n) - \hat{x}'(n) \\ \hat{x}(n) &= \hat{x}'(n) + a r(n) \\ \hat{\dot{x}}(n) &= \hat{\dot{x}}'(n) + \frac{b}{\Delta t} r(n) \end{aligned} \tag{1}$$

and

$$\begin{aligned}\hat{x}'(n+1) &= \hat{x}(n) + \hat{\dot{x}}(n) \Delta t \\ \hat{\dot{x}}'(n+1) &= \hat{\dot{x}}(n)\end{aligned}\tag{2}$$

in which

- $\hat{x}(n)$  is the smoothed estimate of  $x$  at step  $n$
- $\hat{\dot{x}}(n)$  is the smoothed estimate of  $\dot{x}$  at step  $n$
- $\hat{x}'(n)$  is the predicted value of  $x$  at step  $n$  and usually made at step  $n-1$
- $\hat{\dot{x}}'(n)$  is the predicted value of  $\dot{x}$  at step  $n$  and usually made at step  $n-1$
- $a$  position smoothing gain
- $b$  rate smoothing gain

The equations in (1) update the predictions (primed quantities) made for step  $n$  to estimates of  $x$  and  $\dot{x}$ . The quantity  $r(n)$  is the error in the prediction of  $x(n)$  referenced to  $x^*(n)$ . Note that if  $a=0$ ,  $\hat{x}(n)=\hat{x}'(n)$  and no weight is given to the measurement  $x^*(n)$ ; however if  $a=1$ ,  $\hat{x}(n)=x^*(n)$  and the measurement at step  $n$  is given full weight. The equations in (2) define the prediction for one time step in advance.

Equations (1) and (2) can be reduced to the second-order difference equation

$$\hat{x}(n+2) - (2-a-b)\hat{x}(n+1) + (1-a)\hat{x}(n) = ax^*(n+2) + (b-a)x^*(n+1).$$

The performance of the second-order filter depends on the choice of the smoothing gains  $a$  and  $b$ .

For stability of  $\hat{x}(n)$  and  $\hat{\dot{x}}(n)$  it is required that

$$b < 4 - 2a, \quad 0 < a < 2.$$

The filter is:

underdamped if  $4b > (a+b)^2$ ;

critically damped if  $4b = (a+b)^2$ ;

overdamped if  $4b < (a+b)^2$ .

The filter is said to be optimum if  $a$  and  $b$  satisfy the relation

$$b = \frac{a^2}{2 - a}$$

which results in a slightly underdamped filter.

We shall now explain what is meant above by the term 'optimum filter'. Assume the noise on each input sample has zero mean, variance (mean square)  $\sigma_N^2$  and that the noise on different samples is uncorrelated. The ability of the filter to smooth the data is frequently measured by the index

$$R_x(0) = \frac{\text{Variance in smoothed position output}}{\text{Variance in raw position input}}$$

which is referred to as the variance reduction ratio. There is also a variance reduction ratio for the smoothed output velocity sequence,  $\hat{x}(n)$ , which is denoted by  $R_{\dot{x}}(0)$ . For any stable combination of  $a$  and  $b$

$$R_{\dot{x}}(0) = \frac{2a^2 + b(2 - 3a)}{a(4 - b - 2a)}$$

$$R_{\dot{x}}(0) = \frac{1}{\Delta t^2} \cdot \frac{2b^2}{a(4 - b - 2a)}.$$

It is a general characteristic of the second-order filter that, given sufficient time, it will settle onto a linear input sequence, i.e.,

$$x^*(n) = An + B$$

with negligible error. That is

$$\lim_{n \rightarrow \infty} [\hat{x}(n) - x^*(n)] = 0$$

for such a linear sequence. This property is usually referred to as 'zero velocity lag'.

A useful index is one based on the unit-ramp response. Let

$$h_x(n) = \hat{x}(n) \text{ for } x^*(n) = n$$

assuming the filter is initially at rest. Then the index is

$$C_x = \sum_{n=0}^{\infty} (n - h_x(n))^2.$$

One can, similarly, define a velocity index

$$C_{\dot{x}} = \sum_{n=0}^{\infty} (1 - h_{\dot{x}}(n))^2$$

where

$$h_x(n) = \hat{x}(n) \text{ if } x^*(n) = n.$$

For any stable combination of a and b

$$C_x = \frac{(2-a)(1-a)^2}{ab(4-b-2a)}$$

$$C_x^* = \frac{1}{\Delta t^2} \cdot \frac{a^2(2-a) + 2b(1-a)}{ab(4-b-2a)}.$$

The indices  $C_x$  and  $R_x(0)$  each depend on the variables a and b, and one might compute contours of these functions in the a,b-plane using the formulas given above. The following problem in optimization is posed by the two indices and may be formulated in terms of two questions:

- (i) For what values of a and b is  $C_x$  minimized for a given desired value of  $R_x(0)$ ?
- (ii) Conversely, for what values of a and b is  $R_x(0)$  minimized for a given desired value of  $C_x(0)$ ?

The same two questions can be asked with the velocity index  $R_x^*(0)$  replacing  $R_x(0)$  and  $C_x^*$  replacing  $C_x$ . It is proved in Ref. [2] that all four questions have the same answer:  $b=a^2/(2-a)$ , as asserted above. It is in this sense then that the relationship of position and rate gains stated above define an optimum filter.



In Table I-1 there are listed some characteristics first, of a critically damped and then an optimum second-order filter. In each case six values of the position gain are specified in column 1 and the corresponding value of the rate gain,  $b$ , computed by means of the formula given at the top of the table, appears in column 2. The quantities  $\sigma_{POS}$  and  $\sigma_{VEL}$  are the square roots of  $R_x(0)$  and  $R'_x(0)$  defined above. The values of the filter time constant were determined using formulas for the position response function given in Ref. [1] but not reproduced here.

#### I-1.2 Conventional Filter with Aged Measurement and Display Delay

Assume that at time  $t_n = n\Delta t$  the measurement  $x^*$  has an age  $\Delta t_A \geq 0$  (i.e., the measurement is made at  $t_n - \Delta t_A$ ). Also assume that the measurement will not be displayed until after a delay  $\Delta t_D \geq 0$  at  $t_n + \Delta t_D$ . The equations for updating the estimate at  $t_n - \Delta t_A$  are

$$r(n - \Delta t_A) = x^*(n - \Delta t_A) - \hat{x}'(n - \Delta t_A) \quad (3)$$

$$\hat{x}(n - \Delta t_A) = \hat{x}'(n - \Delta t_A) + a r(n - \Delta t_A) \quad (4)$$

$$\hat{\dot{x}}(n - \Delta t_A) = \hat{\dot{x}}'(n - \Delta t_A) + \frac{b}{\Delta t} r(n - \Delta t_A). \quad (5)$$

The forward predictions to the next update time  $t_{n+1} - \Delta t_A$  are made by

$$\hat{x}'(n+1 - \Delta t_A) = \hat{x}(n - \Delta t_A) + \hat{\dot{x}}(n - \Delta t_A) \Delta t \quad (6)$$

$$\hat{\dot{x}}'(n+1 - \Delta t_A) = \hat{\dot{x}}(n - \Delta t_A) \quad (7)$$

The forward predictions to the display time  $t_n + \Delta t_D$  are made by:

$$\hat{x}^D(n + \Delta t_D) = \hat{x}(n - \Delta t_A) + \hat{\dot{x}}(n - \Delta t_A)(\Delta t_A + \Delta t_D) \quad (8)$$

$$\hat{\dot{x}}^D(n + \Delta t_D) = \hat{\dot{x}}(n - \Delta t_A). \quad (9)$$

We shall next arrange the equations above so that updating is done at  $t_n + \Delta t_D$ . First we evaluate (8) and (9) at  $t_{n+1} + \Delta t_D$  and obtain

$$\hat{x}^D(n+1 + \Delta t_D) = \hat{x}(n+1 - \Delta t_A) + \hat{\dot{x}}(n+1 - \Delta t_A)(\Delta t_A + \Delta t_D) \quad (10)$$

$$\hat{\dot{x}}^D(n+1 + \Delta t_D) = \hat{\dot{x}}(n+1 - \Delta t_A). \quad (11)$$

Next we evaluate (3), (4) and (5) at  $t_{n+1} - \Delta t_A$  and find

$$r(n+1 - \Delta t_A) = x^*(n+1 - \Delta t_A) - \hat{x}'(n+1 - \Delta t_A) \quad (12)$$

$$\hat{x}(n+1 - \Delta t_A) = \hat{x}'(n+1 - \Delta t_A) + a r(n+1 - \Delta t_A) \quad (13)$$

$$\hat{\dot{x}}(n+1 - \Delta t_A) = \hat{\dot{x}}'(n+1 - \Delta t_A) + \frac{b}{\Delta t} r(n+1 - \Delta t_A) \quad (14)$$

By means of (13) and (14), (10) and (11) become

$$\begin{aligned} \hat{x}^D(n+1 + \Delta t_D) &= \hat{x}'(n+1 - \Delta t_A) + a r(n+1 - \Delta t_A) \\ &\quad + [\hat{\dot{x}}'(n+1 - \Delta t_A) + \frac{b}{\Delta t} r(n+1 - \Delta t_A)](\Delta t_A + \Delta t_D) \end{aligned} \quad (15)$$

$$\hat{\dot{x}}^D(n+1 + \Delta t_D) = \hat{\dot{x}}'(n+1 - \Delta t_A) + \frac{b}{\Delta t} r(n+1 - \Delta t_A). \quad (16)$$

AD-A086 001

COAST GUARD WASHINGTON D C OFFICE OF RESEARCH AND DE--ETC F/8 17/7  
PRECISION LORAN-C NAVIGATION FOR THE HARBOR AND HARBOR ENTRANCE--ETC(U)  
MAY 80 D L OLSEN, J M LISON, A J SEDLOCK  
USCG-D-34-80

UNCLASSIFIED

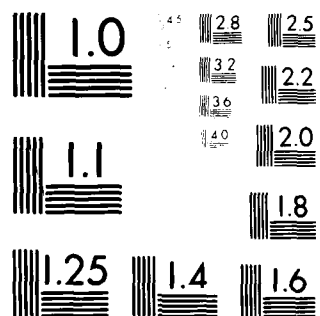
NL

2 of 2

AD-A086 001




END  
DATE  
FILMED  
18-80  
DTIC



MICROCOPY RESOLUTION TEST CHART  
NATIONAL BUREAU OF STANDARDS-1963-A

Then, by means of (6) and (7), (12), (15) and (16) become

$$r(n+1-\Delta t_A) = x^*(n+1-\Delta t_A) - \hat{x}(n-\Delta t_A) - \hat{x}(n-\Delta t_A)\Delta t \quad (17)$$

$$\begin{aligned} \hat{x}^D(n+1+\Delta t_D) &= \hat{x}(n-\Delta t_A) + \hat{x}(n-\Delta t_A)\Delta t + a r(n+1-\Delta t_A) \\ &\quad + [\hat{x}(n-\Delta t_A) + \frac{b}{\Delta t}r(n+1-\Delta t_A)](\Delta t_A + \Delta t_D) \end{aligned} \quad (18)$$

$$\hat{x}^D(n+1+\Delta t_D) = \hat{x}(n-\Delta t_A) + \frac{b}{\Delta t}r(n+1-\Delta t_A). \quad (19)$$

Equations (8) and (9) can be used to express (17), (18) and (19) in the forms

$$\begin{aligned} r(n+1-\Delta t_A) &= x^*(n+1-\Delta t_A) - \hat{x}^D(n+\Delta t_D) + \hat{x}^D(n+\Delta t_D)(\Delta t_A + \Delta t_D) \\ &\quad - \hat{x}^D(n+\Delta t_D)\Delta t \\ &= x^*(n+1-\Delta t_A) + \hat{x}^D(n+\Delta t_D)(\Delta t_A + \Delta t_D) \\ &\quad - [\hat{x}^D(n+\Delta t_D) + \hat{x}^D(n+\Delta t_D)\Delta t]. \end{aligned} \quad (20)$$

$$\begin{aligned} \hat{x}^D(n+1+\Delta t_D) &= \hat{x}^D(n+\Delta t_D) + \hat{x}^D(n+\Delta t_D)\Delta t \\ &\quad + [a + \frac{b}{\Delta t}(\Delta t_A + \Delta t_D)] r(n+1-\Delta t_A) \end{aligned} \quad (21)$$

$$\hat{x}^D(n+1+\Delta t_D) = \hat{x}(n+\Delta t_D) + \frac{b}{\Delta t}r(n+1-\Delta t_A) \quad (22)$$

Let

$$\Delta t_{AD} = \Delta t_A + \Delta t_D. \quad (23)$$

The predicted values at time  $t_{n+1+\Delta t_D}$  are

$$\hat{x}^{D'}(n+1+\Delta t_D) = \hat{x}^D(n+\Delta t_D) + \hat{\dot{x}}^D(n+\Delta t_D)\Delta t \quad (24)$$

$$\hat{\dot{x}}^{D'}(n+1+\Delta t_D) = \hat{\dot{x}}^D(n+\Delta t_D) \quad (25)$$

Then by means of (23), (24) and (25) equations (20), (21) and (22) become

$$\begin{aligned} r(n+1-\Delta t_A) &= x^*(n+1-\Delta t_A) + \hat{\dot{x}}^D(n+1+\Delta t_D)\Delta t_{AD} \\ &\quad - \hat{\dot{x}}^{D'}(n+1+\Delta t_D) \end{aligned} \quad (26)$$

$$\hat{x}^D(n+1+\Delta t_D) = \hat{x}^{D'}(n+1+\Delta t_D) + [a + \frac{b}{\Delta t}\Delta t_{AD}]r(n+1-\Delta t_A) \quad (27)$$

$$\hat{\dot{x}}^D(n+1+\Delta t_D) = \hat{\dot{x}}^{D'}(n+1+\Delta t_D) + \frac{b}{\Delta t}r(n+1-\Delta t_D). \quad (28)$$

### I-1.3 Addition of a Filtered Acceleration Measurement to Aid Prediction

While the second-order filter defined by (26), (27) and (28) is a zero-velocity lag filter it will develop a lag in the presence of a non-zero acceleration,  $\ddot{x}$ . If acceleration can be measured and introduced into (26) by the addition of a term

$$0.5 \Delta t_{AD}^2 \hat{\ddot{x}}$$

the lag due to acceleration can be greatly reduced. However a noisy measurement of acceleration,  $\ddot{x}^*(n)$ , would first have to be filtered. To accomplish the filtering we propose the first-order acceleration filter represented by

$$\hat{\ddot{x}}(n) = \hat{\ddot{x}}(n-1) + c[\ddot{x}^*(n) - \hat{\ddot{x}}(n-1)]. \quad (29)$$

Note in (29) that if the gain  $c=0$ , no weight is given to the acceleration measurement and  $\hat{\ddot{x}}(n)=\hat{\ddot{x}}(n-1)=0$ ; however, if  $c=1$ ,  $\hat{\ddot{x}}(n)=\ddot{x}^*(n)$  and the measurement receives full weight.

#### I-2. Application of the Acceleration-Aided Second-Order Filter to the Problem of Filtering LORAN TD Measurements

In Ref. [3] the LORAN TD (time difference) is given in 'exact' form by Eq. (1.12) and in linearized form by Eq. (2.1) or the expression

$$\underline{TD}_Q = \underline{TD}_P + A_P [\underline{Z}_Q - \underline{Z}_P] + \underline{n}_Q$$

in which  $\underline{TD}$  denotes a vector of two or three TDs;  $\underline{Z}$  denotes a two-dimensional horizontal position vector of the navigator;  $\underline{n}$  is a vector of zero-mean noise errors in the TD measurement;  $A$  is a matrix of first-order partial derivatives of the TDs with respect to the navigator's position coordinates. Subscript  $P$  denotes a variable whose value is known and associated with a fixed waypoint with coordinates  $\underline{Z}=\underline{Z}_P$ . Subscript  $Q$  denotes a variable associated with the variable point  $Q$  with the generally unknown coordinates  $\underline{Z}=\underline{Z}_Q$ . From the measurement  $\underline{TD}_Q$ , a 'navigated' value  $\underline{Z}_Q$  is to be inferred.

If we consider a single TD rather than two or three as in the vector equation above we can use the equation

$$TD_Q = \overline{TD}_P + a_{11}(x_Q - x_P) + a_{12}(y_Q - y_P) + n \quad (30)$$

in which all quantities are scalars.

There are four time intervals which appear explicitly in the equations representing the TD and heading angle (i.e., acceleration) filters. These are:

- $\Delta T_K$  Time interval between TD measurements
- $\Delta T_L$  Time interval between heading measurements
- $dT_i$  Incremental time step in dead reckoning computation in TD filter
- $\Delta T_A$  Time delay in the measurement of TDs.

In addition, there is a time delay,  $dT_\psi$ , in the measurement of ship's heading angle; however this quantity does not appear explicitly in the filter equations which follow.

In the time interval between TD measurements, i.e., when a TD measurement is not available, predictions are made by means of the formulas

$$\hat{TD}_i = \hat{TD}_{i-1} + \hat{TD}_{i-1} dT_i + 0.5 \hat{TD} dT_i^2 \quad (31)$$

$$\hat{TD}_i = \hat{TD}_{i-1} + \hat{TD} dT_i. \quad (32)$$

When a TD measurement, denoted by  $TD_k^*$ , is available the following computations are made:

$$\hat{TD}_k = \hat{TD}_i \quad (33)$$

$$\hat{TD}_k = \hat{TD}_i \quad (34)$$



$$r_k = TD_k^* + \Delta T_A \hat{TD}_k' + 0.5\Delta T_A^2 \hat{\ddot{TD}} - \hat{TD}_k' \quad (35)$$

$$\hat{TD}_k = \hat{TD}_k' + [a + b(\Delta T_A/\Delta T_K)]r_k \quad (36)$$

$$\hat{\ddot{TD}}_k = \hat{\ddot{TD}}_k' + (b/\Delta T_K)r_k. \quad (37)$$

The function of the heading filter is to provide the filtered term  $\hat{\ddot{TD}}$  appearing in (31) and (35). From (30) we have

$$\ddot{TD} = a_{11}\ddot{x} + a_{12}\ddot{y}$$

and by geometry

$$\dot{x} = v \sin \psi$$

$$\dot{y} = v \cos \psi$$

where  $v$  denotes the constant (i.e., slowly changing) speed of the ship and  $\psi$  is ship's heading angle measured clockwise from north. The accelerations

$$\ddot{x} = v\dot{\psi} \cos \psi$$

$$\ddot{y} = v\dot{\psi} \sin \psi$$

can be approximated using measurements  $\psi_n^*$  and  $\psi_{n-1}^*$  made  $\Delta T_L$  seconds apart. The normal acceleration measurement

$$a_n^* = v[\psi_n^* - \psi_{n-1}^*]/\Delta T_L$$

is filtered in the first-order filter

$$\hat{a}_n = \hat{a}_{n-1} + c[a_n^* - \hat{a}_{n-1}]. \quad (38)$$

Then

$$\hat{TD} = [a_{11} \cos \psi_n^* - a_{12} \sin \psi_n^*] \hat{a}_n. \quad (39)$$

Equations (31) through (39) represent the TD and Heading Filter applied to a single TD. These equations are based on the second-order filter with acceleration aiding which is described in Section I-1. The equations are used in the filter simulation program described in Section II.

Table I-1

Summary of Some Characteristics of  
The Second-Order Filter

Critically Damped Filter:  $4b = (a+b)^2$

a	b	$\sigma_{POS}$	$\sigma_{VEL}$	FILTER TIME CONSTANT	
				No. of $\Delta t$ s	(SEC) *
.6400	.1600	$.713\sigma_N$	$.177\sigma_N/\Delta t$	1	.5
.3392	.0350	$.487\sigma_N$	$.0469\sigma_N/\Delta t$	4	2
.1800	.0089	$.345\sigma_N$	$.0156\sigma_N/\Delta t$	10	5
.13642	.0050	$.298\sigma_N$	$.0099\sigma_N/\Delta t$	13	6.5
.1100	.0032	$.267\sigma_N$	$.0070\sigma_N/\Delta t$	17	8.5
.04422	.0005	$.167\sigma_N$	$.0017\sigma_N/\Delta t$	44	22

Optimum Filter:  $b = a^2/(2-a)$

a	b	$\sigma_{POS}$	$\sigma_{VEL}$	FILTER TIME CONSTANT	
				No. of $\Delta t$ s	(SEC) *
.6400	.3010	$.738\sigma_N$	$.342\sigma_N/\Delta t$	1	.5
.3392	.0690	$.519\sigma_N$	$.093\sigma_N/\Delta t$	2	1
.1800	.0178	$.373\sigma_N$	$.031\sigma_N/\Delta t$	4	2.0
.13642	.0100	$.324\sigma_N$	$.0198\sigma_N/\Delta t$	5	2.5
.1100	.0064	$.290\sigma_N$	$.0141\sigma_N/\Delta t$	6	3
.04422	.0010	$.183\sigma_N$	$.0034\sigma_N/\Delta t$	17	8.5

\*Assuming  $\Delta t = 0.5$  sec

$\sigma_N = \sigma$  of measured noise

$\Delta t =$  time interval between updates

## II FILTER SIMULATION

The digital simulation of the filters defined in Section I imposed the requirement that we also model the ship's course as a function of time in order to provide a basis for computing the ideal (geometric) TD as well as ship's heading angle. It was decided to simulate the typical pattern of ship maneuver in a river channel: a straight-line segment, followed by a turn and then another straight-line segment. By repeating this pattern it would be possible, if desired, to simulate the passage of a ship over a course of arbitrary shape and length. Obviously the sudden imposition and removal of an acceleration normal to the ship's course at the start and at the end of the turn will reveal the dynamic response of the filter.

The organization of the filter simulation program is represented by the nine blocks in Fig. II-1 which have some, but not all, of the properties of a flow chart. Each row in the blocks of the figure is divided into two or three columns. The number in the left-hand column represents a point of entry into the block; the number in the right-hand column represents a point of entry in the same or a different block to which control is passed. The center column, when it is present (blocks 1, 2, 7, 8) represents the setting of control parameters or the testing of variables (generally not explicitly indicated on the figure) for control purposes.

Sections II-1 through II-9 describe in appropriate detail the operations performed in the nine blocks of Fig. II-1. The principal symbols used in these sections are defined in the following glossary and table of input parameters.

### Glossary of Symbols

$x, y$	Cartesian position coordinates of the ship relative to the master LORAN station.
$\dot{x}, \dot{y}$	First time derivatives of $x, y$ . Velocity coordinates of the ship.
$\ddot{x}, \ddot{y}$	Acceleration coordinates of the ship.
$\psi$	Ship's heading angle, measured clockwise from north.
$\dot{\psi}$	Ship's turning rate
$a$	Normal acceleration of the ship.
$\phi$	At any waypoint, the angle between the lines of bearing to the preceding and succeeding waypoints. (The ship must turn through the angle $\phi$ at each waypoint.)
$T$	Time variable.
$TD$	Time difference between the arrival times at the ship of LORAN pulses from a slave and from the master station.
$\dot{TD}$	Time derivative of $TD$ .
$\ddot{TD}$	Second time derivative of $TD$ .
$\hat{TD}, \hat{\dot{TD}}, \hat{\ddot{TD}}$	Filtered values of $TD$ , $\dot{TD}$ and $\ddot{TD}$ .
$\delta\hat{TD}$	Error in $\hat{TD}$ . $\delta\hat{TD} = \hat{TD} - TD$ where $TD$ denotes the true value.
$\delta\hat{\dot{TD}}$	Error in $\hat{\dot{TD}}$ . $\delta\hat{\dot{TD}} = \hat{\dot{TD}} - \dot{TD}$ where $\dot{TD}$ denotes the true value.
$TDP$	Value of $TD$ at an arbitrary waypoint, $P$
$x_p, y_p$	Cartesian position coordinates of an arbitrary waypoint, $P$

Input Parameters

$v$	Ship's speed.
$\dot{\psi}_{\max}$	Ship's maximum turning rate.
$\Delta T_i$	Incremental time step in TD filter
$\Delta T_\psi$	Time delay in the measurement of ship's heading angle
$\Delta T_A$	Time delay in the measurement of TDs.
$\Delta T_K$	Time interval between TD measurements for TD filter
$\Delta T_L$	Time interval between measurements of ship's heading for Heading Filter.
A	Gain in TD filter (position gain).
B	Gain in TD filter (rate gain).
C	Gain in Heading Filter
NSIGMA	Standard deviation of noise in measured TDs.

## II-1 Controller

The TD filter simulation consists of three consecutive phases: (1) a straight-line run of the ship; (2) a constant-radius turn; (3) a straight-line run. Each phase requires the precomputation and setting of initial values of certain parameters. These initializations are accomplished in Section II-2, II-3 and II-4.

The function of the controller section is to route control of the computation to the appropriate section as each of the phases is completed. At the end of the simulation control is passed to Section II-9 where the tapes for generating the CALCOMP plots of the TD and  $\dot{T}D$  errors are created.

## II-2 Initialization (Straight-Line Segment Preceding Turn)

Input Parameters:  $v, \psi_1, x_1, y_1, T_S$

Output Parameters:  $\psi_0, \dot{x}_0, \dot{y}_0, x_0, y_0, \ddot{x}, \ddot{y},$   
 $T_0, T_{MAX}, \hat{T}D_{i-1}, \hat{T}D_{i-1}, \hat{a}_{n-1}, \psi_{n-1}$

At the start of the TD filter simulation the ship is on a straight-line, constant-speed course of duration  $T_S$  seconds. This is followed by a turn at the same constant speed and also at a constant angular rate. The values of  $\psi, x$  and  $y$  at the start of the turn are precomputed and are denoted by  $\psi_1, x_1$  and  $y_1$ .

The initial conditions for the straight-line segment are given by:

$$\psi_0 = \psi_1 \quad (2.1)$$

$$\dot{x}_0 = v \sin \psi_0 \quad (2.2)$$

$$\dot{y}_0 = v \cos \psi_0 \quad (2.3)$$

$$x_0 = x_1 - \dot{x}_0 T_S \quad (2.4)$$

$$y_0 = y_1 - \dot{y}_0 T_S \quad (2.5)$$

$$\ddot{x} = 0 \quad (2.6)$$

$$\ddot{y} = 0 \quad (2.7)$$

The times at the start and at the end of the straight-line segment,  $T_0$  and  $T_{MAX}$  are given by

$$T_0 = 0 \quad (2.8)$$

$$T_{MAX} = T_S \quad (2.9)$$

The quantities  $\hat{T}D_{i-1}$  and  $\hat{T}\dot{D}_{i-1}$  are required in Section II-7 to initialize the TD filter. These are obtained from

$$\hat{T}D_{i-1} = TD, \quad T = -dT_i \quad (2.10)$$

$$\hat{T}\dot{D}_{i-1} = T\dot{D}, \quad T = -dT_i \quad (2.11)$$

in which the  $TD$  and  $T\dot{D}$  computations are made in Section II-6.

Initializing values required in Section II-8 for the Heading Filter are given by

$$\hat{a}_{n-1} = 0 \quad (2.12)$$

$$\hat{\psi}_{n-1} = \psi_0 \quad (2.13)$$



### II-3 Initialization (Constant Speed and Radius Turn)

Input Parameters:  $v, \dot{\psi}_{\max}, \phi$

Input Variables:  $x, y, \psi, T$

Output Parameters:  $\dot{\psi}, x_0, y_0, \psi_0, a, T_0, T_{\max}$

At each way station in the chain, the angle,  $\phi$ , between the lines of bearing to the preceding and succeeding way stations is the angle through which the ship must turn in the neighborhood of the waypoint. We assume the turn is accomplished symmetrically about the waypoint and at the maximum turning rate of the ship,  $\dot{\psi}_{\max}$ . Then for the turning segment the ship's turning rate is

$$\dot{\psi} = \dot{\psi}_{\max}. \quad (3.1)$$

The normal acceleration of the ship is

$$a = v\dot{\psi}. \quad (3.2)$$

The initial values of  $x, y, \psi$  and  $T$  are obtained from current values of the simulation (i.e., at the end of the first straight-line segment) and these are denoted in

$$x_0 = x \quad (3.3)$$

$$y_0 = y \quad (3.4)$$

$$\psi_0 = \psi \quad (3.5)$$

$$T_0 = T \quad (3.6)$$

$T_{\max}$ , the value of  $T$  at the end of the turn is given by

$$TMAX = TO + \phi / \dot{\psi}_{max}. \quad (3.7)$$

#### II-4 Initialization (Straight-Line Segment Following Turn)

Input Parameters:  $v, T_S$

Input Variables:  $x, y, \psi, T$

Output Parameters:  $x_0, y_0, \dot{x}_0, \dot{y}_0, TO, TMAX$

At the completion of the waypoint turn, the ship proceeds in a straight line again for a prescribed period of time,  $T_S$ , whereupon the simulation run is concluded. The initial conditions for this segment are obtained from the simulation variables and given by

$$x_0 = x \quad (4.1)$$

$$y_0 = y \quad (4.2)$$

$$\psi_0 = \psi \quad (4.3)$$

$$TO = T \quad (4.4)$$

$$\dot{x}_0 = v \sin \psi_0 \quad (4.5)$$

$$\dot{y}_0 = v \cos \psi_0 \quad (4.6)$$

The terminating value of time is given by

$$TMAX = TO + T_S \quad (4.7)$$

## II-5 Track Generator

Input Parameters:  $x_0, y_0, \dot{x}_0, \dot{y}_0, T_0, \psi_0, \dot{\psi}, v, a$

Input Variables:  $T$

Output Variables:  $x, y, \dot{x}, \dot{y}, \ddot{x}, \ddot{y}$

The Track Generator computes the position, velocity and acceleration coordinates of the ship for prescribed values of the time. Two cases are considered: (1) constant speed and heading of the ship; (2) constant speed and turning radius of the ship. For the case of constant speed and heading, the formulas for the position coordinates are:

$$x = x_0 + \dot{x}_0(T-T_0) \quad (5.1)$$

$$y = y_0 + \dot{y}_0(T-T_0). \quad (5.2)$$

In (5.1) and (5.2)  $T$  denotes an arbitrary time and  $T_0$  denotes the (initial) time at the start of the straight-line run.

For a constant speed and constant turning rate the formulas are:

$$\psi = \psi_0 + \dot{\psi}(T-T_0) \quad (5.3)$$

$$\dot{x} = v \sin \psi \quad (5.4)$$

$$\dot{y} = v \cos \psi \quad (5.5)$$

$$\ddot{x} = a \cos \psi \quad (5.6)$$

$$\ddot{y} = -a \sin \psi \quad (5.7)$$

$$x = x_0 - \dot{y}/\dot{\psi} + (v/\dot{\psi}) \cos \psi_0 \quad (5.8)$$

$$y = y_0 + \dot{x}/\dot{\psi} - (v/\dot{\psi}) \sin \psi_0 \quad (5.9)$$

## II-6 TD Generator

Input Parameters:  $a_{11}$ ,  $a_{12}$ ,  $x_p$ ,  $y_p$ , TDP

Input Variables:  $x$ ,  $y$ ,  $\dot{x}$ ,  $\dot{y}$

Output Variables: TD,  $\dot{TD}$

The input variables to the TD Generator are the 'true' position and velocity coordinates of the ship obtained from the Track Generator. A TD (time difference) and its time derivative are computed as the linear combinations in

$$TD = TDP + a_{11}(x - x_p) + a_{12}(y - y_p) \quad (6.1)$$

$$\dot{TD} = a_{11} \dot{x} + a_{12} \dot{y}. \quad (6.2)$$

The coefficients  $a_{11}$  and  $a_{12}$  in (6.1) and (6.2) represent any of the two elements in the (two-or three-rowed) A-matrix which gives the linear relationship between TDs and ship's position coordinates. In other words, any of the two or three TDs may be represented in the simulation by the linear forms in (6.1) and (6.2)

The values of TD and  $\dot{TD}$  given by (6.1) and (6.2) represent the geometric part of these variables (assuming noise, truncation errors and biases are not present) for the purposes of the simulation. They are also used as the references or 'true' values for computing the errors  $\delta\hat{TD}$  and  $\delta\hat{\dot{TD}}$  defined in Section II-7. They are not to be confused with the surveyed TDs denoted by  $\overline{TD}_p$  in Ref. [3].

## II-7 TD Filter with Dead Reckoning

Input Parameters:  $\delta T_1$ ,  $\Delta T_A$ ,  $\Delta T_K$ , A, B, NSIGMA

Input Variables: T, TD,  $\dot{TD}$ ,  $\hat{\dot{TD}}$

Output Variables:  $\hat{TD}$ ,  $\hat{\dot{TD}}$ ,  $\delta\hat{TD}$ ,  $\delta\hat{\dot{TD}}$

Loran TD measurements are generated at intervals of  $\Delta T_K$  sec. A TD measurement available at time  $T_k$  is delayed or stale by  $\Delta T_A$  sec. The TD measurement is derived from ten equally-spaced TD samples, each of which is truncated to 10 nanosec. The TD measurement is taken to be the average of the ten samples, also truncated to 10 nanosec. The ten sample times,  $\tau_j$ ,  $j=1, \dots, 10$ , are given by

$$\tau_j = T_k - (\Delta T_A + 0.45\Delta T_K) + (j-1)\delta T_j \quad (7.1)$$

in which

$$\delta T_j = \Delta T_K / 10$$

is the time interval between TD samples. The time intervals  $\Delta T_K$ ,  $\Delta T_A$ ,  $\delta T_j$  and the discrete times  $\tau_j$ ,  $T_k$  and  $T_{k-1}$  are illustrated in Fig. II-2.

Let  $TD_j$  denote a true value of a TD at time  $\tau_j$  and  $XRAN_j$  the error in the TD sample. The TD sample, truncated to 10 nanosec (with the 5.0 nanosec truncation bias removed), is denoted by  $TDS_j$  and given by

$$TDS_j = 10[0.1(TD_j + XRAN_j)] + 5.0 \quad (7.2)$$

in which  $[x]$  denotes the integer part of  $x$ .

Finally, the TD measurement, which is the mean of the ten samples, truncated to 10 nanosec, is denoted by  $TDM$  and given by

$$TDM_k = 10[0.1(1/10) \sum_{j=1}^{10} TDS_j] + 5.0. \quad (7.3)$$

In the filter simulation the TD error  $XRAN$  was represented by a normally distributed random variable with zero mean and standard deviation denoted by  $NSIGMA$ .

The integration time step in the TD filter is denoted by  $dt_i$ . During intervals between TD measurements dead-reckoning equations are used to produce the filter outputs, denoted by  $\hat{T}D_i$  and  $\hat{\dot{T}}D_i$ , every  $dt_i$  seconds. The dead-reckoning equations are:

$$\hat{T}D_i = \hat{T}D_{i-1} + (\hat{T}D_{i-1} + 0.5 \hat{\dot{T}}D) dt_i \quad (7.4)$$

$$\hat{\dot{T}}D_i = \hat{\dot{T}}D_{i-1} + \hat{\ddot{T}}D dt_i \quad (7.5)$$

$$\hat{T}D_{i-1} = \hat{T}D_i \quad (7.6)$$

$$\hat{\dot{T}}D_{i-1} = \hat{\dot{T}}D_i \quad (7.7)$$

The value of  $\hat{\ddot{T}}D$  used in (7.4) and (7.5) is taken from the current output of the Heading Filter.

When a new TD measurement first becomes available a different set of filter equations are used to modify  $\hat{T}D_i$  and  $\hat{\dot{T}}D_i$ . In this circumstance the seven applicable filter equations are:

$$\hat{T}D'_k = \hat{T}D_i \quad (7.8)$$

$$\hat{\dot{T}}D'_k = \hat{\dot{T}}D_i \quad (7.9)$$

$$Z_k = TDM_k + \Delta T_A (\hat{T}D'_k + 0.5 \Delta T_A \hat{\dot{T}}D) - \hat{T}D'_k \quad (7.10)$$

$$\hat{T}D_k = \hat{T}D'_k + (A+B(\Delta T_A/\Delta T_K)) Z_k \quad (7.11)$$

$$\hat{\dot{T}}D_k = \hat{\dot{T}}D'_k + (B/\Delta T_K) Z_k \quad (7.12)$$

$$\hat{T}D_i = \hat{T}D_k \quad (7.13)$$

$$\hat{\dot{T}}D_i = \hat{\dot{T}}D_k \quad (7.14)$$

Finally, the errors in the outputs of the TD Filter are given by

$$\delta \hat{T}D = \hat{T}D_i - TD \quad (7.15)$$

$$\delta \dot{\hat{T}}D = \dot{\hat{T}}D_i - \dot{T}D \quad (7.16)$$

## II-8 Heading Filter

Input Parameters:  $\Delta T_L$ ,  $C$ ,  $a_{11}$ ,  $a_{12}$ ,  $v$

Input Variables:  $\psi$ ,  $\ddot{x}$ ,  $\ddot{y}$

Output Variables:  $\psi^t$ ,  $\hat{T}D$ ,  $\delta \hat{T}D$

The Heading Filter uses a measurement of ship's heading angle to produce a filtered value of ship's normal acceleration from which is obtained  $\hat{T}D$  used in the dead-reckoning computations in (7.4), (7.5) and (7.10) of the TD Filter. The time interval between heading measurements (and hence updates in the value of  $\hat{T}D$ ) is denoted by  $\Delta T_L$  and the measurement of ship's heading angle is delayed or stale by  $\Delta T_\psi$ .

The true value of ship's heading angle at time  $t=t_n$  is denoted by  $\psi_n$  and expressed in radians. To express the heading angle in degrees we write

$$\psi_n^o = \psi_n (180/\pi). \quad (8.1)$$

The measured  $\psi$  is expressed in degrees and truncated to the nearest whole degree. We convert this measured value back to radians and denote its value by  $\psi_n^t$ . We have

$$\psi_n^t = [\psi_n^o] (\pi/180) \quad (8.2)$$

and

$$\psi_{n-1}^t = [\psi_{n-1}^o] (\pi/180) \quad (8.3)$$

where  $\psi_{n-1}^t$  denotes the previously measured value of  $\psi$  at  $t=t_n - \Delta T_L$ .  
Let

$$\Delta\psi^t = \psi_n^t - \psi_{n-1}^t. \quad (8.4)$$

The filtered value of ship's normal acceleration, denoted by  $\hat{a}$ , is then given by

$$\hat{a}_n = \hat{a}_{n-1} + C(v(\Delta\psi^t/\Delta T_L) - \hat{a}_{n-1}). \quad (8.5)$$

The components of  $\hat{a}_n$  are

$$\hat{x}_n = \hat{a}_n \cos \psi_n^t \quad (8.6)$$

$$\hat{y}_n = -\hat{a}_n \sin \psi_n^t. \quad (8.7)$$

Then the filtered value of  $\ddot{T}D$  is obtained from

$$\hat{\ddot{T}D} = \hat{x}_n a_{11} + \hat{y}_n a_{12} \quad (8.8)$$

and

$$\ddot{T}D = \ddot{x} a_{11} + \ddot{y} a_{12}. \quad (8.9)$$

The error in  $\hat{\ddot{T}D}$  is given by



$$\delta \ddot{T}D = \hat{\ddot{T}}D - \ddot{T}D. \quad (8.10)$$

Finally,

$$\hat{a}_{n-1} = \hat{a}_n \quad (8.11)$$

$$\psi_{n-1} = \psi_n. \quad (8.12)$$

#### II-9 CALCOMP Plots

At the conclusion of the simulation control is passed to block 9 in which the tapes for creating the CALCOMP plots are made. In this block the means and standard deviations of the TD error and its derivative are also computed.

After a plot tape is made the program reads the input tape to see if there is another simulation to be made.

# U.S.C.G LORAN-C TD FILTER SIMULATION

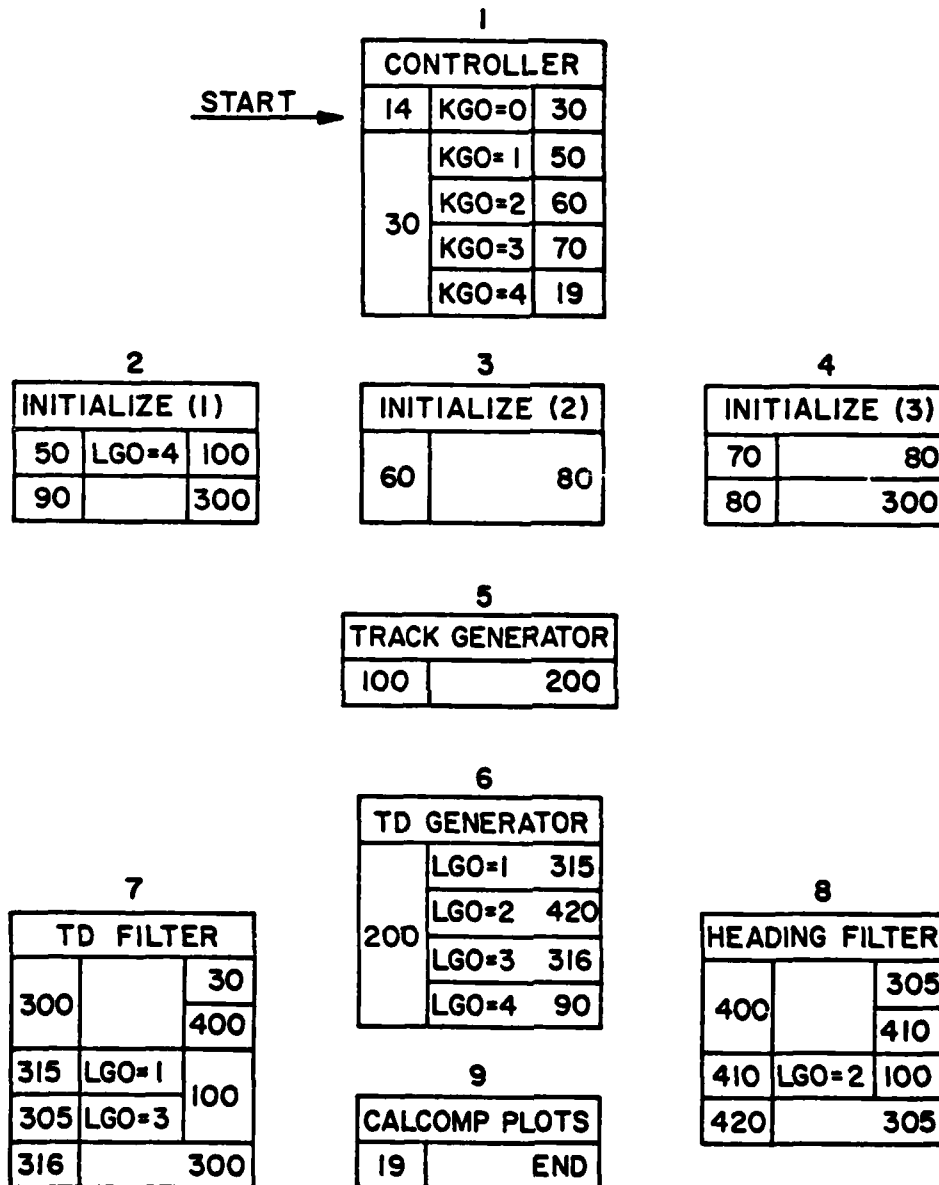
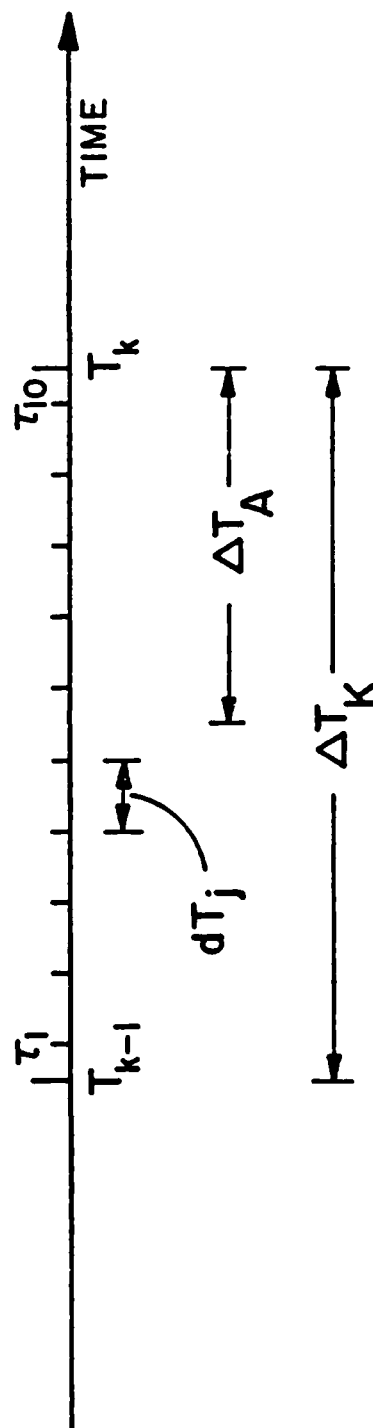


FIG. II-1

# PRINCIPAL TD MEASUREMENT PARAMETERS



$\Delta T_k$  TIME INTERVAL BETWEEN TD MEASUREMENTS

$dT_j$  TIME INTERVAL BETWEEN TD SAMPLES

$\Delta T_A$  TIME DELAY IN TD MEASUREMENT

FIG. II-2

### III FILTER PERFORMANCE

The waypoint chosen for the sample simulations presented in this section was numbered 2 in the numbering scheme employed in the spring of 1979. This was the second waypoint on the downbound summer route and required a turn through 64.5 deg.

Numerical values of system parameters common to all simulations reported here are given in Table III-1. The turn, executed at 0.5 deg/sec, required 129.0. sec. Straight-line runs of 10 sec preceded and followed the turn. Therefore a simulation run extended over an interval of 149 sec.

In Plots 1, 2, 3 and 4 the gain C in the Heading Filter is given the values 0, 0.2, 0.5, 0.9, respectively. The means and standard deviations of the TD error and its derivative for these four simulations are tabulated in Table III-2.

In each of the four plots the scale for the TD error in nanosec is given at the left of the plot and the TD error scale in nanosec/sec is on the right. Observe the changes in scale which occur in going from plot to plot.

In each plot the lower curve, which also has the larger-amplitude, high-frequency oscillations, represents the TD error.

In Plot #1 the gain C in the heading filter is zero, so that this run corresponds to the conventional second-order filter without acceleration-aiding. Note the large velocity lag (TDDT error) which exists at the end of the run. The TD error is nearly 240 nanosec - a value much too large to be tolerated.

In Plots #2, 3, and 4 as the gain C is increased the TD error is correspondingly decreased.

While the runs shown in the plots represent the case of a critically damped filter (compare values of A and B in Table III-1

with a and b in Table I-1) we do not intend to imply that this is the 'best' choice of filter gains for an operational system. They are presented because they indeed exhibit the behavior one might expect of a critically damped filter and thus add to our confidence in the simulation.

Table III-1  
Numerical Values of System Parameters

$v$	=	10.0 knots
$\psi_{\max}$	=	0.5 deg/sec
$dT_i$	=	0.01 sec
$dT_\psi$	=	0.5 sec
$\Delta T_A$	=	0.5 sec
$\Delta T_K$	=	1.0 sec
$\Delta T_L$	=	1.0 sec
$A$	=	0.04422
$B$	=	0.0005
$NSIGMA$	=	5.0 nanosec

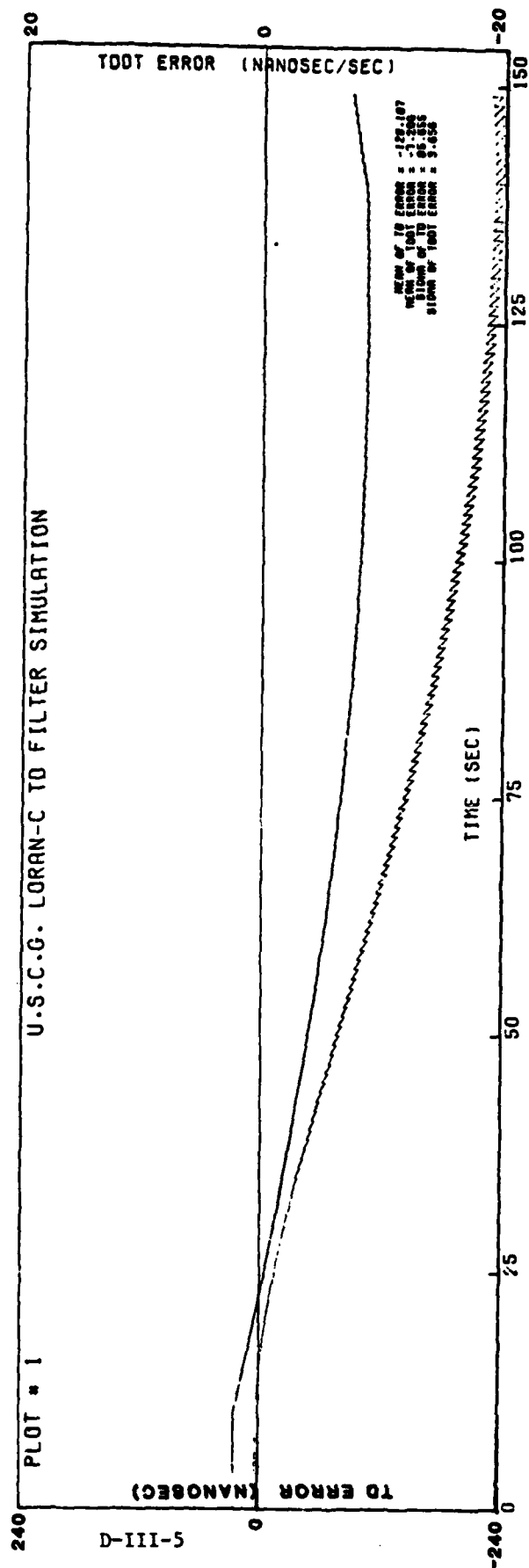
Table III-2  
Mean and Standard Deviation of  
TD Error and TD Error

Plot	C	TD ERROR*			TD ERROR**	
		Mean	Std. Dev.		Mean	Std. Dev.
1	0	-128.107	85.655		-7.200	3.656
2	0.2	-10.273	5.855		-0.468	0.319
3	0.5	-4.974	3.361		-0.215	0.180
4	0.9	-3.390	2.643		-0.142	0.137

\* Nanosec

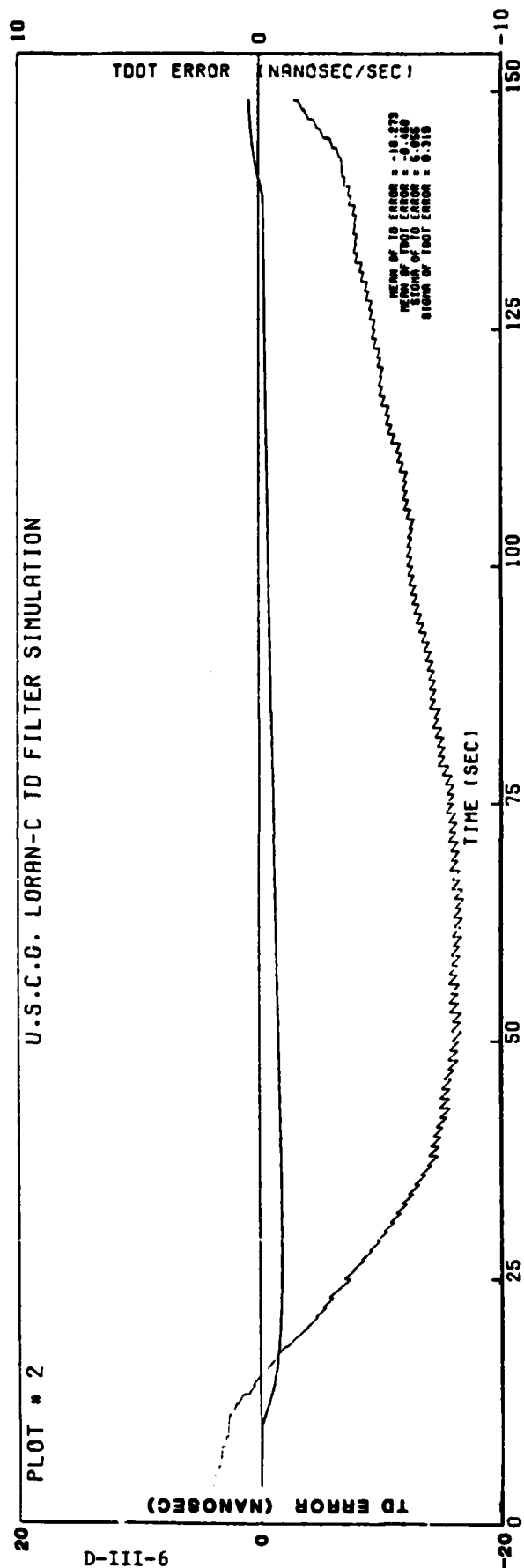
\*\* Nanosec/sec

S2R-79-166  
 Section III  
 Page -5-

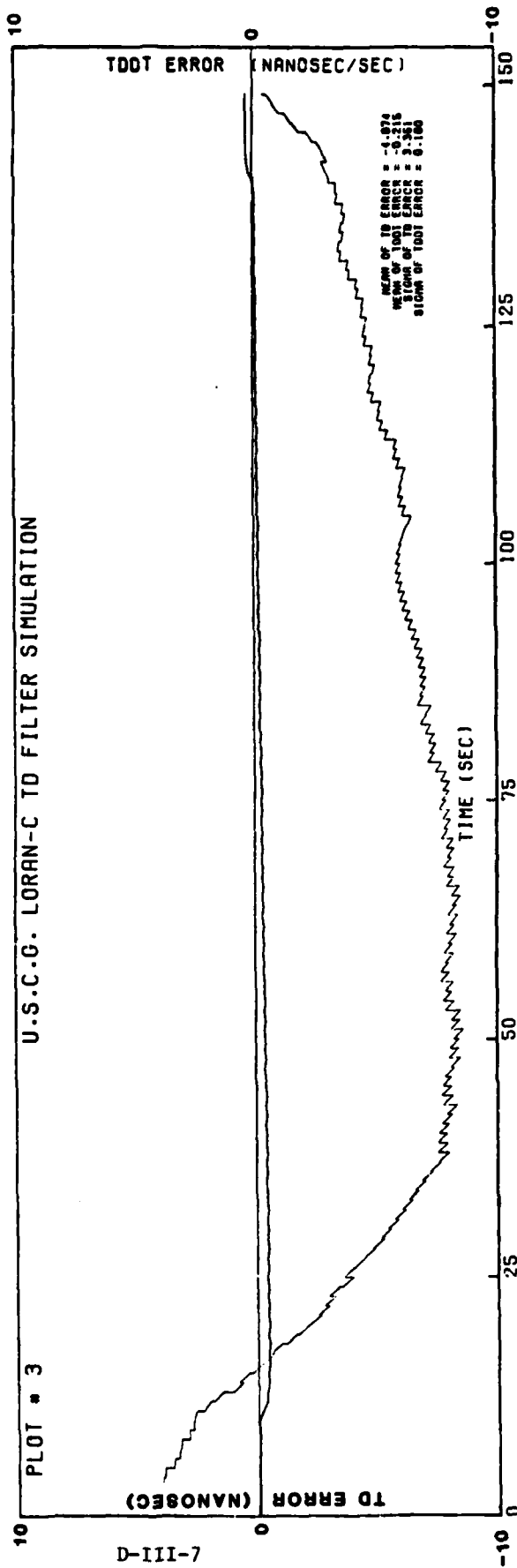




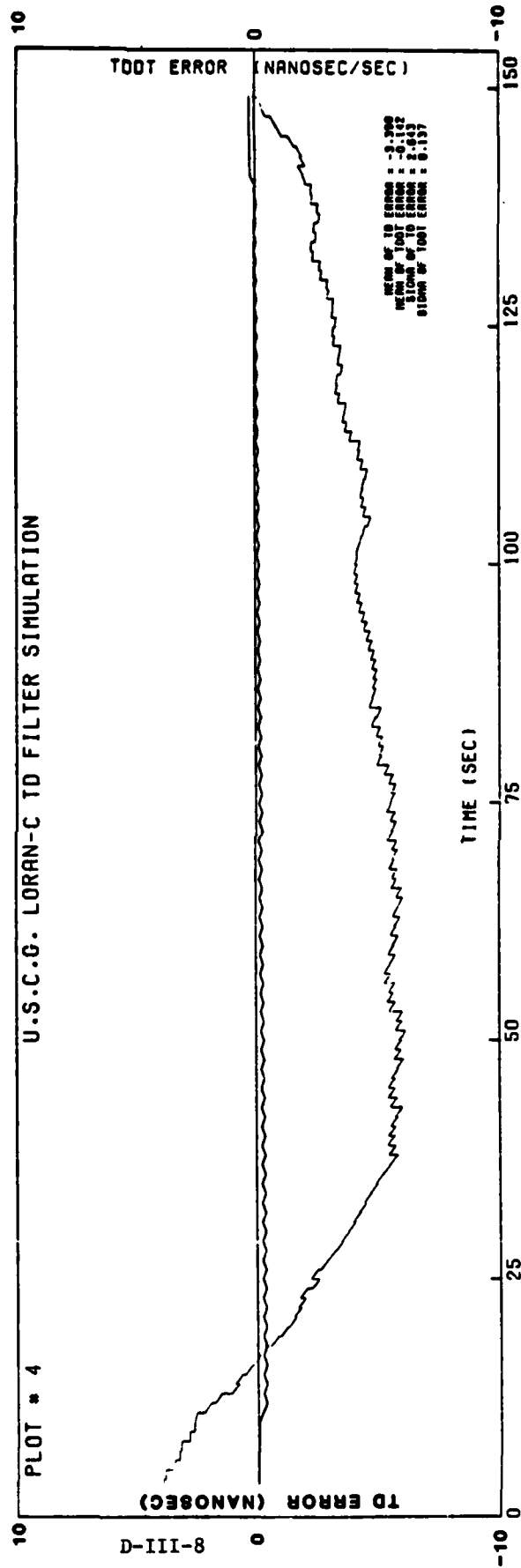
S2R-79-166  
 Section III  
 Page -6-



S2R-79-166  
 Section III  
 Page -7-



S2R-79-166  
 Section III  
 Page -8-



S2R-79-169  
ZT70S2R0  
October 30, 1979

TO: C. R. Edwards

FROM: V. Schwab

SUBJECT: The Effect of Uncompensated TD Truncation Biases  
on TD and TD Errors in the USCG LORAN-C HHE  
Navigation Program

REFERENCE: S2R-79-166, Design, Simulation and Performance of  
Digital TD and Heading Filter for the USCG LORAN-C  
HHE Navigation Program, by L. J. Levy and V. Schwab,  
October 22, 1979

In the USCG LORAN-C HHE Navigation Program a 10-nanosec truncation is performed on each of ten equally-spaced TD samples which are then averaged in the receiver. The average of the ten truncated samples is itself then truncated at the 10-nanosec level to produce a TD measurement. The truncation of the samples produces a 5.0-nanosec bias in the average and the truncation of the average creates an additional 5.0 nanosec bias in the TD measurement for a total bias of 10 nanosec.

It is desirable to compensate for these biases and quite easy to do so. A compensation of 5.0 nanosec should be added either to each TD sample in the receiver or to the average of the ten TD samples before it is truncated. Then the truncated average should be compensated by the addition of 5.0 nanosec. However if separate 5.0-nanosec compensations are not made to the samples and the measurement, a single 10.0-nanosec compensation may be added to the measurement with almost equal beneficial effect.

IBM 3033 Computer Simulations Which Show the Effect of Compensated and Uncompensated Truncation Biases

The USCG TD Filter Simulation Program described in the reference was used to study the behavior of TD and  $\dot{T}$ D errors in the presence of biases, uncompensated and compensated, resulting from TD sample and measurement truncations.

In Table 1 the results of five simulation runs are shown. The filter gains and system constants, defined in the reference memorandum, had the same values indicated in the Table in each of the five runs. What was varied from run to run were the compensations made for the biases resulting from the sample and measurement truncations.

In Run 1 no compensation is made for truncation bias and the mean of the TD error is 11.268 nanosec - close to the total 10.0-nanosec bias present in the TD measurement.

In Runs 2 and 3 the sample and measurement truncations are compensated, but not both in the same run. As a result the mean TD errors are not far from the expected 5.0 nanosec bias.

The proper compensations for the truncation biases are made in Run 4 and here the mean TD error is less than a quarter of a nanosec.

The single 10.0-nanosec compensation made in Run 5 is not quite as effective as the dual compensations of Run 4; still, the mean TD error in this case is only a little greater than one nanosec.

The simulations in Table 1 were made for a stationary ship ( $V=0$ ) and no heading filter was used ( $C=0$ ). The filter was slightly underdamped ( $B>0.005$ ).

*V. Schwab*  
\_\_\_\_\_  
V. Schwab

VS:nt

TABLE 1  
THE EFFECTS OF BIASES DUE TO 10-NANOSEC  
TRUNCATIONS OF TD SAMPLES AND MEASUREMENTS  
IN USCG LORAN-C HHE NAVIGATION PROGRAM

RUN	SAMPLE TRUNCATION	MEASUREMENT TRUNCATION	TD ERROR* (NANOSEC)		TD ERROR* (NANOSEC/SEC)	
			MEAN	STD DEV.	MEAN	STD DEV.
1	UNCOMPENSATED	UNCOMPENSATED	11.268	1.780	0.061	0.131
2	COMPENSATED (5)	UNCOMPENSATED	5.252	0.872	0.029	0.057
3	UNCOMPENSATED	COMPENSATED (5)	6.240	1.466	0.033	0.088
4	COMPENSATED (5)	COMPENSATED (5)	0.225	0.711	0.002	0.031
5	SINGLE COMPENSATION (10)		1.212	1.395	0.005	0.066

Filter Gains: A = 0.13642      System Constants: DTI = 0.01      V = 0.0  
 B = 0.0075      DTPSI = 0.5      PSIDOT = 0.0  
 C = 0.0      DTA = 0.5      NSIGMA = 8.0  
 DELTK = 1.0  
 DELTL = 1.0

E-3

\*THREE-MINUTE AVERAGES

S2R-79-187  
ZT70S2R0  
November 20, 1979

TO: C. R. Edwards

FROM: L. J. Levy/V. Schwab

SUBJECT: Formulas for Making Short-Range Predictions of Ship's Course in the USCG LORAN-C HHE Navigation Program

REFERENCES: [1] APL/JHU S2R-79-162, Methods for Obtaining Approximate and Exact Solutions to a LORAN Navigation Equation, by L. J. Levy and V. Schwab, October 8, 1979

[2] APL/JHU S2R-79-166, Design, Simulation and Performance of Digital TD and Heading Filters for the USCG LORAN-C HHE Navigation Program, by L. J. Levy and V. Schwab, October 22, 1979

It may prove helpful to a pilot in steering his ship to provide him with pictures (CRT displays) of the predicted position of the ship a short time into the future. By observing how the predicted position responds to changes in engine speed and rudder position he may be significantly aided in anticipating the maneuvers required to follow a prescribed or desired course.

The purpose of this memorandum is to provide the formulas for making simple short-range predictions of ship position based on: present ship's velocity alone; present ship's velocity as well as present turning rate. We consider how the initial conditions of position and velocity might be derived from LORAN-C measurements. It is proposed that initial turning rate be obtained from filtered differences of gyrocompass readings.

1. Formulas for Predicting Ship's Course

We define the following terms:

$x_0, y_0$  present cartesian position coordinates of the ship  
 $\dot{x}_0, \dot{y}_0$  present velocity coordinates of the ship  
 $\psi_0$  present heading angle of the ship (measured clockwise from north)  
 $\dot{\psi}_0$  present turning rate of the ship  
 $v_0$  present speed of the ship  
 $T$  time interval over which course predictions are to be made  
 $D$  distance interval over which course predictions are to be made  
 $\Delta t$  time interval between predictions  
 $t(k)$  time of  $k^{\text{th}}$  prediction ( $k=0,1,2,\dots,KMAX$ )  
 $\Delta x(k), \Delta y(k)$  predicted coordinates of the ship at time  $t(k)$  relative to predicted position at time  $t(k-1)$ .

Initially ( $t(0)=0$ ) the ship is at  $x=x_0$  and  $y=y_0$ . At  $t(1)=\Delta t$  the predicted coordinates are  $x_1=x_0+\Delta x(1)$  and  $y_1=y_0+\Delta y(1)$ ; at  $t(2)=2\Delta t$ ,  $x_2=x_0+\Delta x(1) + \Delta x(2)$  and  $y_2=y_0+\Delta y(1) + \Delta y(2)$ . We shall compute the increments  $\Delta x(k)$  and  $\Delta y(k)$  rather than  $x_k$  and  $y_k$  since the CRT plotter makes use of these increments. We consider two cases: one in which the prediction is based upon the ship's present translational velocity alone and the other in which account is also taken of the present turning rate of the ship.

Given:  $x_0, y_0, \dot{x}_0, \dot{y}_0, T$  or  $D$

Compute:

$$\Delta t = T/KMAX \text{ or } \Delta t = D/(KMAX v_0)$$



$$v_0 = \sqrt{\dot{x}_0^2 + \dot{y}_0^2}$$

DO 1 K=1, KMAX

$$t(K) = K\Delta t$$

$$\Delta x(K) = \dot{x}_0 \Delta t$$

$$1 \Delta y(K) = \dot{y}_0 \Delta t$$

Given:  $x_0, y_0, \dot{x}_0, \dot{y}_0, \dot{\psi}_0, T \text{ or } D$

Compute:

$$\Delta t = T/KMAX \text{ or } \Delta t = D/(KMAX v_0)$$

$$\Delta \psi = \dot{\psi}_0 \Delta t$$

$$v_0 = \sqrt{\dot{x}_0^2 + \dot{y}_0^2}$$

$$\sin \psi_0 = \dot{x}_0/v_0$$

$$\cos \psi_0 = \dot{y}_0/v_0$$

$$\sin \Delta \psi = \Delta \psi - \Delta \psi^3/3! + \dots$$

$$\cos \Delta \psi = 1 - \Delta \psi^2/2! + \dots$$

DO 2 K=1, KMAX

$$\sin \psi = \sin \psi_0 \cos \Delta \psi + \cos \psi_0 \sin \Delta \psi$$

$$\cos \psi = \cos \psi_0 \cos \Delta \psi - \sin \psi_0 \sin \Delta \psi$$

$$t(K) = K\Delta t$$

$$\Delta x(K) = (v_0/\dot{\psi}_0) [\cos \psi_0 - \cos \psi]$$

$$\Delta y(K) = (v_0/\dot{\psi}_0) [\sin \psi_0 - \sin \psi]$$

$$\sin \psi_0 = \sin \psi$$

$$2 \cos \psi_0 = \cos \psi$$

## 2. Source of $x_0$ and $y_0$

The present horizontal coordinates of the ship,  $x_0$  and  $y_0$ , are obtained as the exact solution

$$\begin{bmatrix} x_0 \\ y_0 \end{bmatrix} = \underline{z}_Q$$

of equation (4.1) of Ref. [1]. The iterative scheme for obtaining  $\underline{z}_Q$  is given by (4.12).

## 3. Source of $\dot{x}_0$ and $\dot{y}_0$

It would be possible to produce  $\dot{x}_0$  and  $\dot{y}_0$  as the exact solution  $\dot{\underline{z}}_Q$ , of a LORAN rate equation analogous to (4.1). For the intended purpose that accuracy is not required and the computational burden could not be justified. On the other hand the linear G-matrix approach would probably result in errors that are larger than we can stand.

Instead we recommend that the x- and y- outputs of the LORAN equation be differentiated and then passed through a first-order filter to produce  $\dot{x}_0$  and  $\dot{y}_0$ . In Ref. [2] the time interval between TD updates is denoted by  $\Delta T_K$ . We shall assume here that predictions based on the updated values of  $x_0$  and  $y_0$  are to be made

at the same time frequency. We denote the differentiated LORAN position outputs,  $x_0$  and  $y_0$ , by  $\dot{x}_0^*$  and  $\dot{y}_0^*$  and write

$$\dot{x}_0^* = \frac{x_0(t) - x_0(t - \Delta T_K)}{\Delta T_K}$$

$$\dot{y}_0^* = \frac{y_0(t) - y_0(t - \Delta T_K)}{\Delta T_K}$$

The filtered velocity coordinates  $\dot{x}_0(t)$  and  $\dot{y}_0(t)$  are then obtained from the first-order filter equations

$$\dot{x}_0(t) = \dot{x}_0(t - \Delta T_K) + H[\dot{x}_0^* - \dot{x}_0(t - \Delta T_K)]$$

$$\dot{y}_0(t) = \dot{y}_0(t - \Delta T_K) + H[\dot{y}_0^* - \dot{y}_0(t - \Delta T_K)]$$

in which the gain constant  $H$  will be chosen to produce the desired performance of the predictor.  $H$  will depend on the gain settings in the TD filter which control the noise levels in  $x_0$  and  $y_0$ .

#### 4. Source of $\dot{\psi}_0$

The first-order heading filter which supplies a filtered value of  $\ddot{\psi}$  is defined by equation (8.5) of Section II of Ref. [2] and is reproduced below:

$$\hat{a}_n = \hat{a}_{n-1} + C[v(\Delta\psi^t/\Delta T_L) - \hat{a}_{n-1}].$$

In the equation above  $\hat{a}_n = v\dot{\psi}$  is the filtered acceleration normal to the path of the ship, C is the gain constant, v denotes ship's speed,  $\Delta T_L$  is the time interval between  $\hat{a}_n$  and  $\hat{a}_{n-1}$  and  $\Delta\psi^t$  denotes the difference of truncated gyrocompass readings.

One possibility for obtaining  $\dot{\psi}_0$  for the predictor would be to use the formula

$$\dot{\psi}_0 = \hat{a}_n / v_0 = \hat{a}_n / \sqrt{\dot{x}_0^2 + \dot{y}_0^2}.$$

The possible disadvantage resulting from this source for  $\dot{\psi}_0$  is the value of C used in the  $\hat{a}$ -filter. For the TD-filter a large value of C (near unity) is to be preferred in order to obtain a rapid response to a turn. For the predictor application, a smaller value of C might prove to be a better choice. Therefore we recommend that the following separate  $\dot{\psi}_0$ -filter be employed for the predictor:

$$\dot{\psi}_0(t) = \dot{\psi}_0(t - \Delta T_L) + K[\Delta\psi^t / \Delta T_L - \dot{\psi}_0(t - \Delta T_L)].$$

In the equation above K denotes the gain constant and  $\Delta\psi^t$  is the same term which appears in the heading filter.

L. J. Levy  
L. J. Levy

V. Schwab  
V. Schwab

LJL/VS:nt

S2R-79-189  
ZT70S2R0  
November 26, 1979

TO: C. R. Edwards

FROM: V. Schwab

SUBJECT: Additional Performance Evaluations for the Second-Order a,b-Filter

REFERENCE: S2R-79-166 Design, Simulation and Performance of Digital TD and Heading Filters for the USCG LORAN-C HHE Navigation Program, by L. J. Levy and V. Schwab, October 22, 1979

In Table I-1 of the reference, reproduced in this memorandum, we present evaluations of some of the performance characteristics of the a,b-filter used to filter LORAN TDs in the USCG HHE Navigation Program. Table I-1 offers examples of two filter designs: (1) a critically-damped filter defined by the gain relation,  $4b=(a+b)^2$ ; (2) an optimum filter, defined by the gain relation,  $b=a^2/(2-a)$ , which results in a slightly underdamped filter.

We have added to Table I-1 a third case in which the rate gain b is chosen to be the mean of the values of the first two cases, i.e.,  $b=0.5\{2-a-2\sqrt{1-a}+a^2/(2-a)\}$ .

V. Schwab  
V. Schwab

VS:nt

Table I-1

Summary of Some Characteristics of  
The Second-Order Filter

Critically Damped Filter:  $4b = (a+b)^2$

a	b	$\sigma_{POS}$	$\sigma_{VEL}$	FILTER TIME CONSTANT	
				No. of $\Delta t$ s	(SEC) *
.6400	.1600	$.713\sigma_N$	$.177\sigma_N/\Delta t$	1	.5
.3392	.0350	$.487\sigma_N$	$.0469\sigma_N/\Delta t$	4	2
.1800	.0089	$.345\sigma_N$	$.0156\sigma_N/\Delta t$	10	5
.13642	.0050	$.298\sigma_N$	$.0099\sigma_N/\Delta t$	13	6.5
.1100	.0032	$.267\sigma_N$	$.0070\sigma_N/\Delta t$	17	8.5
.04422	.0005	$.167\sigma_N$	$.0017\sigma_N/\Delta t$	44	22

Optimum Filter:  $b = a^2/(2-a)$

a	b	$\sigma_{POS}$	$\sigma_{VEL}$	FILTER TIME CONSTANT	
				No. of $\Delta t$ s	(SEC) *
.6400	.3010	$.738\sigma_N$	$.342\sigma_N/\Delta t$	1	.5
.3392	.0690	$.519\sigma_N$	$.093\sigma_N/\Delta t$	2	1
.1800	.0178	$.373\sigma_N$	$.031\sigma_N/\Delta t$	4	2.0
.13642	.0100	$.324\sigma_N$	$.0198\sigma_N/\Delta t$	5	2.5
.1100	.0064	$.290\sigma_N$	$.0141\sigma_N/\Delta t$	6	3
.04422	.0010	$.183\sigma_N$	$.0034\sigma_N/\Delta t$	17	8.5

\*Assuming  $\Delta t = 0.5$  sec

$\sigma_N = \sigma$  of measured noise

$\Delta t =$  time interval between updates

Table I-1 (Cont'd)

Mean of Critically Damped and Optimum Filters

$$b = (1/2)\{2-a - 2\sqrt{1-a} + a^2/2-a\}.$$

a	b	$\sigma_{pos}$	$\sigma_{vel}$	FILTER TIME CONSTANT	
				No. of $\Delta t$ s	(sec)
.64000	.23059	$.725\sigma_N$	$.258\sigma_N/\Delta t$	1	.5
.33920	.05214	$.504\sigma_N$	$.070\sigma_N/\Delta t$	2	1
.18000	.01336	$.359\sigma_N$	$.023\sigma_N/\Delta t$	4	2.0
.13642	.00749	$.311\sigma_N$	$.015\sigma_N/\Delta t$	5	2.5
.11000	.00480	$.279\sigma_N$	$.011\sigma_N/\Delta t$	7	3.5
.04422	.00075	$.175\sigma_N$	$.0026\sigma_N/\Delta t$	18	9.0

S2R-79-200  
ZT70S2R0  
December 18, 1979

TO: C. R. Edwards

FROM: L. J. Levy/V. Schwab

SUBJECT: Exact Method for Obtaining Horizontal Components of Ship's Velocity from TD Measurements

REFERENCES: [1] S2R-79-187, Formulas for Making Short-Range Predictions of Ship's Course in the USCG LORAN-C HHE Navigation Program, by L. J. Levy and V. Schwab, November 20, 1979

[2] S2R-79-162, Methods for Obtaining Approximate and Exact Solutions to a LORAN Navigation Equation, by L. J. Levy and V. Schwab, October 8, 1979

[3] S2R-79-008, G-Matrix Analysis for USCG LORAN-C HHE Navigation Program, by L. J. Levy and V. Schwab, January 19, 1979

In Ref. [1] we proposed that the horizontal velocity components of the ship be determined by passing differentiated navigated positions through first-order filters. The alternative method, much to be preferred if the computing capacity is available, is to make use of the relation

$$\dot{\underline{Z}}_Q = G_Q \dot{\underline{TD}}_Q$$

in which  $\dot{\underline{TD}}_Q$  is the vector of TD time derivatives obtained from the LORAN TD filter and  $G_Q$  is the G-matrix evaluated at  $\underline{Z}=\underline{Z}_Q$ , the current navigated position of the ship. In this method, the velocity computation is performed after the position fix has been obtained (i.e., after the value of  $\underline{Z}_Q$  has been determined by means of the iterative procedure outlined in Section 4 of Ref. [2]). The relation given above between  $\dot{\underline{Z}}_Q$  and  $\dot{\underline{TD}}_Q$  is exact since  $G_Q$  is evaluated at  $\underline{Z}=\underline{Z}_Q$ . It



therefore fully exploits the velocity information contained in the TDs that are generated by the TD filter.

In the following sections we list the computations required to produce  $\dot{\underline{z}}_Q$  for the cases where there are three and two TD measurements available.

### 1. Velocity Computation Employing Three TDs

In the notation of Ref. [3], the linearized relation between horizontal position, represented by the 2x1 vector  $\underline{z}$ , and LORAN time differences, represented by the 3x1 vector  $\underline{TD}$ , is given by

$$\underline{TD}_Q - \underline{TD}_p = A_p (\underline{z}_Q - \underline{z}_p). \quad (1.1)$$

In (1.1) the elements of the 3x2  $A_p$ -matrix depend upon  $\underline{z}_p$  and the coordinates of the master and slave stations. If we 'solve' (1.1) for  $(\underline{z}_Q - \underline{z}_p)$  we obtain

$$\underline{z}_Q - \underline{z}_p = G_p (\underline{TD}_Q - \underline{TD}_p) \quad (1.2)$$

in which  $G_p = (A_p A_p^T)^{-1} A_p^T$ .

Equations (1.1) and (1.2) are linear approximations in which p denotes a fixed waypoint and Q a variable nearby point. If we differentiate (1.2) with respect to the time we obtain the approximation

$$\dot{\underline{z}}_Q \approx G_p \dot{\underline{TD}}_Q. \quad (1.3)$$

However, at p=Q equation (1.3) becomes exact, i.e.,

$$\dot{\underline{z}}_Q = G_Q \dot{\underline{TD}}_Q \quad (1.4)$$

and provides the basis for the computation of ship's velocity. In Section 3 we present a comparison of numerical results obtained by means of (1.3) and (1.4).

We next list the equations used to compute the elements of the  $G_Q$  matrix. First let

$$\underline{z}_Q = \begin{bmatrix} x_Q \\ y_Q \end{bmatrix} \quad (1.5)$$

represent the navigated horizontal position coordinates of the ship. Then  $r_1$  denotes the slant range from the point Q to the master station  $(x_m, y_m)$  and  $r_{2j}$  the slant range from the point Q to the  $j^{\text{th}}$  slave station  $(x_j, y_j)$ . Evidently

$$r_1 = \left[ (x_Q - x_m)^2 + (y_Q - y_m)^2 \right]^{1/2}$$

$$r_{2j} = \left[ (x_Q - x_j)^2 + (y_Q - y_j)^2 \right]^{1/2}, \quad j=1,2,3.$$

The elements of the  $A_Q$ -matrix are

$$A_{Qj1} = \frac{1}{v} \left[ \frac{x_Q - x_j}{r_{2j}} - \frac{x_Q - x_m}{r_1} \right], \quad j=1,2,3$$

$$A_{Qj2} = \frac{1}{v} \left[ \frac{y_Q - y_j}{r_{2j}} - \frac{y_Q - y_m}{r_1} \right], \quad j = 1,2,3$$

where  $v$  denotes the signal propagation velocity.

Next let

$$D11 = AQ11^2 + AQ21^2 + AQ31^2$$

$$D12 = AQ11 \cdot AQ12 + AQ21 \cdot AQ22 + AQ31 \cdot AQ32$$

$$D21 = D12$$

$$D22 = AQ12^2 + AQ22^2 + AQ32^2$$

$$\Delta = D22 \cdot D11 - D21 \cdot D12.$$

Then

$$GQ1j = (D22 \cdot AQj1 - D21 \cdot AQj2) / \Delta, \quad j=1,2,3$$

$$GQ2j = (D11 \cdot AQj2 - D12 \cdot AQj1) / \Delta, \quad j=1,2,3.$$

Finally

$$\dot{x}_Q = GQ11 \cdot \dot{TD1} + GQ12 \cdot \dot{TD2} + GQ13 \cdot \dot{TD3}$$

$$\dot{y}_Q = GQ21 \cdot \dot{TD1} + GQ22 \cdot \dot{TD2} + GQ23 \cdot \dot{TD3}.$$

## 2. Velocity Computation Employing Two TDs

In Section 1 it was assumed that three  $\dot{TD}s$ ,  $\dot{TD1}$ ,  $\dot{TD2}$  and  $\dot{TD3}$  were available to determine  $\dot{x}_Q$  and  $\dot{y}_Q$ . Here we shall assume that only two are available and these two we shall denote by  $\dot{TDj}$  and  $\dot{TDk}$ . The possible values for  $j$  and  $k$  are the pairs:

$$j = 1, \quad k = 2$$

$$j = 1, \quad k = 3$$

$$j = 2, \quad k = 3$$

No other values of  $j$  and  $k$  are admitted.

AQ is the 2x2 matrix

$$AQ = \begin{bmatrix} AQj1 & AQj2 \\ AQk1 & AQk2 \end{bmatrix}$$

whose elements are defined by expressions given in Section 1. Let

$$\Delta = AQj1 \cdot AQk2 - AQk1 \cdot AQj2$$

and

$$GQ11 = AQk2/\Delta$$

$$GQ21 = -AQk1/\Delta$$

$$GQ12 = -AQj2/\Delta$$

$$GQ22 = AQj1/\Delta.$$

Then

$$\dot{x}_Q = GQ11 \cdot \dot{T}Dj + GQ12 \cdot \dot{T}Dk$$

$$\dot{y}_Q = GQ21 \cdot \dot{T}Dj + GQ22 \cdot \dot{T}Dk$$

### 3. Comparison of Numerical Results Obtained Using $G_p$ and $G_Q$ Matrix

In this section we compare numerical results computed for the St. Mary's River LORAN-C mini chain using equations (1.3) and (1.4) of Section 1. The approximation given by (1.3) which uses the  $G_p$  matrix would offer some advantages in that the  $G_p$  matrices are precomputed and stored on tape. However, as we shall see, the errors in the velocity determined by means of the  $G_p$  matrix can be quite large.

In Table I we list the along-track (ATE) and cross-track (CTE) navigation errors in position and velocity at a number of points in the St. Mary's River. The index I denotes the waypoint number and K=1 means downbound, summer. S denotes linear distance between successive waypoints and ITER represents the number of iterations of the navigation computation. The navigation position errors are expressed in feet.

The navigation velocity errors in Table I are zero since the  $G_Q$ -matrix is used to compute  $\underline{\dot{Z}}$ . The components of ship's velocity remain constant between successive waypoints and ship's speed is 12 mph.

Table II is the same as Table I except that the  $G_p$ -matrix is used to compute  $\underline{\dot{Z}}$ . In this case the along-track and cross-track velocity errors are no longer zero but increase monotonically with S.

  
L. J. Levy

  
V. Schwab

LJL/VS:nt  
Distribution  
GEBaer  
CREdwards  
WDKelley, Jr.  
LJLevy  
JBMoffett  
JNagrant  
BSOgorzalek  
VSchwab  
JETarr  
TThompson  
JGWall (5)  
Archives  
S2R File

Table I  
(Q-Matrix)

S2R-79-200  
Page -7-

EXACT SOLUTIONS OF LUNAR EQUATIONS FOR HORIZONTAL POSITION AND VELOCITY COORDINATES

I	K	S (KYDS)	ITER	ATE (FT)	CTE (FT)	ITER	ATE (MPH)	CTE (MPH)	XDOT (MPH)	YDOT (MPH)
1	1	0.0	1	0.0	0.0	0	0.00000	0.00000	7.95	-8.96
1	1	1.10	3	0.03	-0.01	0	0.00000	0.00000	7.95	-8.96
1	1	2.20	5	0.03	-0.00	0	0.00000	-0.00000	7.95	-8.96
1	1	3.30	6	-0.11	0.01	0	0.00000	-0.00000	7.95	-8.96
1	1	4.40	7	0.22	-0.03	0	0.00000	-0.00000	7.95	-8.96
1	1	5.50	9	0.22	-0.02	0	0.00000	0.00000	7.95	-8.96
1	1	6.60	11	0.20	-0.02	0	0.00000	-0.00000	7.95	-8.96
1	1	7.70	13	0.23	-0.02	0	0.00000	0.00000	7.95	-8.96
1	1	8.80	15	0.24	-0.03	0	-0.00000	-0.00000	7.95	-8.96
1	1	9.90	17	0.37	-0.02	0	0.00000	-0.00000	7.95	-8.96
1	1	11.00	19	0.49	-0.04	0	-0.00000	-0.00000	7.95	-8.96
1	1	11.19	20	-0.37	0.03	0	0.00000	-0.00000	7.95	-8.96
2	1	0.0	1	0.0	0.0	0	0.00000	-0.00000	11.53	3.32
2	1	1.00	3	0.00	0.00	0	0.00000	-0.00000	11.53	3.32
2	1	2.00	4	-0.01	-0.01	0	0.00000	0.00000	11.53	3.32
2	1	3.00	5	0.02	0.01	0	0.00000	-0.00000	11.53	3.32
2	1	4.00	6	-0.03	-0.02	0	-0.00000	-0.00000	11.53	3.32
2	1	5.00	7	0.04	0.03	0	-0.00000	0.00000	11.53	3.32
2	1	5.42	7	0.08	0.05	0	-0.00000	-0.00000	11.53	3.32
3	1	0.0	1	-0.00	-0.00	0	-0.00000	0.00000	10.64	5.56
3	1	0.80	2	-0.02	-0.02	0	-0.00000	0.00000	10.64	5.56
4	1	0.0	1	-0.00	-0.00	0	-0.00000	-0.00000	5.27	10.78
4	1	1.00	2	0.00	0.00	0	-0.00000	-0.00000	5.27	10.78
4	1	1.56	2	0.01	0.02	0	-0.00000	-0.00000	5.27	10.78
5	1	0.0	1	-0.00	-0.00	0	-0.00000	-0.00000	9.63	7.16
5	1	1.00	3	0.00	0.00	0	-0.00000	-0.00000	9.63	7.16
5	1	2.00	3	0.03	0.04	0	-0.00000	-0.00000	9.63	7.16
5	1	3.00	4	-0.02	-0.03	0	-0.00000	-0.00000	9.63	7.16
5	1	4.00	5	0.02	0.02	0	-0.00000	-0.00000	9.63	7.16
5	1	4.29	5	0.03	0.04	0	0.00000	0.00000	9.63	7.16
6	1	0.0	1	-0.00	-0.00	0	0.00000	0.00000	11.67	2.79
6	1	1.00	3	0.00	0.00	0	-0.00000	0.00000	11.67	2.79
6	1	2.00	3	0.04	0.02	0	-0.00000	0.00000	11.67	2.79
6	1	3.00	4	-0.02	-0.01	0	0.00000	0.00000	11.67	2.79
6	1	3.60	4	-0.06	-0.04	0	-0.00000	0.00000	11.67	2.79
7	1	0.0	1	0.0	0.0	0	-0.00000	0.00000	11.99	0.57
7	1	1.00	2	-0.02	-0.00	0	-0.00000	-0.00000	11.99	0.57
7	1	2.00	3	0.01	0.00	0	-0.00000	-0.00000	11.99	0.57
7	1	3.00	4	-0.00	-0.00	0	-0.00000	0.00000	11.99	0.57
7	1	3.30	4	-0.01	-0.00	0	0.00000	0.00000	11.99	0.57
8	1	0.0	1	0.0	0.0	0	0.00000	0.00000	10.53	-5.75
8	1	0.91	2	-0.00	0.00	0	0.00000	0.00000	10.53	-5.75
9	1	0.0	1	0.0	0.0	0	-0.00000	0.00000	11.30	-4.04
9	1	1.00	2	-0.00	0.00	0	0.00000	0.00000	11.30	-4.04
9	1	2.00	3	0.00	-0.00	0	-0.00000	0.00000	11.30	-4.04
9	1	2.03	3	0.00	-0.00	0	0.00000	0.00000	11.30	-4.04

Table II  
(p-Matrix)

SOLUTIONS OF LORAN EQUATIONS FOR HORIZONTAL POSITION AND VELOCITY COORDINATES

I	K	S (KYDS)	ITER	ATE (FT)	CTE (FT)	ITER	ATE (MPH)	CTE (MPH)	XDOT (MPH)	YDOT (MPH)
1	1	0.0	1	0.0	0.0	0	0.00000	-0.00000	7.95	-8.98
1	1	1.10	3	0.05	-0.01	0	-0.85570	0.07196	7.95	-8.98
1	1	2.20	5	0.02	-0.00	0	-1.68949	0.13937	7.95	-8.98
1	1	3.30	6	-0.11	0.01	0	-2.49070	0.20070	7.95	-8.98
1	1	4.40	7	0.28	-0.03	0	-3.25013	0.25459	7.95	-8.98
1	1	5.50	9	0.21	-0.02	0	-3.96068	0.30013	7.95	-8.98
1	1	6.60	11	0.20	-0.02	0	-4.61720	0.33654	7.95	-8.98
1	1	7.70	13	0.22	-0.02	0	-5.21656	0.36336	7.95	-8.98
1	1	8.80	15	0.28	-0.03	0	-5.75746	0.38042	7.95	-8.98
1	1	9.90	17	0.37	-0.03	0	-6.24007	0.38774	7.95	-8.98
1	1	11.00	19	0.45	-0.04	0	-6.66574	0.38552	7.95	-8.98
1	1	11.19	20	-0.37	0.03	0	-6.73357	0.38428	7.95	-8.98
2	1	0.0	1	0.0	0.0	0	0.00000	-0.00000	11.53	3.32
2	1	1.00	3	0.00	0.00	0	-0.38800	-0.20716	11.53	3.32
2	1	2.00	4	-0.01	-0.01	0	-0.78824	-0.43418	11.53	3.32
2	1	3.00	5	0.02	0.01	0	-1.20032	-0.68107	11.53	3.32
2	1	4.00	6	-0.03	-0.02	0	-1.62325	-0.94732	11.53	3.32
2	1	5.00	7	0.04	0.03	0	-2.05627	-1.23193	11.53	3.32
2	1	5.42	7	0.08	0.05	0	-2.23974	-1.35595	11.53	3.32
3	1	0.0	1	-0.00	-0.00	0	-0.00000	0.00000	10.64	5.56
3	1	0.86	2	-0.02	-0.02	0	-0.19319	-0.21767	10.64	5.56
4	1	0.0	1	-0.00	-0.00	0	0.00000	-0.00000	5.27	10.78
4	1	1.00	2	0.00	0.00	0	0.09326	0.06097	5.27	10.78
4	1	1.56	2	0.01	0.02	0	0.15061	0.09031	5.27	10.78
5	1	0.0	1	-0.00	-0.00	0	0.00000	0.00000	9.63	7.16
5	1	1.00	3	0.00	0.00	0	-0.09101	-0.25746	9.63	7.16
5	1	2.00	3	0.03	0.04	0	-0.17764	-0.54267	9.63	7.16
5	1	3.00	4	-0.02	-0.03	0	-0.25776	-0.85530	9.63	7.16
5	1	4.00	5	0.02	0.02	0	-0.33305	-1.19420	9.63	7.16
5	1	4.29	5	0.03	0.04	0	-0.35344	-1.29532	9.63	7.16
6	1	0.0	1	-0.00	-0.00	0	-0.00000	-0.00000	11.67	2.79
6	1	1.00	3	0.00	0.00	0	-0.31214	-0.27939	11.67	2.79
6	1	2.00	3	0.04	0.02	0	-0.61304	-0.54644	11.67	2.79
6	1	3.00	4	-0.02	-0.01	0	-0.90026	-0.79762	11.67	2.79
6	1	3.60	4	-0.06	-0.04	0	-1.06412	-0.93850	11.67	2.79
7	1	0.0	1	0.0	0.0	0	0.00000	-0.00000	11.99	0.57
7	1	1.00	2	-0.02	-0.00	0	-0.27325	-0.09572	11.99	0.57
7	1	2.00	3	0.01	0.00	0	-0.52859	-0.16935	11.99	0.57
7	1	3.00	4	-0.00	-0.00	0	-0.76651	-0.22267	11.99	0.57
7	1	3.30	4	-0.01	-0.00	0	-0.83388	-0.23482	11.99	0.57
8	1	0.0	1	0.0	0.0	0	0.00000	-0.00000	10.53	-5.75
8	1	0.91	2	-0.00	0.00	0	-0.03665	0.11823	10.53	-5.75
9	1	0.0	1	0.0	0.0	0	0.00000	-0.00000	11.30	-4.04
9	1	1.00	2	-0.00	0.00	0	-0.09741	0.13381	11.30	-4.04
9	1	2.00	3	0.00	-0.00	0	-0.18754	0.27544	11.30	-4.04
9	1	2.03	3	0.00	-0.00	0	-0.19071	0.27923	11.30	-4.04

S2R-80-019  
ZT70S2R0  
January 28, 1980

TO: C. R. Edwards  
FROM: V. Schwab  
SUBJECT: Computation of GDOP for St. Mary's River Data File

The formulas used to compute GDOP for the St. Mary's River Data File are summarized below.

1. General Formulas

The scalar variable GDOP (geometric dilution of precision) depends on the G-matrix and is given by

$$\text{GDOP} = [\text{tr}(\mathbf{G}\mathbf{G}^T)]^{1/2} \quad (1)$$

in which  $\mathbf{G}^T$  denotes the transpose of the matrix  $\mathbf{G}$  and  $\text{tr}(\mathbf{M})$  denotes the sum of the diagonal elements of  $\mathbf{M}$ . The matrix  $\mathbf{M} = \mathbf{G}\mathbf{G}^T$  is  $n \times n$  where  $n=2$  or  $3$  according as  $2$  or  $3$  LORAN TDs are used in the navigation fix.

In the case of  $2$  TDs the G-matrix is given by

$$\mathbf{G} = \mathbf{A}^{-1} \quad (2)$$

where  $\mathbf{A}$  is  $2 \times 2$  and of rank  $2$ .

In the case of  $3$  TDs minimum variance estimation is used and  $\mathbf{G}$  is given by

$$\mathbf{G} = (\mathbf{A}^T \mathbf{R}^{-1} \mathbf{A})^{-1} \mathbf{A}^T \mathbf{R}^{-1}. \quad (3)$$

In this case  $\mathbf{A}$  is  $3 \times 3$  and of rank  $3$  and the  $3 \times 3$  matrix  $\mathbf{R}$  is the



covariance matrix of the noise in the TD measurements. In both (2) and (3) the elements of A depend only on the relative geometry of the navigator, master station and slave stations and the nominal propagation velocity of the LORAN signals.

We define the following coordinates which enter into the definitions of the elements of A and R:

$x_m, y_m$	horizontal cartesian position coordinates of the master station
$x_i, y_i$	horizontal cartesian position coordinates of ith slave station
$x_p, y_p$	horizontal cartesian position coordinates of a known, arbitrary point
$v$	nominal propagation velocity of the LORAN signals
$R_1$	slant range from master station to arbitrary point
$R_{2i}$	slant range from ith slave station to arbitrary point
$a_{ij}$	element of A-matrix

The formulas for  $R_1$ ,  $R_{2i}$ ,  $a_{i1}$  and  $a_{i2}$  are

$$R_1 = [(x_p - x_m)^2 + (y_p - y_m)^2]^{1/2} \quad (4)$$

$$R_{2i} = [(x_p - x_i)^2 + (y_p - y_i)^2]^{1/2}, \quad i=1,2,3 \quad (5)$$

$$a_{i1} = [(x_p - x_i)/R_{2i} - (x_p - x_m)/R_1]/v, \quad i=1,2,3 \quad (6)$$

$$a_{i2} = [(y_p - y_i)/R_{2i} - (y_p - y_m)/R_1]/v, \quad i=1,2,3 \quad (7)$$

## 2. Formulas for GDOP in the Case of Two TDs

In the case of two TDs eqs (1) and (2) give

$$GDOP_2 = [a_{11}^2 + a_{12}^2 + a_{21}^2 + a_{22}^2]^{1/2} / (a_{11}a_{22} - a_{12}a_{21}). \quad (8)$$

## 3. Formulas for GDOP in the Case of Three TDs

The elements of the noise covariance matrix, R, are

$$r_{ii} = (R_1^2 + R_{2i}^2)/R_1^2, \quad i=1,2,3$$

$$r_{ij} = 1.0, \quad i \neq j.$$

The determinant of R is

$$\Delta = r_{11}r_{22}r_{33} + 2r_{12}r_{23}r_{13} - r_{13}^2r_{22} - r_{12}^2r_{33} - r_{11}r_{23}^2.$$

The elements of  $R^{-1}$  are

$$r_{11}^{-1} = (r_{22}r_{33} - r_{23}^2)/\Delta$$

$$r_{12}^{-1} = (r_{13}r_{23} - r_{33}r_{12})/\Delta$$

$$r_{13}^{-1} = (r_{12}r_{23} - r_{22}r_{13})/\Delta$$

$$r_{22}^{-1} = (r_{11}r_{33} - r_{13}^2) / \Delta$$

$$r_{23}^{-1} = (r_{12}r_{13} - r_{11}r_{23}) / \Delta$$

$$r_{33}^{-1} = (r_{11}r_{22} - r_{12}^2) / \Delta$$

$$r_{21}^{-1} = r_{12}^{-1}$$

$$r_{31}^{-1} = r_{13}^{-1}$$

$$r_{32}^{-1} = r_{23}^{-1}$$

The elements of  $B = A^T R^{-1}$  are

$$b_{11} = a_{11}r_{11}^{-1} + a_{21}r_{21}^{-1} + a_{31}r_{31}^{-1}$$

$$b_{12} = a_{11}r_{12}^{-1} + a_{21}r_{22}^{-1} + a_{31}r_{32}^{-1}$$

$$b_{13} = a_{11}r_{13}^{-1} + a_{21}r_{23}^{-1} + a_{31}r_{33}^{-1}$$

$$b_{21} = a_{12}r_{11}^{-1} + a_{22}r_{21}^{-1} + a_{32}r_{31}^{-1}$$

$$b_{22} = a_{12}r_{12}^{-1} + a_{22}r_{22}^{-1} + a_{32}r_{32}^{-1}$$

$$b_{23} = a_{12}r_{13}^{-1} + a_{22}r_{23}^{-1} + a_{32}r_{33}^{-1}$$

The elements of  $C = (A^T R^{-1} A)$  are

$$c_{11} = b_{11}a_{11} + b_{12}a_{21} + b_{13}a_{31}$$

$$c_{12} = b_{11}a_{12} + b_{12}a_{22} + b_{13}a_{32}$$

$$c_{21} = b_{21}a_{11} + b_{22}a_{21} + b_{23}a_{31}$$

$$c_{22} = b_{21}a_{12} + b_{22}a_{22} + b_{23}a_{32}$$

The elements of  $C^{-1} = (A^T R^{-1} A)^{-1}$  are

$$\Delta = c_{22}c_{11} - c_{12}c_{21}$$

$$c_{11}^{-1} = c_{22}/\Delta$$

$$c_{12}^{-1} = -c_{12}/\Delta$$

$$c_{21}^{-1} = c_{21}/\Delta$$

$$c_{22}^{-1} = c_{11}/\Delta$$

The elements of  $G = (A^T R^{-1} A)^{-1} A^T R^{-1}$  are

$$g_{11} = c_{11}^{-1}b_{11} + c_{12}^{-1}b_{21}$$

$$g_{12} = c_{11}^{-1}b_{12} + c_{12}^{-1}b_{22}$$

$$g_{13} = c_{11}^{-1}b_{13} + c_{12}^{-1}b_{23}$$

$$g_{21} = c_{21}^{-1}b_{11} + c_{22}^{-1}b_{21}$$

$$g_{22} = c_{21}^{-1}b_{12} + c_{22}^{-1}b_{22}$$

$$g_{23} = c_{21}^{-1}b_{13} + c_{22}^{-1}b_{23}$$

Finally

$$GDOP_3 = [g_{11}^2 + g_{12}^2 + g_{13}^2 + g_{21}^2 + g_{22}^2 + g_{23}^2]^{1/2} \quad (9)$$

#### 4. The Units in Which GDOP is Expressed

The units in which  $GDOP_2$  given by (8) and  $GDOP_3$  given by (9) are expressed depend on the units used to express the propagation velocity,  $v$ . For the St. Mary's River Data File the position coordinates are expressed in kiloyards and propagation velocity in kiloyards/nanosec.  $GDOP_2$  and  $GDOP_3$  as given by (8) and (9) are also then in kiloyards/nanosec. However, in the Data File it was desired to express GDOP in yds/nanosec, so the numerical values given by (8) and (9) are multiplied by 1000 to make the conversion.

V. Schwab  
V. Schwab

VS:nt  
Distribution  
GEBaer  
CREdwards  
LJLevy  
JBMoffett  
VSchwab  
TThompson  
JGWall (5)  
Archives  
S2R File

## REFERENCES

1. Ligon, J.M. and Edwards, C.R., PILOT: PRECISION INTRACOASTAL LORAN TRANSLOCATION—EXPLOITING LORAN-C IN THE HARBOR AND RIVER ENVIRONMENT, Wild Goose Association Eighth Annual Technical Symposium, October 17-19, 1979.
2. Sedlock, A.J., SURVEYING IN THE TIME-DIFFERENCE DOMAIN, Wild Goose Association Eighth Annual Technical Symposium, October 17-19, 1979.
3. Olsen, D.L., and Isgett, C.E., PRELIMINARY STABILITY ANALYSIS OF THE ST. MARYS RIVER MINI-CHAIN, Wild Goose Association Eighth Annual Technical Symposium, October 17-19, 1979.
4. Ilgen, J.D. and Feldman, D.A., LORAN-C SIGNAL ANALYSIS EXPERIMENTS "AN OVERVIEW," Proceedings of Conference on Navigation in Transportation, September 19-21, 1978.
5. Johler, J.R., Doherty, R.H., Samaddar, S.N., and Campbell, L.W., A METEOROLOGICAL PREDICTION TECHNIQUE FOR LORAN-C TEMPORAL VARIATIONS, Wild Goose Association Eighth Annual Technical Symposium, October 17-19, 1979.
6. Warren, R.S., Gupta, R.R., and Healy, R.D., "Design and Calibration of a Grid Prediction Algorithm for the St. Marys River Loran-C Chain." The Analytic Sciences Corporation, Technical Information Memorandum TIM-1119-2, March 1978. Published as U.S. Coast Guard Report No. CG-D-32-80. Available from the National Technical Information Service, Springfield, Virginia 22161.
7. DePalma, L.M., and Gupta, R.R., "Seasonal Sensitivity Analysis of the St. Marys River Loran-C Time Difference Grid." The Analytic Sciences Corporation, Technical Information Memorandum TIM-1119-3, June 1978. Published as U.S. Coast Guard Report No. CG-D-33-80. Available from the National Technical Information Service, Springfield, Virginia 22161.
8. Doherty, R.H., and Johler, J.R., "Meteorological Influences on Loran-C Ground Wave Propagation." Journal of Atmospheric and Terrestrial Physics, Vol. 37, pp 1117-1124, 1975.
9. Campbell, L.W., Doherty, R.H., and Johler, J.R., "Loran-C System Dynamic Model: Temporal Propagation Variation Study." Final Report. Analytical Systems Engineering Corporation, Report No. ASECR 79-107, July 1979. Published as U.S. Coast Guard Report No. CG-D-57-79. Available from the National Technical Information Service, Springfield, Virginia 22161 as AD-A076214.

